Implication of carbon monoxide signaling in cellular stress response

Inaugural-Dissertation

zur Erlangung des Doktorgrades
der Mathematisch-Naturwissenschaftlichen Fakultät
der Heinrich-Heine-Universität Düsseldorf

vorgelegt von

David Stucki
aus Moers

Düsseldorf, September 2020

aus dem Institut für Biochemie und Molekularbiologie I
der Heinrich-Heine-Universität Düsseldorf

Gedruckt mit der Genehmigung der
Mathematisch-Naturwissenschaftlichen Fakultät der
Heinrich-Heine-Universität Düsseldorf

Berichterstatter:

1. Prof. Dr. Wilhelm Stahl

2. Prof. Dr. Vlada Urlacher

Tag der mündlichen Prüfung: 23.03.2021

It’s a crazy world out there. Be curious.

Stephen Hawking

TABLE OF CONTENTS

PREFACE

This work about the implication of carbon monoxide signaling in cellular stress response was written as a cumulative thesis consisting of four published manuscripts, including one review article and three research articles, and additional data sets.

The thesis is set up in three major parts. In part one, a general introduction about cellular stress response, the biochemical requirements for carbon monoxide (CO) signaling and the connection of these processes with cellular energy metabolism is provided along with the review article *Manuscript 1*, a key part of the introduction. In *Manuscript 1*, an overview of biochemical research tools for detection and delivery of CO in model systems is presented together with a detailed view on the current understanding of CO signaling and its regulation of mitochondrial homeostasis.

The experimental data of this study is presented in part two. First, the selection of biochemical tools for the study of CO signaling, including its delivery to sensitive model systems via CO releasing molecules (CORMs) is shown in *Manuscript 2*, highlighting advantages and limitations of three frequently applied CORMs. *Manuscript 3* builds up on this and demonstrates how quick and direct effects of CO, from CORM-401 or endogenously produced by heme oxygenases, on mitochondrial function are transduced in secondary signaling pathways, likely contributing to the antioxidant defense. These findings are complemented by additional data showing the connection of CO signaling with mitochondrial quality control mechanisms via modulation of energy metabolism. *Manuscript 4* shows the modulation of cytochrome P450-dependent monooxygenases by CO signaling and the subsequent connection with other stress response pathways and xenobiotic metabolism.

Finally, the results of this thesis are put into context with current literature and are discussed with respect to the overall question of this study: how is CO signaling implicated in cellular stress response?

ABBREVIATIONS

AK	adenylate kinase
AMPK	AMP-activated protein kinase
ANT	adenine nucleotide translocase
ARE	antioxidant response element
BK_{Ca}	large-conductance Ca^{2+}-activated K^+ channel
CO	carbon monoxide
CORM	carbon monoxide releasing molecule
CYP	cytochrome P450-dependent monooxygenase
DHE	dihydroethidium
DRP1	dynamin-related protein 1
ECAR	extracellular acidification rate
ER	endoplasmatic reticulum
EROD	ethoxyresorufin-*O*-deethylase
ETC	electron transport chain
FUNDC1	FUN14 domain containing 1
GPx	glutathione peroxidase
GRX	glutaredoxin
GSH	glutathione, reduced
GSSG	glutathione, oxidized
GST	glutathione-S-transferase
Hb	hemoglobin
HO-1	heme oxygenase-1
IC-MS	ion chromatography mass spectometry
iCORM	inactive carbon monoxide releasing molecule
Keap1	kelch-like ECH-associated protein 1
LC3	microtubule-associated protein 1A/1B-light chain 3
Mb	myoglobin
MEFs	murine embryonic fibroblasts
MFF	mitochondrial fission factor
NADPH	nicotinamide adenine dinucleotide phosphate
NQO1	NAD(P)H quinone oxidoreductase 1

NRF1	nuclear respiratory factor 1
Nrf2	nuclear factor (erythroid derived 2)-like 2
OCR	oxygen consumption rate
OXPHOS	oxidative phosphorylation system
PER	proton efflux rate
PGC	proliferator-activated receptor gamma coactivator
P_iC	phosphate carrier
Pink1	PTEN-induced kinase 1
PPAR	peroxisome proliferator-activated receptor
PPP	pentose phosphate pathway
ROS	reactive oxygen species
SDH	succinate dehydrogenase
SOD	superoxide dismutase
SRB	sulforhodamine B
TFAM	mitochondrial transcription factor A
TRX	thioredoxin
UGT	UDP-glucuronosyltransferase
ULK1	Unc-51 like autophagy activating kinase 1
XF	extracellular flux

ABSTRACT

All organisms are exposed to potentially hazardous noxae, including xenobiotics, natural compounds, toxins, drugs, or heavy metals, challenging the organism on the cellular level. For cytoprotection, different stress response pathways have evolved to counteract various noxae and enable survival of the organism. The Nrf2/Keap1 system orchestrates cellular defense against electrophilic compounds, including prooxidative and alkylating agents. Upon activation of the Nrf2/Keap1 system, gene expression of enzymes related to antioxidant defense or phase II xenobiotic metabolism for elimination of electrophilic alkylating agents, is induced. Furthermore, heme oxygenase-1 (HO-1) is typically highly upregulated upon Nrf2/Keap1 activation. HO-1 catalyzes the degradation of heme to biliverdin, iron and carbon monoxide (CO). CO is a small gaseous signaling molecule and HO-1 is therefore thought to play a key role in stress-induced CO signaling.

Here, the implication of CO signaling in cellular stress response was investigated. A selection of suitable tools, CO releasing molecules (CORMs), for the study of CO signaling was performed first, leading to the use of CORM-401 as appropriate model compound for intracellular CO delivery. Biological effects determined upon exposure of cells to CORM-401 were also found after endogenous CO production by heme oxygenases and provision of substrate (heme). It was shown, that the initial CO signal modulates mitochondrial respiratory chain activity, further triggering two different signaling pathways. One implicated the formation of ROS and a subsequent metabolic rewiring from glycolysis to pentose phosphate pathway for NADPH regeneration, which is needed for antioxidant defense. The other pathway comprised the inhibition of mitochondrial ATP production, leading to elevated AMP levels and activation of AMP-activated protein kinase (AMPK) signaling. AMPK likely activated the target kinase ULK1, which is an inducer of mitophagy. Since AMPK activity is also known to induce mitochondrial biogenesis, a regulatory role of CO signaling on preservation of mitochondrial function upon exogenous stress is suggested to be mediated by this pathway.

It was further shown, that CO delivered by CORM-401 modulates the activity of cytochrome P450-dependent monooxygenases (CYPs) in HepG2 cells. This finding may hint to a putative feedback inhibition of electrophilic stress, since CYPs can form electrophiles from xenobiotics (bioactivation). It also demonstrates the interconnection of CO signaling with other stress response pathways (xenobiotic metabolism).

1 INTRODUCTION

1.1 General introduction

All organisms, from simple bacteria or single-celled eukaryotes to complex multicellular systems like humans, are exposed to exogenous stressors. Exogenous stressors include, potentially hazardous chemical or physical noxae such as xenobiotics, secondary plant constituents or other natural compounds, drugs, heavy metals or radiation (Fig 1). In order to survive, these noxae have to be recognized and eliminated by the organism. In mammals, various stress response pathways have evolved on the cellular level to counteract the diverse exogenous stressors. Cellular stress response includes sensing of the stressor and subsequent adaptation of the cell, e.g. via regulation of gene expression for stress-specific defense (Fig 1, box 1-4). An exogenous stressor can be sensed via activation of a receptor or transcription factor, ultimately leading to an adapted gene expression profile and induction of defense enzymes for protection against the respective stressor. Defense enzymes can act either directly on the stressor, leading to its elimination, implicate repair of structural damage caused by the stressor, or trigger secondary events via signal transduction leading to the degradation and replacement of the structurally damaged molecules or even organelles.

Obviously, optimal cellular stress response needs to exert some specificity towards characteristic structures of xenobiotics for efficient counteraction. For example, classes of large lipophilic hydrocarbon compounds activate the aryl hydrocarbon receptor, thus inducing the expression of cytochrome P450-dependent monooxygenases (CYPs) (Vogel et al., 2020, Whitlock, 1999). CYPs in turn catalyze the oxidation of lipophilic hydrocarbons to more hydrophilic metabolites, which can more easily be eliminated from the body than the parent compounds (Nebert et al., 2013). The enzyme catalase is another example for a defense enzyme acting directly and specifically on the stressor. Catalase converts the prooxidant hydrogen peroxide to molecular oxygen and water (Fig 1, box 1) and thus prevents the oxidation of macromolecules within the cell (Nandi et al., 2019).

A central hub of cellular stress response is the nuclear factor (erythroid derived 2)-like 2 (Nrf2) / kelch-like ECH-associated protein 1 (Keap1) system activated by electrophilic compounds, such as direct alkylating agents (e.g. secondary plant constituents containing α,β-unsaturated carbonyl functions) or reactive oxygen species (ROS) (Baird and Yamamoto, 2020). As a consequence of Nrf2/Keap1 activation, the expression of enzymes related to the antioxidant defense such as superoxide dismutase (SOD) for ROS scavenging (reduction) or glutathione

peroxidase (GPx) to reduce organic peroxides or the glutaredoxin (GRX) and thioredoxin (TRX) systems for protein repair (Fig 1, box 2) is induced (Sies et al., 2017). Additionally, phase II enzymes of the xenobiotic metabolism such as glutathione-S-transferase (GST) or UDP-glucuronosyltransferase (UGT) are induced via Nrf2/Keap1 in order to further increase hydrophilicity of electrophilic compounds and thereby promote their elimination (Otsuki and Yamamoto, 2020, Galal et al., 2015, Xu et al., 2005).

Induction of these enzymes results in a direct defense against the environmental stressor, however, activation of Nrf2/Keap1 can also activate secondary/indirect counteractions. One enzyme which is strongly upregulated upon Nrf2/Keap1 activation is heme oxygenase-1 (HO-1) (Medina et al., 2020), which catalyzes the degradation of heme to biliverdin, iron and carbon monoxide (CO) (Coburn et al., 1963). Endogenously produced CO is suggested to act as a gaseous signaling molecule which participates in cellular stress response via signal transduction processes leading to the activation of secondary events including metabolic rewiring of the cell or modulation of mitochondrial homeostasis (Fig 1, box 3+4). Since damaged mitochondria are a potent source of ROS, which in turn could facilitate a structural damage throughout the cell via oxidation of other constituents such as membrane lipids or DNA, they must be removed. CO is suggested to trigger the degradation and replacement of damaged mitochondria via mitophagy and mitochondrial biogenesis, respectively (Fig 1, box 4) (Stucki and Stahl, 2020). By preventing mitochondrial-based damage and restoring the population of functional mitochondria, CO is integrated into the cellular stress response network. Effects, however, are indirectly as compared to the antioxidant defense mediated by catalase, SOD and GPx or the xenobiotic metabolism related to CYPs, GST and UGT. The role of CO signaling on mitochondrial function upon exogenous stress is reviewed in *Manuscript 1*, which is an essential part of the introduction.

Briefly, it is well-established, that CO can bind to heme moieties of proteins via competing with oxygen for the binding site. In mammals, no other target molecules are known. Via this mechanism, CO can modulate activity of different heme proteins such as NADPH oxidases, CYPs or cytochrome *c* oxidase (complex IV of the respiratory chain) (Taillé et al., 2005, Leemann et al., 1994, Ishigami et al., 2017). Application of high amounts of CO gas to isolated mitochondria typically blocks the electron transport through the respiratory chain and produces reactive oxygen species (ROS) via one-electron transfer to oxygen (Zuckerbraun et al., 2007). Obviously, this implies a loss of mitochondrial ATP production. For the study of low amounts of CO, CO releasing molecules (CORMs) have been developed, in order to mimic CO signaling more accurately than the application of CO gas (Motterlini et al., 2002, Schatzschneider, 2015).

By the use of CORMs, it was found, that CO signaling modulates mitochondrial homeostasis on different levels. On the one hand, an upregulation of mitochondrial biogenesis und subsequent increased mitochondrial mass as well as ATP levels are described (Pecorella et al., 2015, Choi et al., 2016). On the other hand, in contrast, it was reported, that CO signaling drives the process of mitophagy (Kim et al., 2018, Chen et al., 2019), a mitochondria-selective form of autophagy, and an essential process for the preservation of a functional mitochondrial population. The simultaneous regulation of both processes (mitophagy and mitochondrial biogenesis) is needed for the removal and replacement of defective and dysfunctional mitochondria. Otherwise the cellular energy metabolism would be affected by dysfunctional mitochondrial population on the long-term. Although such secondary effects of CO signaling, as described here and in more detail in *Manuscript 1*, are well-documented in the literature, it is not fully understood, how the CO signal is transduced into a signaling pathway for the regulation of mitochondrial homeostasis. With respect to mitochondria, inhibition of cytochrome *c* oxidase was suggested as starting point for signal transduction pathways. This also implies a CO-dependent modulation of the cells main ATP-providing pathway and related energy status sensing systems such as the AMP-activated protein kinase (AMPK).

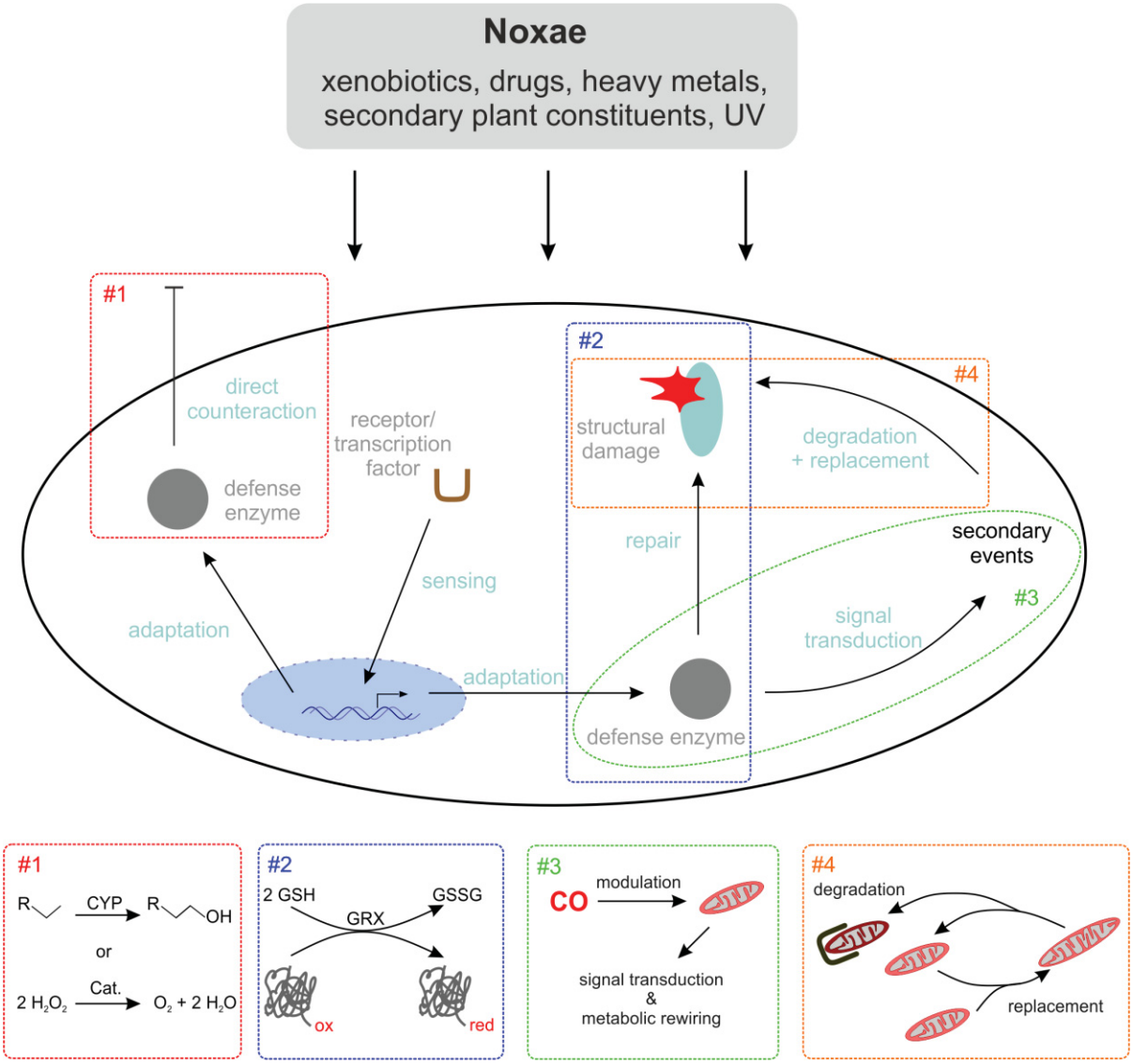

Figure 1: Different cellular stress response pathways. Selected examples of the different pathways are highlighted in the respective boxes below. Cat. = catalase, CYP = cytochrome P450-dependent monooxygenase, GRX = glutaredoxin, GSH = glutathione (reduced), GSSG = glutathione (oxidized).

1.2 Energy status sensing via AMP-activated protein kinase (AMPK) and mitochondrial homeostasis

The ability of cells to transfer energy from production sites to feed energy-consuming processes is essential for their survival. Intracellular energy transfer is mainly mediated via the adenine nucleotide system (ATP, ADP, AMP). Chemical energy of the phosphoanhydridic bonds in ATP (28 to 33 kJ/mol) is used to drive energy demanding processes such as the maintenance of membrane potential, intracellular movement and signaling, cell division or anabolic processes. ATP can be regenerated from ADP either via oxidative phosphorylation system (OXPHOS) or substrate level phosphorylation. Alternatively, ATP is also formed by adenylate kinase (AK)

(Dzeja and Terzic, 2009). The enzyme catalyzes the transfer of a phosphoryl group from one ADP molecule to another, thereby generating ATP and AMP. If ATP consuming and producing processes are at equilibrium, the molar ratio of ATP to ADP is about 10:1 and of ATP to AMP about 100:1 (Beis and Newsholme, 1975). The overall proportions between ATP, ADP and AMP describe the energy status of a cell, which can be calculated as the adenylate energy charge given in Eq 1.

(Eq 1) $$adenylate\ energy\ charge = \frac{[ATP]+\frac{1}{2}[ADP]}{[ATP]+[ADP]+[AMP]}$$

Adenylate energy charge values typically vary between 0.7 and 0.95 for cells of most organisms, including bacteria, fungi, plants, and mammals (De la Fuente et al., 2014). The interconversion of ATP, ADP and AMP by AK occurs close to the enzymatic and is highly reversible (De la Fuente et al., 2014). As a consequence of these enzymatic properties and the high levels of ATP compared to AMP, even minor changes of ATP concentrations cause major shifts in AMP concentrations (Hardie, 2004). Thus, increased AMP concentrations can be used by the cell as a sensitive marker for low energy status.

A key AMP-sensor is the AMP-activated protein kinase (AMPK). AMPK consists of three different subunits: α, β and γ. The α-subunit contains the catalytically active kinase domain as well as a critical threonine residue (Thr172), which is phosphorylated upon AMPK activation by upstream kinases and can therefore be used as a biochemical marker for AMPK activity (Herzig and Shaw, 2018). The β- and γ-subunits have regulatory function. Via its γ-subunit the AMPK complex directly binds and thereby senses adenine nucleotides with the highest affinity for AMP (Ross et al., 2016). While AMP-binding to γ-subunit and resulting phosphorylation of Thr172 is a well-established process for AMPK activation, the exact molecular mechanism is not fully understood. Inhibition of phosphatases (dephosphorylation of Thr172) or allosteric activation of already phosphorylated AMPK have been proposed (Hawley et al., 2003, Davies et al., 1995). Nevertheless, activation of AMPK leads to phosphorylation of downstream proteins involved in cellular metabolism, increasing catabolism and decreasing anabolism to counteract a lowered energy status of the cell. Some AMPK target proteins such as Acetyl-CoA carboxylase, HMG-CoA reductase or phosphofructokinase 2 are involved in metabolic pathways and their regulation allows for a fast rewiring of metabolism (Carling et al., 1987, Munday et al., 1988, Marsin et al., 2000). Additionally, AMPK also targets proteins such as members of the proliferator-activated receptor gamma coactivator (PGC) protein family which

are more indirectly involved in cell metabolism via a stimulating action on mitochondrial biogenesis (Herzig and Shaw, 2018). With this two-sited response, AMPK activity ensures ATP replenishment on the short- and long-term.

Since mitochondria are the main source for ATP and underly a complex quality control machinery, it is not surprising, that the AMPK signaling pathway not only targets mitochondrial biogenesis, but also other processes involved in the regulation of mitochondrial homeostasis. Damaged mitochondria are separated from the mitochondrial network via fission processes. These fission events are mediated by GTPases of the dynamin protein family such as dynamin-related protein 1 (DRP1). Upon energetic stress, AMPK phosphorylates the mitochondrial fission factor (MFF) at Ser155 and Ser173. MFF, which is located on the outer mitochondrial membrane, then recruits DRP1 to the mitochondria, mediating mitochondrial fission (Toyama et al., 2016). A separated, dysfunctional mitochondrion can be degraded via the mitochondria-selective autophagy pathway called mitophagy. Therefore, AMPK phosphorylates Unc-51 like autophagy activating kinase 1 (ULK1) at multiple sites, including Ser555 (Egan et al., 2011, Kim et al., 2011). ULK1 in turn phosphorylates mitophagy receptors located on the outer mitochondrial membrane, such as FUN14 domain containing 1 (FUNDC1) and thereby regulates their interaction with autophagosomal adaptor proteins such as microtubule-associated protein 1A/1B-light chain 3 (LC3) (Wu et al., 2014, Park and Koh, 2020). The mitochondrion is then engulfed by the autophagosome and degraded, providing biomolecules and nutrients for further use.

Induction of mitochondrial fission and subsequently removal via mitophagy as a mode of action for ATP replenishment seems to be counterintuitive, since ATP generating organelles are degraded. However, two considerations should be taken into account: (i) damaged mitochondria are a potent source of ROS, which in turn might distribute the damage over the entire mitochondrial network and (ii) damaged mitochondria are insufficient ATP producing systems. Hence, to counteract cellular ATP deficits, defect mitochondria need to be removed and replaced via mitophagy and mitochondrial biogenesis, respectively. The interplay between cellular energy metabolism and AMPK regulated mitochondrial homeostasis is summarized in Fig 2.

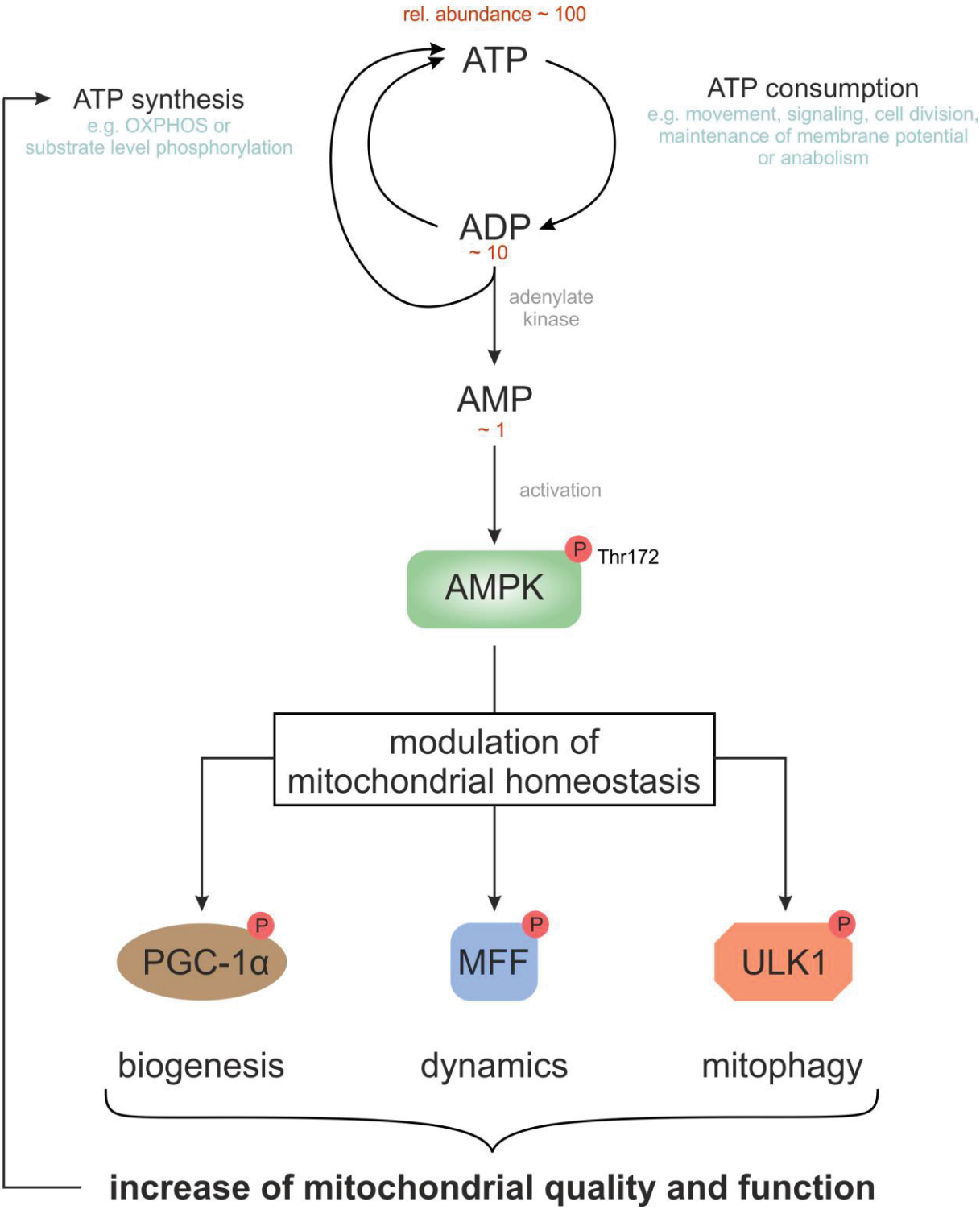

Figure 2: Overview of the regulation of mitochondrial homeostasis via AMP-mediated AMPK activation. AMPK = AMP-activated protein kinase, MFF = mitochondrial fission factor, PGC-1α = proliferator-activated receptor gamma coactivator-1α, ULK1 = Unc-51 like autophagy activating kinase1.

1.3 *Manuscript 1*: Carbon monoxide – beyond toxicity?

David Stucki[1] and Wilhelm Stahl[1]

[1] Institute of Biochemistry and Molecular Biology I, Medical Faculty, Heinrich Heine University Düsseldorf, D-40001 Düsseldorf, Germany.

Received: 20th July 2020; Accepted: 20th August 2020; Published: 26th August 2020

Published in: *Toxicology Letters*, **333**: 251-260.

DOI: 10.1016/j.toxlet.2020.08.010

Contribution statement:
The work on this manuscript was equally distributed between authors.

Toxicology Letters 333 (2020) 251–260

Contents lists available at ScienceDirect

Toxicology Letters

journal homepage: www.elsevier.com/locate/toxlet

Carbon monoxide – beyond toxicity?

D. Stucki, W. Stahl*

Institute of Biochemistry and Molecular Biology I, University of Düsseldorf, Medical Faculty, Germany

ARTICLE INFO

Keywords:
heme oxygenase
carbon monoxide
CORMs
stress response
electrophiles
mitochondria
respiration

ABSTRACT

Carbon monoxide (CO) intoxication is one of the most frequent causes of accidental poisoning, mechanistically related to the inhibition of oxygen transport following blockage of the oxygen binding site of hemoglobin. However, it has become evident that CO is also a gaseous signaling molecule like nitric oxide and capable to trigger cellular stress responses in complex organisms. Endogenously, CO is synthesized upon degradation of heme by heme oxygenases (HOs) of which two enzymatically active isoenzymes are known in mammals; the stress-inducible HO-1 and the constitutively expressed HO-2. Among other pathways, HO-1 expression is stimulated by the Nrf2/Keap1 system which senses electrophilic compounds including alkylating agents and reactive oxygen species (ROS) such as superoxide or hydrogen peroxide. In context with ROS, HO-1 expression has been associated with antioxidant defense related to the heme-metabolite redox pair biliverdin/bilirubin. Studies on CO signaling were facilitated by the introduction of so called "CO releasing molecules" (CORMs), which allow for the controlled release of the compound in biological systems. Obviously, major biological targets of CO comprise intracellular heme-proteins such as cytochrome *c* oxidase of the respiratory chain, cytochrome P450-dependent monooxygenases (CYPs), or NADPH oxidases. From toxicological studies it is known that exposure to high amounts of CO provokes an inhibition of mitochondrial respiration and increased generation of ROS. In contrast, biological response to low amounts of CO comprises moderate mitochondrial uncoupling (proton leakage) due to the activation of channels including phosphate carrier (P_iC), adenine nucleotide translocase (ANT) or large-conductance Ca^{2+}-activated K^+ channels (BK_{Ca}). Uncoupling of mitochondrial respiration from ATP production is accompanied by a loss of mitochondrial membrane potential – a key sensor and regulator of mitochondrial quality control and mitophagy. Inhibitory effects of CO on mitochondrial respiration are compensated by an increased glycolysis. However, on a short term, utilization of glucose is shifted to the pentose phosphate pathway, to provide NADPH for detoxification. It is notable that endogenous CO production is associated with the physiological response against exogenous electrophilic insult like Nrf2-dependent expression of phase II enzymes or glutathione synthesis. In contrast phase I enzymes such as CYPs which usually generate more electrophiles are inhibited by CO. Together with direct and indirect transient effects on energy metabolism and mitochondrial quality control CO may be an important regulator in cellular stress response.

1. Introduction: carbon monoxide toxicity – and then?

Carbon monoxide (CO) poisoning is still among the most frequent toxicological causes of mortality (Rose et al., 2017). The gas is generated upon incomplete combustion of carbon compounds and exogenous exposure can for instance result from fires, charcoal grills, car exhaust, faulty heaters, or industrial accidents (Tadevosyan et al., 2020, Estrella et al., 2019, Golob et al., 2018, Markey and Zumwalt, 2001). In recent years hookah smoking became a major cause of CO intoxication. Relative incidence of hookah-associated CO toxicity increased from 9.5% in 2015 to 41.6% in 2018 (Nguyen et al., 2020). Typical symptoms of CO poisoning are headache, dizziness, weakness, vomiting, chest pain, and confusion often mistaken for a flu. Prolonged exposure will cause brain damage and death (Kinoshita et al., 2020).

According to textbook knowledge, CO toxicity is directly related to the impaired delivery of oxygen to tissues. CO binds to hemoglobin (Hb) with a 200-fold greater affinity compared to oxygen, thus forming an HbCO complex and subsequently blocking an oxygen binding site and decreasing oxygen transport capacity (Veronesi et al., 2017). Additionally, CO binding to one heme group of hemoglobin increases the affinity of the other binding sites for oxygen, hampering its release in peripheral tissues. Following exogenous exposure, hemoglobin in

* Corresponding author at: Institute of Biochemistry and Molecular Biology I, University of Düsseldorf, Medical Faculty, POB 101007, D-40001 Düsseldorf, Germany
E-mail address: wilhelm.stahl@hhu.de (W. Stahl).

https://doi.org/10.1016/j.toxlet.2020.08.010
Received 20 July 2020; Received in revised form 18 August 2020; Accepted 20 August 2020
Available online 26 August 2020
0378-4274/

erythrocytes is the primary target of CO and provides a biological sink thus protecting other tissues from high level exposure to some extent. Binding to the heme group of Hb is reversible and depends on oxygen tension. Exhalation of CO via the lung is the most important way of detoxification (Ryter and Choi, 2013).

Once the biological barrier (Hb sink) is overcome, CO can also bind to other proteins. The presence of a heme moiety as prosthetic group with the central ferrous iron is the structural requirement for efficient binding. Usually CO competes with oxygen for the binding site – other reactions of CO under physiological conditions are not known in mammals.

Cytochrome *c* oxidase of the mitochondrial respiratory chain is inhibited by exogenously applied CO gas which results in impairment of ATP synthesis and an elevated production of superoxide and other reactive oxygen species (ROS). Cellular response includes a switch to glycolysis for energy production and an adaptive defense against oxidative stress. Other targets are myoglobin or cytochrome P450-dependent monooxygenases (CYPs), which are inactivated by CO binding to the central heme group. However, with respect to poisoning due to inhalation of CO, the impaired oxygen transport is most relevant.

Apart from exogenous CO sources, the molecule is also produced endogenously (Coburn et al., 1963). Of course, the same mechanisms underly the modulation of proteins by endogenous CO (competition with oxygen for heme binding site). However, it is important to point out, that biological responses can differ significantly, since location, concentration and target proteins are different. Endogenous CO production gained increasing scientific interest over the past decades and CO is nowadays considered as a gaseous signaling molecule along with nitric oxide and hydrogen sulfide. In the current review we summarize the most important findings about endogenous CO production, its role as a mediator of cellular stress response and technological advances for the study of these processes.

2. Cellular stress response and endogenous CO synthesis – role of heme oxygenases

In animals and humans, highly conserved stress response pathways exist on the cellular level in order to defend against environmental, but also endogenous insults of different origin. Among different stress response pathways, the nuclear factor (erythroid derived 2)-like 2 (Nrf2) / kelch-like ECH-associated protein 1 (Keap1) system (Fig. 1) is mainly responsible for the regulation of cellular defense against oxidative/electrophilic stress and is activated by various noxae such as ROS, xenobiotics, drugs, transition metals, secondary plant constituents or UV irradiation (Dinkova-Kostova et al., 2005, Saito et al., 2016, Dinkova-Kostova et al., 2001, Zhang et al., 1992, Hirota et al., 2005). At resting state, Nrf2 is anchored in the cytosol via binding to Keap1. Upon reaction of an oxidant/electrophile with Cys residues of Keap1 this interaction is abrogated. Thereby, oxidant/electrophilic stressors with various chemical properties react with different Cys residues of Keap1. While ROS such as hydrogenperoxide mostly react with Cys226/613/622/624, sulforaphane- and bardoxolone-dependent Nrf2 activation is specifically mediated via Cys151 (Saito et al., 2016, Baird and Yamamoto, 2020). After release from Keap1 Nrf2 translocates into the nucleus and forms a heterodimer with small masculoaponeurotic fibrosarcoma (sMaf) proteins. This complex ultimately binds to the antioxidant response element (ARE) and triggers transcription of genes associated with either antioxidant defense such as superoxide dismutase (SOD), NAD(P)H quinone oxidoreductase 1 (NQO1) and glutathione peroxidase (GPx) or phase II xenobiotic metabolizing system such as glutathione-S-transferase (GST) and UDP-glucuronosyltransferase (UGT) (Otsuki and Yamamoto, 2020, Baird and Yamamoto, 2020). Activating stressors can be classified as either alkylating or prooxidant agents. These two groups are in line with the cellular defense enzymes they induce. While electrophilic alkylating agents such as α,β-unsaturated carbonyls or epoxides are typically eliminated via phase II xenobiotic metabolism (Galal et al., 2015), prooxidants need to be scavenged via antioxidant defense (Sies et al., 2017). In this context Nrf2 functions as a xenobiotic-activated receptor regulating the adaptive response to prooxidants and alkylating electrophiles.

Interestingly, heme oxygenase-1 (HO-1) is typically highly induced upon activation of the Nrf2/Keap1 signaling pathway (Medina et al., 2020), but its task in antioxidant scavenging and defense against electrophiles is not clearly understood.

Heme oxygenases catalyze the degradation of heme to biliverdin, thereby generating equimolar amounts of CO as well as ferrous iron. This reaction is the main source for endogenous CO production in mammals and consumes molecular oxygen and electrons which are provided by cytochrome P450 reductase from NADPH (Fig. 2). In mammals, two enzymatically active isoenzymes are known: heme oxygenase-1 (HO-1), the stress-inducible isoform (via Nrf2/Keap1; Fig. 1) encoded by the *HMOX1* gene and heme oxygenase-2 (HO-2), which is encoded by the *HMOX2* gene and expressed constitutively (Applegate et al., 1995). Furthermore, HO-3 is described as an enzymatically inactive variant probably involved in heme sensing. HO-1 induction is a widely accepted strategy used by cells to counteract a number of different stress conditions such as electrophilic or prooxidative stress. Many natural compounds have been confirmed to be effective non-cytotoxic HO-1 inducers. A majority of HO-1 inducers are present in plants that are being widely used as flavoring agents, food, or spices and are discussed to exert protective effect on human health against oxidative stress (Becker and Juvik, 2016). However, it is still under debate how HO-1 derived cell protection is mediated and different strategies are discussed as potential mechanisms.

Since heme is an important prosthetic group not only in hemoglobin but also in other heme-containing enzymes, its degradation by heme oxygenases is involved in the regulation of enzyme levels. Several of these enzymes such as nitric oxide synthase, cyclooxygenases or guanylate cyclase play key roles in cellular signaling processes (Mancuso et al., 2006, Jones et al., 2010, Jia et al., 2018). Ferrous iron is a co-product of heme catabolism and HO activity is linked to the co-expression of ferritin, which is required to avoid prooxidant effects of free iron (Gozzelino and Soares, 2014, Fang and Aust, 1997).

For decades, heme oxygenase activity was directly associated with the network of antioxidant defense (for review see: (Dennery, 2014)). Biliverdin, the primary product of heme oxygenases is reduced by biliverdin reductase under consumption of NADPH to form bilirubin (Fig. 2) (Sedlak and Snyder, 2004). ROS such as lipidperoxides (LOOH) or hydrogenperoxide are scavenged (reduced) via the oxidation of bilirubin to biliverdin and the system thereby provides an antioxidant protection. However, the physiological relevance and role of this antioxidant redox cycle is still debated (Jansen and Daiber, 2012).

In addition to the effects described above, heme oxygenases are thought to modulate cellular processes via CO-dependent signaling. Apparently, major targets include intracellular heme-containing proteins such as cytochrome *c* oxidase (complex IV of the respiratory chain), cytochrome P450-dependent monooxygenases, NADPH oxidases and others (Motterlini and Foresti, 2017). The implication of CO as a second messenger molecule is still under debate, especially since mechanisms for the control of cellular CO levels are not fully understood. It has been questioned if sufficient CO amounts are generated by heme oxygenases for proper signaling (Levitt and Levitt, 2015), but it should be noted – as already known for other low molecular weight signals – that the concentrations of the signaling molecules at specific subcellular locations can be considerably high if the generating enzymes are spatially recruited (García-Cardeña et al., 1996, Iwakiri et al., 2006). The HO-1 isoform is usually anchored in the endoplasmatic reticulum at its C-terminus facing the cytosol (Yoshida and Sato, 1989). However, upon cellular stress, it was found in different subcellular compartments including nuclei, caveolae, or mitochondria (Lin et al., 2007, Kim et al., 2004, Zhang et al., 2019). In addition to the induction of HO-1 expression, intracellular translocation may account

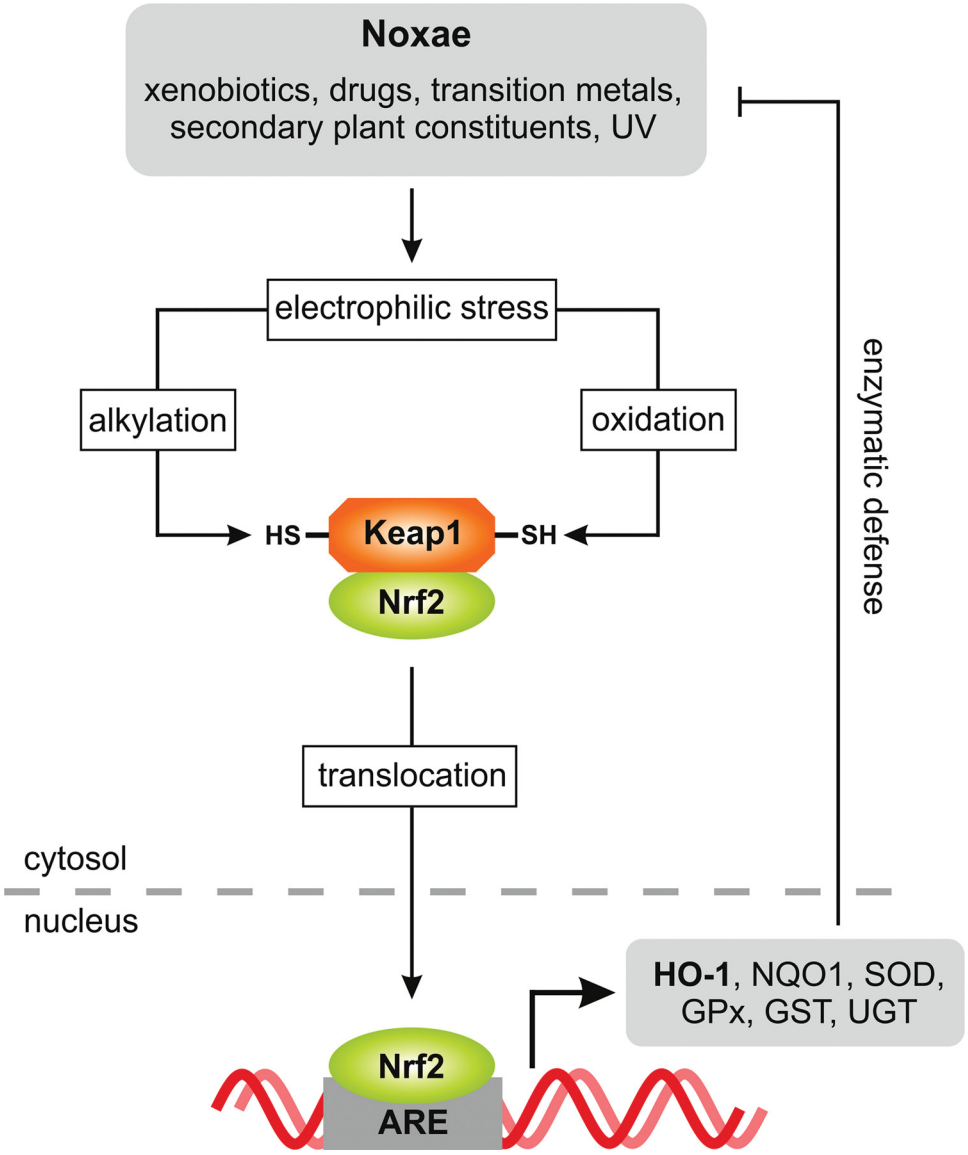

Fig. 1. Schematic depiction of Nrf2/Keap1 pathway activation and subsequent induction of enzymatic defense.

for the regulation of cytoprotective pathways. Continuous removal of CO from the intracellular space is thought to be triggered by a concentration gradient driven by hemoglobin. Hb acts as a nearly infinite sink due to its high affinity for CO, forming HbCO complexes. CO is then transported to the lung and eliminated from the body via exhalation (Moscato et al., 2014, Ryter and Choi, 2013). This continuous passive elimination of CO implies that intracellular CO levels are mainly regulated via its biosynthesis depending on enzyme activity of HOs and provision of substrate. For purpose of signaling differentiation and variety, the affinity of CO towards target heme groups differs over a wide range (Motterlini and Foresti, 2017). This is a comparable mechanism to thiol groups exhibiting different reactivities towards signaling ROS such as hydrogenperoxide, thereby contributing to the orchestration of the redox signaling network (Jones and Sies, 2015).

3. Application and detection of CO in biological systems

To study CO in biological models, suitable delivery systems are required for application in cell and animal experiments. Since dosing with CO gas is quite complicated, other delivery systems have been developed. For this purpose, a number of chemically different compounds was synthesized summarized under the term “CO releasing molecules” or CORMs (Motterlini et al., 2002, Schatzschneider, 2015). CORMs are low-molecular weight compounds which release one or more CO molecules upon decomposition. They can be applied to biological systems and CO release is triggered by different conditions such as pH, temperature, UV-exposure, enzymatic reactions, presence of exchangeable ligands or availability of high affinity acceptor proteins (Schatzschneider, 2015).

The majority of CORMs applied in biological systems are metal complexes of transition metals with CO and other ligands. Essential trace elements such as iron, cobalt and manganese as well as non-physiological metals such as ruthenium or rhenium were used as central ions. The ruthenium-based CORM-2 and CORM-3 or CORM-401 which contains a manganese ion in the center (Motterlini et al., 2002, Clark et al., 2003, Crook et al., 2011, Schatzschneider, 2015) are among the most widely studied CORMs. These three compounds, together with ALF-186 – a molybdenum-based CORM (Seixas et al., 2013) – are representatives of a class of ligand exchangeable CORMs. CO release from CORMs can also be triggered by enzymatic activity of e.g. esterases, producing a labile carbonyl complex that subsequently releases CO (Romanski et al., 2011) or exposure to UV light (PhotoCORMs) (Nagel et al., 2014). However, non-metallic CORMs based on different lead structures such as hydroxyflavone derivatives, boron dipyrromethene

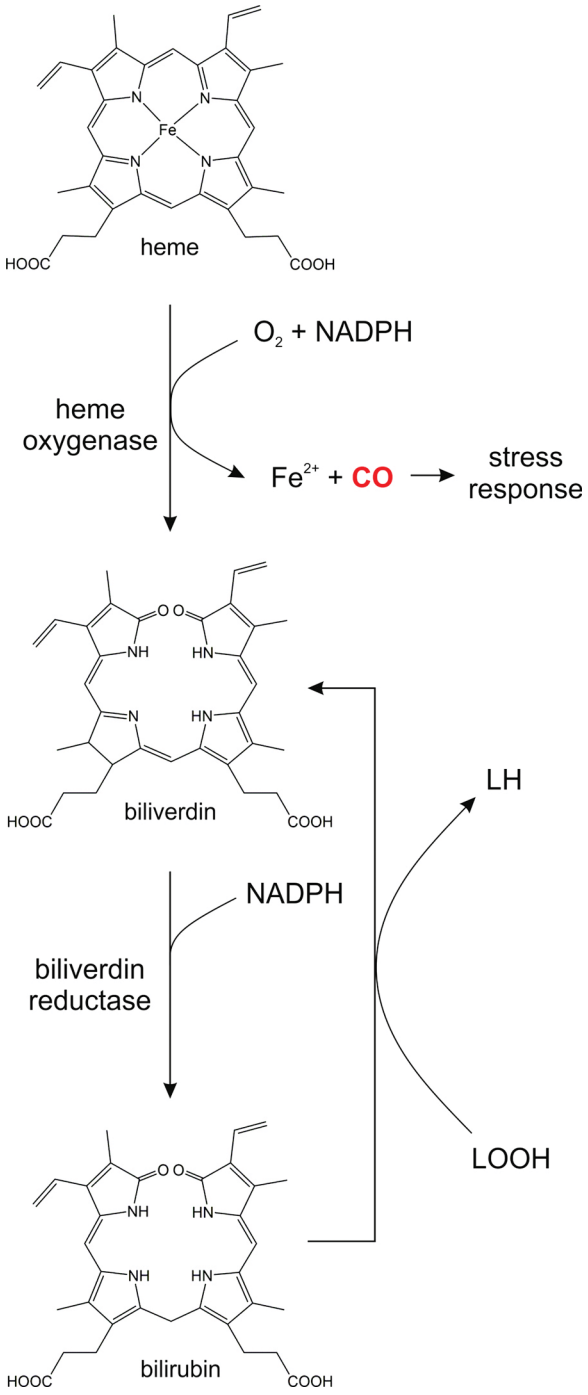

Fig. 2. Heme catabolism.

difluoride (BODIPY) chromophores and others have also been introduced (Anderson et al., 2015, Palao et al., 2016, Pan et al., 2017). Exemplary structures of different CORMs are given in Fig. 3.

Depending on their chemical properties CORMs behave differently in biological systems and experimental settings with respect to the kinetics of CO release, toxicity, affinity to heme groups and subsequent inhibition of heme-enzymes (Stucki et al., 2020a, Soboleva et al., 2018). Also, interference with oxygen detection systems hampers the use of some CORMs in measurements of CO effects on the respiratory chain and related read outs. Hence, the selection of a suitable CORM is essential for successful experiments. In this context, the selection of a proper control is also important. Usually an inactive CORM (so called iCORM) is used as additional control. Only the comparison of a mock treated control with both CORM and iCORM groups allows for correct data interpretation as well as differentiation between CO-related effects and those mediated by the CORM-backbone. In some cases, non-CO related effects of CORMs have been reported and were e.g. ascribed to the biological activity of the central metal ion (Nielsen, 2019, Southam et al., 2018). Solutions of the decomposed CORMs are often applied as respective iCORMs. Alternatively, non-active components of the CORM are used, e.g. an equimolar mixture of sarcosine-N-dithiocarbamate and $MnSO_4$ as surrogate iCORM-401. Experimental problems associated with iCORMs may be related to residual CO releasing activity. It should be stated that more sophisticated CORMs are under development, for instance with ligands targeting specific compartments (Soboleva et al., 2018) or inherent fluorogenic properties to monitor availability of the compound in biological test systems (Sakla et al., 2019, Feng et al., 2019). Notably, these compounds were only developed recently and are not yet extensively studied for their suitability in biological research.

Another important task in CO research is the detection of CO in model systems, both *in vitro* and *in vivo*. For simple, cell-free settings, binding of CO to myoglobin can be spectrophotometrically assessed following the formation of carboxymyoglobin which was used to determine the release of CO from CORMs (Atkin et al., 2011). For detection of CO in biological systems, fluorescent probes are available. One of the first CO sensing molecules developed was CO probe-1 (COP-1), which contains a BODIPY structure linked to a cyclometalated dimeric palladium (II) unit (Michel et al., 2012). Upon CO binding, the fluorescent BODIPY is released from the non-fluorescent parent compound for detection. Further advances among CO sensing probes include ratiometric fluorescent switches for differentiated detection before and after CO exposure, shorter reaction times and increasing sensitivity (Madea et al., 2020, Zhou et al., 2020). Additionally, CO can be detected using a genetically encoded CO sensor (COser). This biosensor consists of a yellow fluorescent protein as a reporter unit and CooA from *Rhodospirillum rubrum* as a dimeric heme-containing CO recognition unit (Wang et al., 2012). Both CORMs and CO detection systems are still undergoing further development and optimization.

4. Biological effects of CO

On the one hand, mitochondria are a major source of electrophilic compounds such as superoxide and hydrogenperoxide, but on the other hand also possess a high abundance of target structures for electrophiles, namely thiol-containing proteins (Koenitzer and Freeman, 2010, Wong and Liebler, 2008). Targeting of electrophiles to mitochondria has been shown to modulate protein function and/or induce apoptosis (Diers et al., 2010, Beavers et al., 2017).

Mitochondria also exhibit a high number of heme-containing proteins - putative targets of CO - needed for their biological function including respiration and consequently ATP production. Some of them, such as cytochrome *c* oxidase, are already known to be addressed by CO (Ishigami et al., 2017), which in turn is endogenously generated by heme oxygenases. Among these, the HO-1 isoform is regulated via the electrophile-sensitive Nrf2/Keap1 pathway (Fig. 1). Here, we will therefore mainly focus on regulatory effects of CO, as a stress response mediator, on mitochondrial homeostasis.

4.1. Regulation of mitochondrial homeostasis by CO

Application of CO gas is limited in terms of proper dosing and was for a long time the only available tool to study CO effects on biological systems. The most important findings, however, contribute significantly to the current understanding of regulatory CO effects. The main mitochondrial target for CO is cytochrome *c* oxidase in complex IV of the electron transport chain (ETC), which can be blocked by CO, thus inhibiting respiration. This has often been demonstrated by treatment of isolated mitochondria or cells with CO gas (Wohlrab and Ogunmola, 1971, Wagner and Erecinska, 1971, Zuckerbraun et al., 2007). Closely

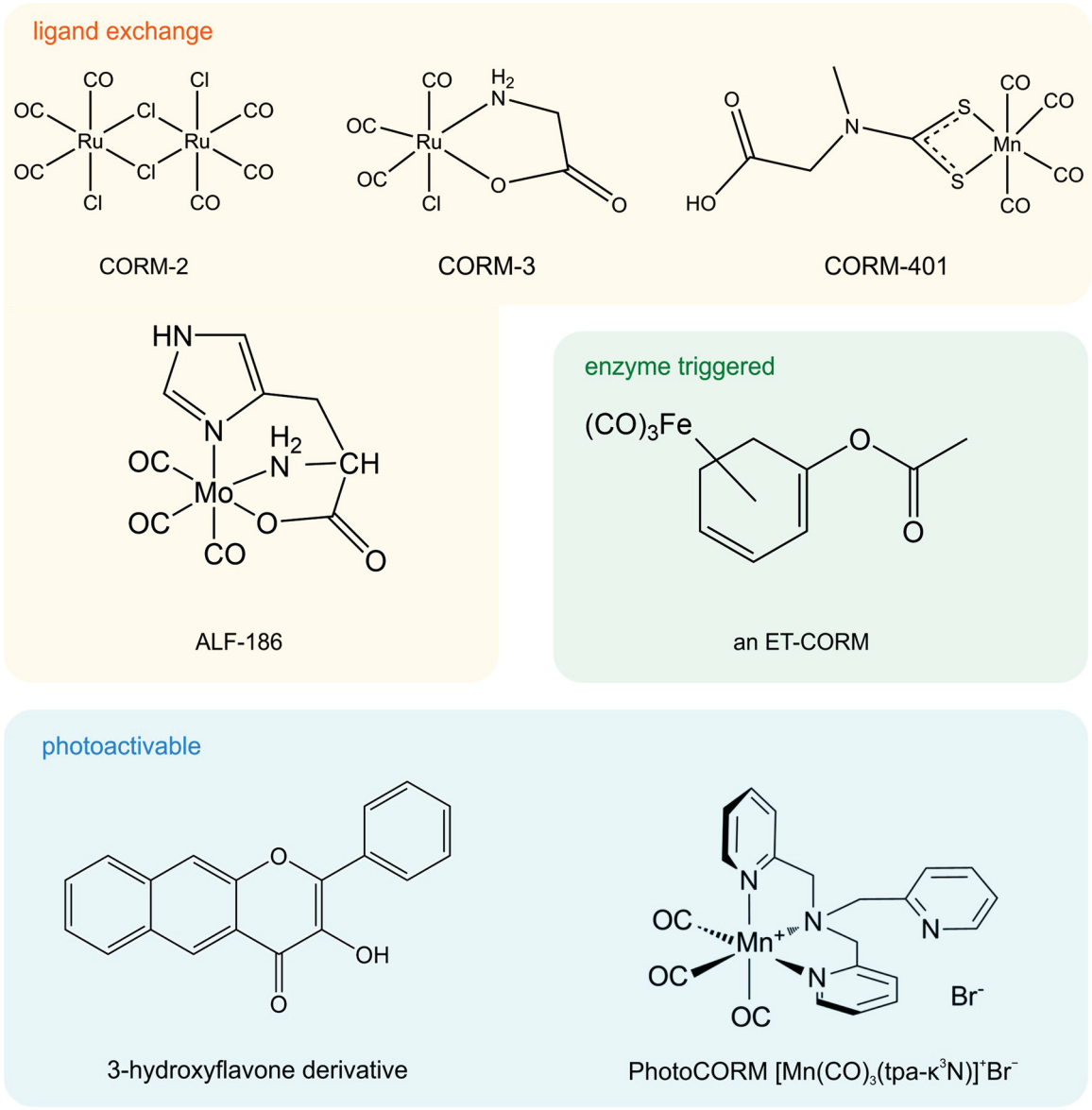

Fig. 3. Chemical structures of selected CORMs – mechanisms of CO release are indicated.

related to this effect is the finding of increased levels of ROS with mitochondrial origin (Bilban et al., 2006, Zuckerbraun et al., 2007), most likely following blockage of ETC and consequently unintended electron transfer to oxygen. More indirect observations were made by the group of H.B. Suliman, when applying different doses of CO gas to either mice or humans. It was found that markers of mitochondrial biogenesis, such as peroxisome proliferator-activated receptor gamma coactivator 1-alpha (PGC-1α), mitochondrial transcription factor A (TFAM) and nuclear respiratory factor 1 (NRF1), were upregulated on mRNA and protein level in healthy subjects treated with 100 – 200 ppm CO gas for 1 h on 5 consecutive days (Rhodes et al., 2009, Pecorella et al., 2015) or in mice (single dose at 50 – 1250 ppm for 1 h) (Suliman et al., 2007). This effect was accompanied by elevated levels of mtDNA and citrate synthase, suggesting an increase of mitochondrial mass (Pecorella et al., 2015). Interestingly, in H9c2 rat cardiomyocytes similar effects were observed following dichloromethane (DCM) treatment (Suliman et al., 2007). DCM undergoes cytochrome P450-mediated metabolism, thereby producing CO as a by-product (Pankow and Jagielki, 1993, Kubic and Anders, 1978). However, it should be taken into account that xenobiotic metabolism of DCM also leads to the formation of other metabolites, possibly interfering with CO-related read outs.

In studies with CORMs and biological CO generating systems (heme oxygenases) these findings were confirmed. It was found that the effect of CO on mitochondrial function depends on the concentration of CO. As already known, comparatively high amounts of CO administered by CORMs provoke inhibition of mitochondrial respiration, which was confirmed in isolated mitochondria from rat hearts and in endothelial cells (Lo Iacono et al., 2011, Long et al., 2014, Kaczara et al., 2015). Decreased respiration of mitochondria isolated from mice hearts was also found in HO-1 overexpressing animals (Wang et al., 2010) as well as a decreased cytochrome *c* oxidase activity (complex IV) and increased ROS levels in cells subjected to HO-1 overexpression. These effects were enhanced by a truncated HO-1 variant that co-locates with mitochondria (Bansal et al., 2014). Translocation of HO-1 from ER to mitochondria is not only described for genetically modified variants, but also upon treatment of cells with exogenous stressors such as $CoCl_2$, hemin, cigarette smoke or the isoflavone ME-344 (Bansal et al., 2014, Converso et al., 2006, Slebos et al., 2007, Zhang et al., 2019). On the short-term induction of ROS formation by CO is accompanied by an intracellular modified glucose utilization from glycolysis towards pentose phosphate pathway (PPP) (Stucki et al., 2020b; Kaczara et al., 2018). This increased flux through the PPP regenerates reduction

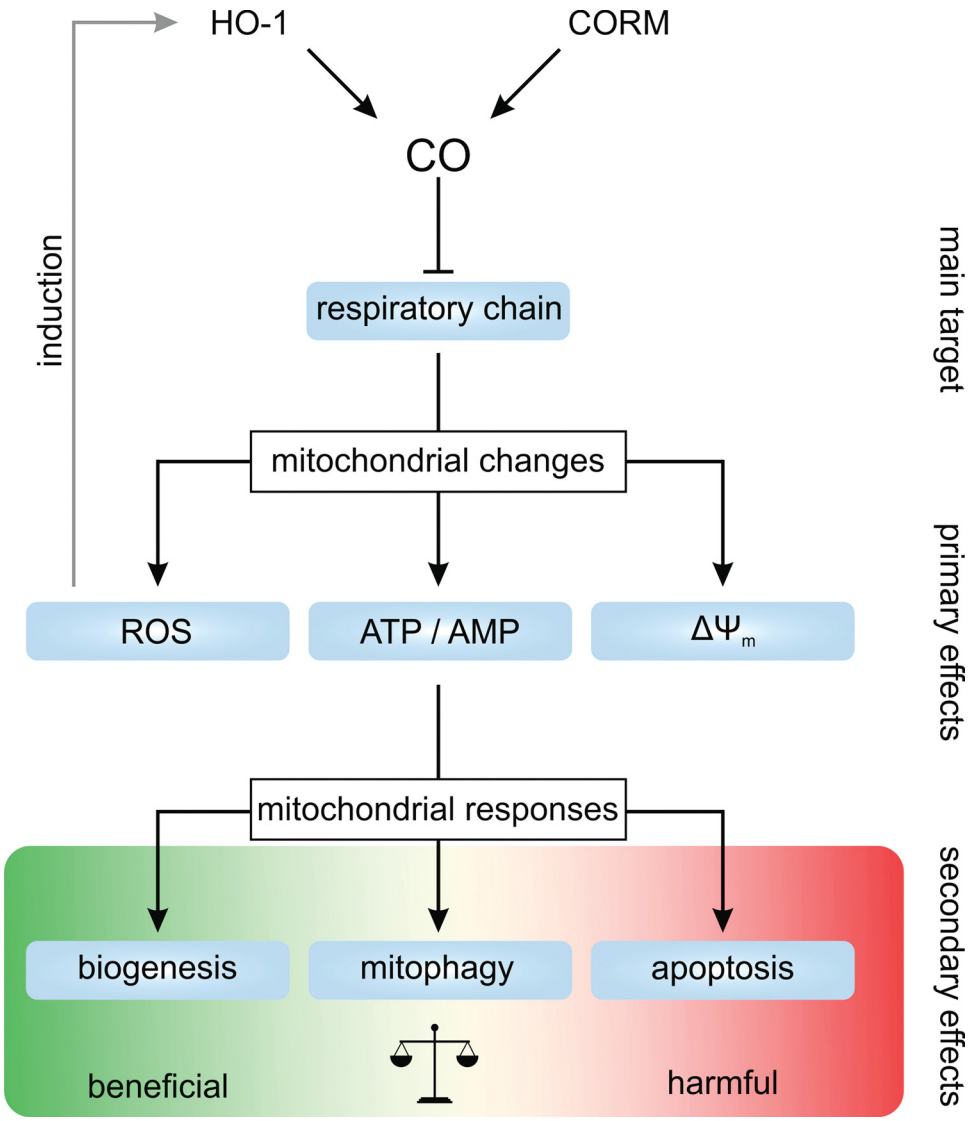

Fig. 4. Role of carbon monoxide on mitochondrial homeostasis.

equivalents (NADPH) required for antioxidant defense and thus provides an additional mechanism for the antioxidant properties of the HO-1/CO system.

Exposure to low amounts of CO leads to moderate mitochondrial uncoupling that is assigned to the activation of different channels such as phosphate carrier (P_iC), adenine nucleotide translocase (ANT) or large-conductance Ca^{2+}-activated K^+ channels (BK_{Ca}) by CO (Lo Iacono et al., 2011, Long et al., 2014, Kaczara et al., 2015). The exact mechanism is not understood, particularly since none of the mentioned channels contains a heme moiety, which is usually needed for a direct CO effect on protein function. Nevertheless, uncoupling of the mitochondrial respiration from ATP production was accompanied by a decrease of mitochondrial membrane potential (Lo Iacono et al., 2011, Long et al., 2014, Kaczara et al., 2016), which in turn is a major regulator of mitochondrial quality control mechanisms and a known inducer of mitochondria selective autophagy: mitophagy (Lemasters, 2014). During mitophagy, defective mitochondria are separated from the mitochondrial network via fission processes. The separated mitochondrion then accumulates the PTEN-induced kinase 1 (Pink1) on its outer membrane, which recruits the E3 ligase Parkin from the cytosol. Parkin then ubiquitinates proteins of the outer mitochondrial membrane, thereby marking the mitochondrion for autophagosomal degradation (Youle and van der Bliek, 2012, Zimmermann and Reichert, 2017). Pink1 and Parkin levels are increased in different cell lines in response to CORM-2 treatment (Kim et al., 2018, Chen et al., 2019) and Pink1 levels are also elevated upon HO-1 overexpression in mice hearts (Hull et al., 2016), indicating induction of CO-mediated mitophagy. These effects are supported by further downstream events observed after CORM treatment. For example, CORM-3 administration led to a conversion of LC3-I to LC3-II in mice (Lancel et al., 2012), an observation which was also made for different CORM-2 treated cell types and was accompanied by increased numbers of autolysosomes per cell (Kim et al., 2018). These findings suggest an increased autophagosomal activity mediated by CO. They are in line with the cumulative observations that heme oxygenases are responsible for mediating the cellular pro-survival mechanisms mitophagy/autophagy upon exposure to exogenous stressors. For example, lipid polysaccharide (LPS)-induced autophagy in macrophages was abrogated upon pharmacological inhibition or genetical knock down of heme oxygenases. Upon heme oxygenase overexpression, however, the autophagic flux was increased (Waltz et al., 2011). A similar observation was made in mice which were subjected to an experimental sepsis or LPS treatment. Induced autophagy was abrogated upon inhibition or knock down of HO-1. Instead, increased levels of cell death were found (Carchman et al., 2011). Furthermore, conditional HO-1 knock out in mice hearts prevented the induction of mitophagy by hyperoxia, resulting in a severe cardiac

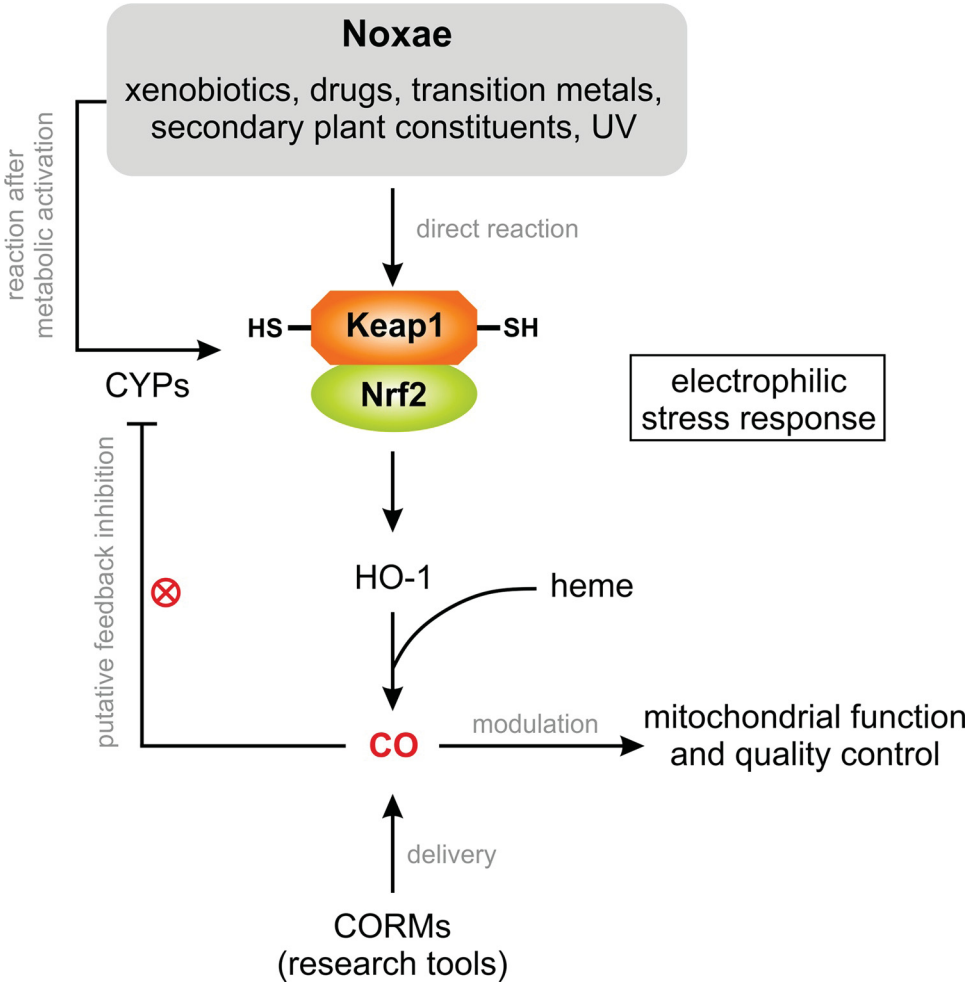

Fig. 5. Proposed model of the integration of CO as signaling molecule in cellular stress response.

fibrosis that was not found in equally treated wildtype animals (Suliman et al., 2017). Mitochondrial quality control mechanisms are not only regulated via CO/HO-1, but are vice versa also suggested to be involved in the regulation of HO-1 induction. In murine embryonic fibroblasts, it was shown that HO-1 induction at least in part depends on the presence of the mitochondrial fission factor dynamin-related protein 1 (DRP1) (Stucki et al., 2018). DRP1 in turn is required for the separation of single mitochondria from the mitochondrial network and thus needed for processes such as mitophagy, but also apoptosis (Ishihara et al., 2009, Tong et al., 2020).

The selective removal of damaged mitochondria for cell protection is a balancing act. Excessive mitophagy or autophagy might be harmful to cells, possibly leading to autophagic cell death (Bialik et al., 2018). Closely associated with these processes is the induction of the mitochondria-mediated intrinsic pathway of apoptosis. It was recently discovered that besides the numerous anti-apoptotic properties described, HO-1 also exerts pro-apoptotic effects. HO-1 dependent cleavage of pro-caspase-3 and poly (ADP-ribose) polymerase was observed in human colorectal carcinoma cells. This effect was only reconstituted by the usage of comparably high doses of CORM-3 (200 – 800 μM), but neither with $FeSO_4$ nor biliverdin, indicating a CO-derived apoptosis induction by HO-1 (Wu et al., 2019). Furthermore, apoptotic cell death triggered by demethoxycurcumin, an inducer of HO-1 expression, was prevented upon gene silencing of *HMOX1* (Chien et al., 2020). Taken together, these findings suggest that low amounts of CO promote cell survival via mitophagy/autophagy, while high amounts of the compound trigger apoptosis. It can therefore be speculated that CO signaling as part of cellular stress response is involved in regulating the balance between these processes.

Mitochondria are essential organelles and need to be resynthesized via mitochondrial biogenesis, counteracting their removal via mitophagy. As discussed above, increasing levels of mitochondrial biogenesis markers were already found in studies using CO gas as a treatment tool. Corresponding to this, elevated protein levels of PGC-1α were found in mice overexpressing HO-1 (Hull et al., 2016). By means of CORMs, these findings were reproduced and refined. Kim et al. showed, that CORM-2 treatment led to increased PGC-1α, NRF1 and TFAM mRNA in different cell types (HepG2, HeLa and hepatocytes). This was accompanied by elevated levels of mtDNA as well as components of the ETC. The activation of transcription factor EB was suggested as the underlying molecular mechanism (Kim et al., 2018). Using CORM-2 it was also discovered that induction of mitochondrial biogenesis is higher when a recovery period is included in the treatment protocol compared to the stand-alone treatment. This resulted not only in increased mitochondrial mass, but also elevated ATP levels (Choi et al., 2016), indicating a transient activity of CO signaling – a typical property of signaling molecules. However, CO might not only increase cellular ATP levels via mitochondrial biogenesis. In mice treated with CORM-401 the ATP-linked respiration was decreased, while lactate and total ATP levels were increased, suggesting a metabolic switch from oxidative phosphorylation system towards glycolysis (Braud et al., 2018). The data highlight the dynamic nature of cellular responses towards intracellular CO exposure, ultimately leading to cytoprotective adaptations. The role of CO on mitochondrial homeostasis is summarized in Fig. 4.

4.2. Non-mitochondrial CO targets

ROS and electrophilic compounds of natural origin are not the only sources of electrophilic stress that cells have to encounter. Oxidation of xenobiotics by CYPs is a known mechanism of electrophile formation and therefore toxification of the parent compounds. CYP activity mechanistically depends on the presence of a prosthetic heme group which is required for oxygen binding and subsequent incorporation into the substrate. This heme group can also be addressed by CO leading to an inactivation of the enzyme. Such an observation was not only made using high amounts of CO gas as a control in CYP activity studies (Parise et al., 2015), but also at comparatively low CO amounts delivered by CORM-401 in cell culture experiments (Walter et al., 2019). This scenario represents a putative additional mechanism for the detoxification of electrophiles. If a xenobiotic is oxidized to an electrophile (e.g. an epoxide) by CYPs, this metabolite could induce phase II xenobiotic metabolizing enzymes (GST, UGT) for its own detoxification via the Nrf2/Keap1 pathway. At the same time, activation of Nrf2/Keap1 would trigger endogenous CO production by HO-1 induction. CO could then inhibit CYP activity and prevent formation of more electrophilic compounds.

5. Conclusion

Research on signaling properties of CO is a developing field and numerous postulated mechanisms of action remain to be revealed. However, present knowledge suggests an implication of CO signaling in the regulation of cellular stress response and related energy metabolism. The latter depends in particular on the activity of the respiratory chain and in general mitochondrial quality control, both addressed by CO for regulation. With the Nrf2/Keap1 system involved in CO production via HO-1, thiol-dependent signaling is linked to the heme protein specific CO signaling thus likely contributing to the integration of endogenous defense against exogenous stressors. A proposed model of the role of CO in cellular stress response upon electrophilic insult is provided in Fig. 5.

Funding

Our research was funded in parts by the Deutsche Forschungsgemeinschaft (DFG, German Research Foundation) project STA699/3-1 (WS).

Declaration of Competing Interest

The authors report no declarations of interest.

References

Anderson, S.N., Richards, J.M., Esquer, H.J., Benninghoff, A.D., Arif, A.M., Berreau, L.M., 2015. A Structurally-Tunable 3-Hydroxyflavone Motif for Visible Light-Induced Carbon Monoxide-Releasing Molecules (CORMs). ChemistryOpen 4, 590–594.
Applegate, L.A., Noël, A., Vile, G., Frenk, E., Tyrrell, R.M., 1995. Two genes contribute to different extents to the heme oxygenase enzyme activity measured in cultured human skin fibroblasts and keratinocytes: implications for protection against oxidant stress. Photochem Photobiol 61, 285–291.
Atkin, A.J., Lynam, J.M., Moulton, B.E., Sawle, P., Motterlini, R., Boyle, N.M., Pryce, M.T., Fairlamb, I.J., 2011. Modification of the deoxy-myoglobin/carbonmonoxy-myoglobin UV-vis assay for reliable determination of CO-release rates from organometallic carbonyl complexes. Dalton Trans 40, 5755–5761.
Baird, L., Yamamoto, M., 2020. The Molecular Mechanisms Regulating the KEAP1-NRF2 Pathway. Mol Cell Biol 40.
Bansal, S., Biswas, G., Avadhani, N.G., 2014. Mitochondria-targeted heme oxygenase-1 induces oxidative stress and mitochondrial dysfunction in macrophages, kidney fibroblasts and in chronic alcohol hepatotoxicity. Redox Biol 2, 273–283.
Beavers, W.N., Rose, K.L., Galligan, J.J., Mitchener, M.M., Rouzer, C.A., Tallman, K.A., Lamberson, C.R., Wang, X., Hill, S., Ivanova, P.T., Brown, H.A., Zhang, B., Porter, N.A., Marnett, L.J., 2017. Protein Modification by Endogenously Generated Lipid Electrophiles: Mitochondria as the Source and Target. ACS Chem Biol 12, 2062–2069.
Becker, T.M., Juvik, J.A., 2016. The Role of Glucosinolate Hydrolysis Products from Brassica Vegetable Consumption in Inducing Antioxidant Activity and Reducing Cancer Incidence. Diseases 4.
Bialik, S., Dasari, S.K., Kimchi, A., 2018. Autophagy-dependent cell death - where, how and why a cell eats itself to death. J Cell Sci 131.
Bilban, M., Bach, F.H., Otterbein, S.L., Ifedigbo, E., D'avila, J.C., Esterbauer, H., Chin, B.Y., Usheva, A., Robson, S.C., Wagner, O., Otterbein, L.E., 2006. Carbon monoxide orchestrates a protective response through PPARgamma. Immunity 24, 601–610.
Braud, L., Pini, M., Muchova, L., Manin, S., Kitagishi, H., Sawaki, D., Czibik, G., Ternacle, J., Derumeaux, G., Foresti, R., Motterlini, R., 2018. Carbon monoxide-induced metabolic switch in adipocytes improves insulin resistance in obese mice. JCI Insight 3.
Carchman, E.H., Rao, J., Loughran, P.A., Rosengart, M.R., Zuckerbraun, B.S., 2011. Heme oxygenase-1-mediated autophagy protects against hepatocyte cell death and hepatic injury from infection/sepsis in mice. Hepatology 53, 2053–2062.
Chen, Y., Park, H.J., Park, J., Song, H.C., Ryter, S.W., Surh, Y.J., Kim, U.H., Joe, Y., Chung, H.T., 2019. Carbon monoxide ameliorates acetaminophen-induced liver injury by increasing hepatic HO-1 and Parkin expression. FASEB J 33, 13905–13919.
Chien, M.H., Yang, W.E., Yang, Y.C., Ku, C.C., Lee, W.J., Tsai, M.Y., Lin, C.W., Yang, S.F., 2020. Dual Targeting of the p38 MAPK-HO-1 Axis and cIAP1/XIAP by Demethoxycurcumin Triggers Caspase-Mediated Apoptotic Cell Death in Oral Squamous Cell Carcinoma Cells. Cancers (Basel) 12 (3), 703.
Choi, Y.K., Park, J.H., Baek, Y.Y., Won, M.H., Jeoung, D., Lee, H., Ha, K.S., Kwon, Y.G., Kim, Y.M., 2016. Carbon monoxide stimulates astrocytic mitochondrial biogenesis via L-type Ca(2+) channel-mediated PGC-1alpha/ERRalpha activation. Biochem Biophys Res Commun 479, 297–304.
Clark, J.E., Naughton, P., Shurey, S., Green, C.J., Johnson, T.R., Mann, B.E., Foresti, R., Motterlini, R., 2003. Cardioprotective actions by a water-soluble carbon monoxide-releasing molecule. Circ Res 93, e2–8.
Coburn, R.F., Blakemore, W.S., Forster, R.E., 1963. Endogenous carbon monoxide production in man. J Clin Invest 42, 1172–1178.
Converso, D.P., Taille, C., Carreras, M.C., Jaitovich, A., Poderoso, J.J., Boczkowski, J., 2006. HO-1 is located in liver mitochondria and modulates mitochondrial heme content and metabolism. FASEB J 20, 1236–1238.
Crook, S.H., Mann, B.E., Meijer, A.J., Adams, H., Sawle, P., Scapens, D., Motterlini, R., 2011. [Mn(CO)4{S2CNMe(CH2CO2H)}], a new water-soluble CO-releasing molecule. Dalton Trans 40, 4230–4235.
Dennery, P.A., 2014. Signaling function of heme oxygenase proteins. Antioxid Redox Signal 20, 1743–1753.
Diers, A.R., Higdon, A.N., Ricart, K.C., Johnson, M.S., Agarwal, A., Kalyanaraman, B., Landar, A., Darley-Usmar, V.M., 2010. Mitochondrial targeting of the electrophilic lipid 15-deoxy-Delta12,14-prostaglandin J2 increases apoptotic efficacy via redox cell signalling mechanisms. Biochem J 426, 31–41.
Dinkova-Kostova, A.T., Liby, K.T., Stephenson, K.K., Holtzclaw, W.D., Gao, X., Suh, N., Williams, C., Risingsong, R., Honda, T., Gribble, G.W., Sporn, M.B., Talalay, P., 2005. Extremely potent triterpenoid inducers of the phase 2 response: correlations of protection against oxidant and inflammatory stress. Proc Natl Acad Sci U S A 102, 4584–4589.
Dinkova-Kostova, A.T., Massiah, M.A., Bozak, R.E., Hicks, R.J., Talalay, P., 2001. Potency of Michael reaction acceptors as inducers of enzymes that protect against carcinogenesis depends on their reactivity with sulfhydryl groups. Proc Natl Acad Sci U S A 98, 3404–3409.
Estrella, B., Sempértegui, F., Franco, O.H., Cepeda, M., Naumova, E.N., 2019. Air pollution control and the occurrence of acute respiratory illness in school children of Quito, Ecuador. J Public Health Policy 40, 17–34.
Fang, R., Aust, A.E., 1997. Induction of ferritin synthesis in human lung epithelial cells treated with crocidolite asbestos. Arch Biochem Biophys 340, 369–375.
Feng, W., Feng, S., Feng, G., 2019. CO release with ratiometric fluorescence changes: a promising visible-light-triggered metal-free CO-releasing molecule. Chem Commun (Camb) 55, 8987–8990.
Galal, A.M., Walker, L.A., Khan, I.A., 2015. Induction of GST and related events by dietary phytochemicals: sources, chemistry, and possible contribution to chemoprevention. Curr Top Med Chem 14, 2802–2821.
García-Cardeña, G., Oh, P., Liu, J., Schnitzer, J.E., Sessa, W.C., 1996. Targeting of nitric oxide synthase to endothelial cell caveolae via palmitoylation: implications for nitric oxide signaling. Proc Natl Acad Sci U S A 93, 6448–6453.
Golob, N., Grenc, D., Brvar, M., 2018. Carbon monoxide poisoning in wood pellet storerooms. Occup Med (Lond) 68, 143–145.
Gozzelino, R., Soares, M.P., 2014. Coupling heme and iron metabolism via ferritin H chain. Antioxid Redox Signal 20, 1754–1769.
Hirota, A., Kawachi, Y., Itoh, K., Nakamura, Y., Xu, X., Banno, T., Takahashi, T., Yamamoto, M., Otsuka, F., 2005. Ultraviolet A irradiation induces NF-E2-related factor 2 activation in dermal fibroblasts: protective role in UVA-induced apoptosis. J Invest Dermatol 124, 825–832.
Hull, T.D., Boddu, R., Guo, L., Tisher, C.C., Traylor, A.M., Patel, B., Joseph, R., Prabhu, S.D., Suliman, H.B., Piantadosi, C.A., Agarwal, A., George, J.F., 2016. Heme oxygenase-1 regulates mitochondrial quality control in the heart. JCI Insight 1, e85817.
Ishigami, I., Zatsepin, N.A., Hikita, M., Conrad, C.E., Nelson, G., Coe, J.D., Basu, S., Grant, T.D., Seaberg, M.H., Sierra, R.G., Hunter, M.S., Fromme, P., Fromme, R., Yeh, S.R., Rousseau, D.L., 2017. Crystal structure of CO-bound cytochrome c oxidase determined by serial femtosecond X-ray crystallography at room temperature. Proc Natl Acad Sci U S A 114, 8011–8016.
Ishihara, N., Nomura, M., Jofuku, A., Kato, H., Suzuki, S.O., Masuda, K., Otera, H., Nakanishi, Y., Nonaka, I., Goto, Y., Taguchi, N., Morinaga, H., Maeda, M., Takayanagi, R., Yokota, S., Mihara, K., 2009. Mitochondrial fission factor Drp1 is essential for embryonic development and synapse formation in mice. Nat Cell Biol 11, 958–966.
Iwakiri, Y., Satoh, A., Chatterjee, S., Toomre, D.K., Chalouni, C.M., Fulton, D.,

Groszmann, R.J., Shah, V.H., Sessa, W.C., 2006. Nitric oxide synthase generates nitric oxide locally to regulate compartmentalized protein S-nitrosylation and protein trafficking. Proc Natl Acad Sci U S A 103, 19777–19782.
Jansen, T., Daiber, A., 2012. Direct Antioxidant Properties of Bilirubin and Biliverdin. Is there a Role for Biliverdin Reductase? Front Pharmacol 3, 30.
Jia, L., Wang, Y., Wang, Y., Ma, Y., Shen, J., Fu, Z., Wu, Y., Su, S., Zhang, Y., Cai, Z., Wang, J., Xiang, M., 2018. Heme Oxygenase-1 in Macrophages Drives Septic Cardiac Dysfunction via Suppressing Lysosomal Degradation of Inducible Nitric Oxide Synthase. Circ Res 122, 1532–1544.
Jones, A.W., Durante, W., Korthuis, R.J., 2010. Heme oxygenase-1 deficiency leads to alteration of soluble guanylate cyclase redox regulation. J Pharmacol Exp Ther 335, 85–91.
Jones, D.P., Sies, H., 2015. The Redox Code. Antioxid Redox Signal 23, 734–746.
Kaczara, P., Motterlini, R., Kus, K., Zakrzewska, A., Abramov, A.Y., Chlopicki, S., 2016. Carbon monoxide shifts energetic metabolism from glycolysis to oxidative phosphorylation in endothelial cells. FEBS Lett 590, 3469–3480.
Kaczara, P., Motterlini, R., Rosen, G.M., Augustynek, B., Bednarczyk, P., Szewczyk, A., Foresti, R., Chlopicki, S., 2015. Carbon monoxide released by CORM-401 uncouples mitochondrial respiration and inhibits glycolysis in endothelial cells: A role for mitoBKCa channels. Biochim Biophys Acta 1847, 1297–1309.
Kaczara, P., Proniewski, B., Lovejoy, C., Kus, K., Motterlini, R., Abramov, A.Y., Chlopicki, S., 2018. CORM-401 induces calcium signalling, NO increase and activation of pentose phosphate pathway in endothelial cells. FEBS J 285, 1346–1358.
Kim, H.J., Joe, Y., Rah, S.Y., Kim, S.K., Park, S.U., Park, J., Kim, J., Ryu, J., Cho, G.J., Surh, Y.J., Ryter, S.W., Kim, U.H., Chung, H.T., 2018. Carbon monoxide-induced TFEB nuclear translocation enhances mitophagy/mitochondrial biogenesis in hepatocytes and ameliorates inflammatory liver injury. Cell Death Dis 9, 1060.
Kim, H.P., Wang, X., Galbiati, F., Ryter, S.W., Choi, A.M., 2004. Caveolae compartmentalization of heme oxygenase-1 in endothelial cells. Faseb j 18, 1080–1089.
Kinoshita, H., Türkan, H., Vucinic, S., Naqvi, S., Bedair, R., Rezaee, R., Tsatsakis, A., 2020. Carbon monoxide poisoning. Toxicol Rep 7, 169–173.
Koenitzer, J.R., Freeman, B.A., 2010. Redox signaling in inflammation: interactions of endogenous electrophiles and mitochondria in cardiovascular disease. Ann N Y Acad Sci 1203, 45–52.
Kubic, V.L., Anders, M.W., 1978. Metabolism of dihalomethanes to carbon monoxide–III. Studies on the mechanism of the reaction. Biochem Pharmacol 27, 2349–2355.
Lancel, S., Montaigne, D., Marechal, X., Marciniak, C., Hassoun, S.M., Decoster, B., Ballot, C., Blazejewski, C., Corseaux, D., Lescure, B., Motterlini, R., Neviere, R., 2012. Carbon monoxide improves cardiac function and mitochondrial population quality in a mouse model of metabolic syndrome. PLoS One 7, e41836.
Lemasters, J.J., 2014. Variants of mitochondrial autophagy: Types 1 and 2 mitophagy and micromitophagy (Type 3). Redox Biol 2, 749–754.
Levitt, D.G., Levitt, M.D., 2015. Carbon monoxide: a critical quantitative analysis and review of the extent and limitations of its second messenger function. Clin Pharmacol 7, 37–56.
Lin, Q., Weis, S., Yang, G., Weng, Y.H., Helston, R., Rish, K., Smith, A., Bordner, J., Polte, T., Gaunitz, F., Dennery, P.A., 2007. Heme oxygenase-1 protein localizes to the nucleus and activates transcription factors important in oxidative stress. J Biol Chem 282, 20621–20633.
Lo Iacono, L., Boczkowski, J., Zini, R., Salouage, I., Berdeaux, A., Motterlini, R., Morin, D., 2011. A carbon monoxide-releasing molecule (CORM-3) uncouples mitochondrial respiration and modulates the production of reactive oxygen species. Free Radic Biol Med 50, 1556–1564.
Long, R., Salouage, I., Berdeaux, A., Motterlini, R., Morin, D., 2014. CORM-3, a water soluble CO-releasing molecule, uncouples mitochondrial respiration via interaction with the phosphate carrier. Biochim Biophys Acta 1837, 201–209.
Madea, D., Martínek, M., Muchová, L., Váňa, J., Vítek, L., Klán, P., 2020. Structural Modifications of Nile Red Carbon Monoxide Fluorescent Probe: Sensing Mechanism and Applications. J Org Chem 85, 3473–3489.
Mancuso, C., Perluigi, M., Cini, C., De Marco, C., Giuffrida Stella, A.M., Calabrese, V., 2006. Heme oxygenase and cyclooxygenase in the central nervous system: a functional interplay. J Neurosci Res 84, 1385–1391.
Markey, M.A., Zumwalt, R.E., 2001. Fatal carbon monoxide poisoning after the detonation of explosives in an underground mine: a case report. Am J Forensic Med Pathol 22, 387–390.
Medina, M.V., Sapochnik, D., Garcia Solá, M., Coso, O., 2020. Regulation of the Expression of Heme Oxygenase-1: Signal Transduction, Gene Promoter Activation, and Beyond. Antioxid Redox Signal 32, 1033–1044.
Michel, B.W., Lippert, A.R., Chang, C.J., 2012. A reaction-based fluorescent probe for selective imaging of carbon monoxide in living cells using a palladium-mediated carbonylation. J Am Chem Soc 134, 15668–15671.
Moscato, U., Poscia, A., Gargaruti, R., Capelli, G., Cavaliere, F., 2014. Normal values of exhaled carbon monoxide in healthy subjects: comparison between two methods of assessment. BMC Pulm Med 14, 204.
Motterlini, R., Clark, J.E., Foresti, R., Sarathchandra, P., Mann, B.E., Green, C.J., 2002. Carbon monoxide-releasing molecules: characterization of biochemical and vascular activities. Circ Res 90, E17–24.
Motterlini, R., Foresti, R., 2017. Biological signaling by carbon monoxide and carbon monoxide-releasing molecules. Am J Physiol Cell Physiol 312, C302–c313.
Nagel, C., Mclean, S., Poole, R.K., Braunschweig, H., Kramer, T., Schatzschneider, U., 2014. Introducing [Mn(CO)3(tpa-κ(3)N)](+) as a novel photoactivatable CO-releasing molecule with well-defined iCORM intermediates - synthesis, spectroscopy, and antibacterial activity. Dalton Trans 43, 9986–9997.
Nguyen, V., Salama, M., Fernandez, D., Sperling, J.D., Regina, A., Rivera, R., Wang, J., Friedman, B.W., Smith, S.W., 2020. Comparison between carbon monoxide poisoning from hookah smoking versus other sources. Clin Toxicol (Phila) 1–6 In press.
Nielsen, V.G., 2019. The anticoagulant effect of Apis mellifera phospholipase A2 is inhibited by CORM-2 via a carbon monoxide-independent mechanism. J Thromb Thrombolysis 49 (1), 100–107.
Otsuki, A., Yamamoto, M., 2020. Cis-element architecture of Nrf2-sMaf heterodimer binding sites and its relation to diseases. Arch Pharm Res 43, 275–285.
Palao, E., Slanina, T., Muchova, L., Solomek, T., Vitek, L., Klan, P., 2016. Transition-Metal-Free CO-Releasing BODIPY Derivatives Activatable by Visible to NIR Light as Promising Bioactive Molecules. J Am Chem Soc 138, 126–133.
Pan, Z., Chittavong, V., Li, W., Zhang, J., Ji, K., Zhu, M., Ji, X., Wang, B., 2017. Organic CO Prodrugs: Structure-CO-Release Rate Relationship Studies. Chemistry 23, 9838–9845.
Pankow, D., Jagielki, S., 1993. Effect of methanol or modifications of the hepatic glutathione concentration on the metabolism of dichloromethane to carbon monoxide in rats. Hum Exp Toxicol 12, 227–231.
Parise, R.A., Eiseman, J.L., Clausen, D.M., Kicielinski, K.P., Hershberger, P.A., Egorin, M.J., Beumer, J.H., 2015. Characterization of the metabolism of benzaldehyde dimethane sulfonate (NSC 281612, DMS612). Cancer Chemother Pharmacol 76, 537–546.
Pecorella, S.R., Potter, J.V., Cherry, A.D., Peacher, D.F., Welty-Wolf, K.E., Moon, R.E., Piantadosi, C.A., Suliman, H.B., 2015. The HO-1/CO system regulates mitochondrial-capillary density relationships in human skeletal muscle. Am J Physiol Lung Cell Mol Physiol 309, L857–71.
Rhodes, M.A., Carraway, M.S., Piantadosi, C.A., Reynolds, C.M., Cherry, A.D., Wester, T.E., Natoli, M.J., Massey, E.W., Moon, R.E., Suliman, H.B., 2009. Carbon monoxide, skeletal muscle oxidative stress, and mitochondrial biogenesis in humans. Am J Physiol Heart Circ Physiol 297, H392–9.
Romanski, S., Kraus, B., Schatzschneider, U., Neudörfl, J.M., Amslinger, S., Schmalz, H.G., 2011. Acyloxybutadiene iron tricarbonyl complexes as enzyme-triggered CO-releasing molecules (ET-CORMs). Angew Chem Int Ed Engl 50, 2392–2396.
Rose, J.J., Wang, L., Xu, Q., Mctiernan, C.F., Shiva, S., Tejero, J., Gladwin, M.T., 2017. Carbon Monoxide Poisoning: Pathogenesis, Management, and Future Directions of Therapy. Am J Respir Crit Care Med 195, 596–606.
Ryter, S.W., Choi, A.M., 2013. Carbon monoxide in exhaled breath testing and therapeutics. J Breath Res 7, 017111.
Saito, R., Suzuki, T., Hiramoto, K., Asami, S., Naganuma, E., Suda, H., Iso, T., Yamamoto, H., Morita, M., Baird, L., Furusawa, Y., Negishi, T., Ichinose, M., Yamamoto, M., 2016. Characterizations of Three Major Cysteine Sensors of Keap1 in Stress Response. Mol Cell Biol 36, 271–284.
Sakla, R., Singh, A., Kaushik, R., Kumar, P., Jose, D.A., 2019. Allosteric Regulation in Carbon Monoxide (CO) Release: Anion Responsive CO-Releasing Molecule (CORM) Derived from (Terpyridine)phenol Manganese Tricarbonyl Complex with Colorimetric and Fluorescence Monitoring. Inorg Chem 58, 10761–10768.
Schatzschneider, U., 2015. Novel lead structures and activation mechanisms for CO-releasing molecules (CORMs). Br J Pharmacol 172, 1638–1650.
Sedlak, T.W., Snyder, S.H., 2004. Bilirubin benefits: cellular protection by a biliverdin reductase antioxidant cycle. Pediatrics 113, 1776–1782.
Seixas, J.D., Mukhopadhyay, A., Santos-Silva, T., Otterbein, L.E., Gallo, D.J., Rodrigues, S.S., Guerreiro, B.H., Gonçalves, A.M., Penacho, N., Marques, A.R., Coelho, A.C., Reis, P.M., Romão, M.J., Romão, C.C., 2013. Characterization of a versatile organometallic pro-drug (CORM) for experimental CO based therapeutics. Dalton Trans 42, 5985–5998.
Sies, H., Berndt, C., Jones, D.P., 2017. Oxidative Stress. Annu Rev Biochem 86, 715–748.
Slebos, D.J., Ryter, S.W., Van Der Toorn, M., Liu, F., Guo, F., Baty, C.J., Karlsson, J.M., Watkins, S.C., Kim, H.P., Wang, X., Lee, J.S., Postma, D.S., Kauffman, H.F., Choi, A.M., 2007. Mitochondrial localization and function of heme oxygenase-1 in cigarette smoke-induced cell death. Am J Respir Cell Mol Biol 36, 409–417.
Soboleva, T., Esquer, H.J., Anderson, S.N., Berreau, L.M., Benninghoff, A.D., 2018. Mitochondrial-Localized Versus Cytosolic Intracellular CO-Releasing Organic PhotoCORMs: Evaluation of CO Effects Using Bioenergetics. ACS Chem Biol 13 (8), 2220–2228.
Southam, H.M., Smith, T.W., Lyon, R.L., Liao, C., Trevitt, C.R., Middlemiss, L.A., Cox, F.L., Chapman, J.A., El-Khamisy, S.F., Hippler, M., Williamson, M.P., Henderson, P.J.F., Poole, R.K., 2018. A thiol-reactive Ru(II) ion, not CO release, underlies the potent antimicrobial and cytotoxic properties of CO-releasing molecule-3. Redox Biol 18, 114–123.
Stucki, D., Brenneisen, P., Reichert, A.S., Stahl, W., 2018. The BH3 mimetic compound BH3I-1 impairs mitochondrial dynamics and promotes stress response in addition to its pro-apoptotic key function. Toxicol Lett 295, 369–378.
Stucki, D., Krahl, H., Walter, M., Steinhausen, J., Hommel, K., Brenneisen, P., Stahl, W., 2020a. Effects of frequently applied carbon monoxide releasing molecules (CORMs) in typical CO-sensitive model systems - A comparative in vitro study. Arch Biochem Biophys 687, 108383.
Stucki, D., Steinhausen, J., Westhoff, P., Krahl, H., Brilhaus, D., Massenberg, A., Weber, A.P.M., Reichert, A.S., Brenneisen, P., Stahl, W., 2020b. Endogenous Carbon Monoxide Signaling Modulates Mitochondrial Function and Intracellular Glucose Utilization: Impact of the Heme Oxygenase Substrate Hemin. Antioxidants (Basel) 9 (8).
Suliman, H.B., Carraway, M.S., Tatro, L.G., Piantadosi, C.A., 2007. A new activating role for CO in cardiac mitochondrial biogenesis. J Cell Sci 120, 299–308.
Suliman, H.B., Keenan, J.E., Piantadosi, C.A., 2017. Mitochondrial quality-control dysregulation in conditional HO-1-/- mice. JCI Insight 2, e89676.
Tadevosyan, A., Mikulski, M.A., Baber Wallis, A., Rubenstein, L., Abrahamyan, S., Arestakesyan, L., Hovsepyan, M., Reynolds, S.J., Fuortes, L.J., 2020. Open fire ovens and effects of in-home lavash bread baking on carbon monoxide exposure and carboxyhemoglobin levels among women in rural Armenia. Indoor Air 30, 361–369.
Tong, M., Zablocki, D., Sadoshima, J., 2020. The role of Drp1 in mitophagy and cell death

in the heart. J Mol Cell Cardiol 142, 138–145.
Veronesi, A., Pecoraro, V., Zauli, S., Ottone, M., Leonardi, G., Lauriola, P., Trenti, T., 2017. Use of carboxyhemoglobin as a biomarker of environmental CO exposure: critical evaluation of the literature. Environ Sci Pollut Res Int 24, 25798–25809.
Wagner, M., Erecinska, M., 1971. Experimental and theoretical studies of the electron transport chain. I. The effect of respiratory chain inhibitors on the carbon monoxide blocked respiratory chain. Arch Biochem Biophys 147, 666–674.
Walter, M., Stahl, W., Brenneisen, P., Reichert, A.S., Stucki, D., 2019. Carbon monoxide releasing molecule 401 (CORM-401) modulates phase I metabolism of xenobiotics. Toxicol In Vitro 59, 215–220.
Waltz, P., Carchman, E.H., Young, A.C., Rao, J., Rosengart, M.R., Kaczorowski, D., Zuckerbraun, B.S., 2011. Lipopolysaccaride induces autophagic signaling in macrophages via a TLR4, heme oxygenase-1 dependent pathway. Autophagy 7, 315–320.
Wang, G., Hamid, T., Keith, R.J., Zhou, G., Partridge, C.R., Xiang, X., Kingery, J.R., Lewis, R.K., Li, Q., Rokosh, D.G., Ford, R., Spinale, F.G., Riggs, D.W., Srivastava, S., Bhatnagar, A., Bolli, R., Prabhu, S.D., 2010. Cardioprotective and antiapoptotic effects of heme oxygenase-1 in the failing heart. Circulation 121, 1912–1925.
Wang, J., Karpus, J., Zhao, B.S., Luo, Z., Chen, P.R., He, C., 2012. A selective fluorescent probe for carbon monoxide imaging in living cells. Angew Chem Int Ed Engl 51, 9652–9656.
Wohlrab, H., Ogunmola, G.B., 1971. Carbon monoxide binding studies of cytochrome a3 hemes in intact rat liver mitochondria. Biochemistry 10, 1103–1106.
Wong, H.L., Liebler, D.C., 2008. Mitochondrial protein targets of thiol-reactive electrophiles. Chem Res Toxicol 21, 796–804.
Wu, M.S., Chien, C.C., Chang, J., Chen, Y.C., 2019. Pro-apoptotic effect of haem oxygenase-1 in human colorectal carcinoma cells via endoplasmic reticular stress. J Cell Mol Med 23, 5692–5704.
Yoshida, T., Sato, M., 1989. Posttranslational and direct integration of heme oxygenase into microsomes. Biochem Biophys Res Commun 163, 1086–1092.
Youle, R.J., Van Der Bliek, A.M., 2012. Mitochondrial fission, fusion, and stress. Science 337, 1062–1065.
Zhang, L., Zhang, J., Ye, Z., Manevich, Y., Ball, L.E., Bethard, J.R., Jiang, Y.L., Broome, A.M., Dalton, A.C., Wang, G.Y., Townsend, D.M., Tew, K.D., 2019. Isoflavone ME-344 Disrupts Redox Homeostasis and Mitochondrial Function by Targeting Heme Oxygenase 1. Cancer Res 79, 4072–4085.
Zhang, Y., Talalay, P., Cho, C.G., Posner, G.H., 1992. A major inducer of anticarcinogenic protective enzymes from broccoli: isolation and elucidation of structure. Proc Natl Acad Sci U S A 89, 2399–2403.
Zhou, E., Gong, S., Hong, J., Feng, G., 2020. Development of a new ratiometric probe with near-infrared fluorescence and a large Stokes shift for detection of gasotransmitter CO in living cells. Spectrochim Acta A Mol Biomol Spectrosc 227, 117657.
Zimmermann, M., Reichert, A.S., 2017. How to get rid of mitochondria: crosstalk and regulation of multiple mitophagy pathways. Biol Chem 399, 29–45.
Zuckerbraun, B.S., Chin, B.Y., Bilban, M., D'avila, J.C., Rao, J., Billiar, T.R., Otterbein, L.E., 2007. Carbon monoxide signals via inhibition of cytochrome c oxidase and generation of mitochondrial reactive oxygen species. Faseb J 21, 1099–1106.

1.4 Objectives

In the present thesis the following questions were experimentally addressed:

1. Which biochemical test systems are suitable to study direct CO effects on heme protein activity?
2. Which CO releasing molecule (CORM) is most suitable to study CO-specific effects in CO-sensitive model systems?
3. Are primary CO effects on mitochondrial function transduced into secondary signals, creating signaling pathways?
4. Are CORM-dependent effects also evoked by endogenously produced CO?
5. Does CO modulate activity of other intracellular target structures besides mitochondria?

2 MAIN PART

2.1 *Manuscript 2*: Effects of frequently applied carbon monoxide releasing molecules (CORMs) in typical CO-sensitive model systems – A comparative *in vitro* study

David Stucki[1], Heide Krahl[1], Moritz Walter[1], Julia Steinhausen[1], Katrin Hommel[1], Peter Brenneisen[1] and Wilhelm Stahl[1]

[1] Institute of Biochemistry and Molecular Biology I, Medical Faculty, Heinrich Heine University Düsseldorf, D-40001 Düsseldorf, Germany.

Received: 20th February 2020; Accepted: 16th April 2020; Published: 23rd April 2020

Published in: *Archives of Biochemistry and Biophysics*, **687**: 108383.

DOI: 10.1016/j.abb.2020.108383

Contribution statement:
D.S. contributed to conceptualization and supervision of the study, performed all experiments except EROD assays. D.S. analyzed and visualized all experiments, wrote the main part of the original draft and contributed to review & editing of the manuscript.

Archives of Biochemistry and Biophysics 687 (2020) 108383

Contents lists available at ScienceDirect

Archives of Biochemistry and Biophysics

journal homepage: www.elsevier.com/locate/yabbi

Effects of frequently applied carbon monoxide releasing molecules (CORMs) in typical CO-sensitive model systems – A comparative *in vitro* study

David Stucki, Heide Krahl, Moritz Walter, Julia Steinhausen, Katrin Hommel, Peter Brenneisen, Wilhelm Stahl*

Institute of Biochemistry and Molecular Biology I, Medical Faculty, Heinrich Heine University Düsseldorf, Postfach 10 10 07, D-40001, Düsseldorf, Germany

ARTICLE INFO

Keywords:
Myoglobin
Heme proteins
Mitochondria
Respiratory chain
Oxygen
CYP

ABSTRACT

Intracellular carbon monoxide (CO) is a gaseous signaling molecule and is generated enzymatically by heme oxygenases upon degradation of heme to billiverdin. Target structures for intracellular produced CO are heme proteins including cytochrome *c* oxidase of the respiratory chain, cytochrome P450-dependent monooxygenases, or myoglobin. For studies on CO signaling, CO-releasing molecules (CORMs) of different structure are available. Here, three frequently used CORMs (CORM-2, CORM-3 and CORM-401) were studied for their properties to provide CO in biological test systems and address susceptible heme proteins. CO release was investigated in the myoglobin binding assay and found to be rapid (< 5 min) with CORM-2- and CORM-3, whereas CORM-401 continuously provided CO (> 50 min). Storage stability of CORM stock solutions was also assessed with the myoglobin assay. Only CORM-401 stock solutions were stable over a period of 7 days. Incubation of CORMs with recombinant cytochrome P450 led to an inhibition of enzyme activity. However, only CORM-3 and CORM-401 proved to be suitable in this test system because controls with the inactivated CORM-2 (iCORM-2) also led to a loss of enzyme activity. The impact of CORMs on the respiratory chain was investigated with high resolution respirometry and extracellular flux technology. In the first approach interferences of CORM-2 and CORM-3 with oxygen measurement occurred, since a rapid depletion of oxygen was detected in the medium even when no cells were present. However, CORM-401 did not interfere with oxygen measurement and the expected inhibition of cellular respiration was observed. CORM-2 was not suitable for use in oxygen measurements with the extracellular flux technology and CORM-3 application did not show any effect in this system. However, CO-dependent inhibition of cellular respiration was observed with CORM-401. Based on the present experiments it is concluded, that CORM-401 produced most reliable CO-specific results for the modulation of typical CO targets. For studies on CO-dependent biological effects on intracellular heme groups, CORM-2 and CORM-3 were less suitable. Depending on the experimental setting, data achieved with these compounds should be evaluated with caution.

1. Introduction

Within cells, carbon monoxide (CO) is generated enzymatically by heme oxygenases upon degradation of heme to yield biliverdin which is further reduced to bilirubin [1]. Evidence accumulated over the last decade that CO is a gaseous, diffusible molecule implicated in intra- and intercellular signaling [2]. For study purposes, the delivery of CO to cells and tissues was formerly restricted to the application of CO-gas associated with limitations of proper dosing and usually administration of high CO amounts to biological systems. With the development of CO-releasing molecules (CORMs) those problems were partially overcome and delivery of low CO amounts, mimicking CO signaling more appropriate, was achievable [3]. Most of these compounds are metal complexes with CO-ligands attached. Depending on the structure of the molecule and the physico-chemical conditions of the environment the complexes release certain amounts of CO and were applied for controlled release of carbon monoxide in animal and cell culture studies [4]. Mode and location of CORM-mediated CO release as well as delivery of CO to intracellular targets are still a matter of debate [5] and questions on the properties of different CORMs with respect to their effects on biological targets remain open.

Primary target structures for CO are porphyrins in heme proteins with ferrous iron as central atom and CO is thought to act as an exchange ligand for other complexants such as molecular oxygen [6]. The

* Corresponding author.
E-mail address: wilhelm.stahl@hhu.de (W. Stahl).

https://doi.org/10.1016/j.abb.2020.108383
Received 20 February 2020; Received in revised form 15 April 2020; Accepted 16 April 2020
Available online 23 April 2020
0003-9861/

affinity of CO towards various heme proteins differs significantly [7], which likely provides the mechanistic principle for selective CO signaling. Well-known intracellular target structures for CO are heme proteins of the respiratory chain, myoglobin, or porphyrin containing oxidoreductases such as cytochrome P450-dependent monooxygenases (CYPs). Cytochrome *c* oxidase (complex IV of the respiratory chain) is addressed by CO leading to an inhibition of oxidative phosphorylation. Here CO interferes directly with the energy metabolism and triggers via secondary signals such as the ATP/ADP ratio other constituents of the energy-providing pathways [8]. Regulatory effects on other signaling pathways may be mediated by a transient inactivation of CYPs [9] which are involved in the biosynthesis, activation, and degradation of several lipophilic signaling compounds including steroid hormones, cholecalciferol, retinoic acid, or eicosanoids [10–12].

In this study, the effects of three structurally different and commercially available CORMs on well-known CO-sensitive systems (CYPs; respiratory chain) were evaluated. All compounds belonged to the group of CO metal complexes. The data highlight pitfalls with frequently used CORMs in biological studies on CO signaling.

2. Materials and methods

2.1. Chemicals

Tricarbonyldichlororuthenium(II) dimer (CORM-2), Tricarbonylchloro(glycinato)ruthenium (II) (CORM-3), Tetracarbonyl[N-(dithiocarboxy-κ*S*,κ*S*′)-N-methylglycine]manganite (CORM-401), Dulbecco's Modified Eagle's Medium (DMEM), manganese sulfate monohydrate, ethoxyresorufin, sodium dithionite, myoglobin (from equine skeletal muscle), NADPH and PBS were from Sigma-Aldrich (Deisenhofen, Germany), trichloroacetic acid from Merck (Darmstadt, Germany), DMSO from Roth (Karlsruhe, Germany) and sarcosine-N-dithiocarbamate was obtained from 3B Scientific Corporation (Wuhan, China).

2.2. Preparation and dissolution of CORMs and iCORMs

Upon arrival all CORMs were stored at −20 °C according to manufacturer's instructions. CORM-2 was freshly dissolved in DMSO prior to all experiments. To prepare inactive CORM-2 (iCORM-2), a 50 mM CORM-2 solution was diluted 1:10 with H_2O, incubated over night at 37 °C for CO liberation and was then bubbled with N_2 for 15 min to remove residual CO.

CORM-3 was freshly dissolved in H_2O prior to all experiments. To prepare iCORM-3, a 50 mM CORM-3 solution was diluted 1:10 with PBS and was further treated as described for CORM-2. Preparation of iCORM-2 and iCORM-3 is, with slight modifications, in accordance with literature [13,14].

CORM-401 was freshly dissolved in PBS. According to literature, an equimolar mixture of sarcosine-N-dithiocarbamate and $MnSO_4$ was used as iCORM-401 [15–17]. All CORMs and iCORMs were protected from light at all times.

2.3. Myoglobin assay

Release of CO from CORMs and iCORMs was assessed with the myoglobin (Mb) assay. In the Mb assay the conversion of deoxymyoglobin (deoxy-Mb) to carboxymyoglobin (Mb-CO) is determined spectrophotometrically in the range of 500–600 nm [3]. Myoglobin (100 μM) was dissolved in PBS and sodium dithionite was added to a final concentration of 0.2% (w/v), for complete oxygen depletion. An absorbance spectrum was recorded at the beginning of the experiment (deoxy-Mb). Then CORMs or iCORMs were added to a final concentration of 30 μM. The solution was covered with N_2 gas and nine further absorbance spectra were recorded. Record intervals were 0.5 min (CORM-2, iCORM-2, CORM-3, iCORM-3) or 5 min (CORM-401, iCORM-401). The myoglobin assay was performed with freshly dissolved CORMs or after storage of aliquots for seven days at either room temperature or −20 °C. Purging of the deoxy-Mb solution with CO gas was applied to achieve a complete conversion from deoxy-Mb to Mb-CO. Quantification of Mb-CO was performed according to a previously published method [18]. For calculations, the Mb extinction coefficient of 14.8 mM^{-1} cm^{-1} at 540 nm [19] and the isobestic point at 585 nm were used.

2.4. Ethoxyresorufin-O-deethylase activity assay

The ethoxyresorufin-*O*-deethylase (EROD) assay was used to determine the activity of CYP1A enzymes. The assay is based on the deethylation of the non-fluorescent substrate ethoxyresorufin to the fluorescent product resorufin [20]. The EROD assay was performed in 48 well plates. The reaction mixture (250 μL per well) consisted of 0.125 pmol recombinant human CYP1A1 enzyme with cytochrome P450 reductase (C3735, Sigma, Deisenhofen, Germany) and 2.5 μM ethoxyresorufin in a 0.1 M potassium phosphate buffer (pH 7.2). CORMs or iCORMs were added to final concentrations of 1–100 μM and the reaction was started by adding NADPH to a final concentration of 200 μM. The reaction was recorded for 10 min at 37 °C by measuring the fluorescence of the newly formed resorufin (λ_{ex}: 535 nm/λ_{em}: 590 nm) every 2 min with a plate reader (Tecan, Infinite M200). EROD activity was calculated as increase of relative fluorescence units (RFU) per min. For comparison the respective solvent control was set to 100%.

2.5. Cell culture

Murine embryonic fibroblasts (MEFs) were a kind gift from N. Ishihara and co-workers [21] and were cultured in DMEM (low glucose), supplemented with 10% fetal bovine serum (FBS, PAN-Biotech, Aidenbach, Germany), penicillin (100 U/mL), streptomycin (100 μg/mL) and GlutaMAX™ (2 mM) at 37 °C and 5% CO_2 in a humidified atmosphere.

2.6. High-resolution respirometry

High-resolution respirometry was performed using an Oroboros O2k (Oroboros Instruments, Innsbruck, Austria). The system consists of two closed reaction chambers. At zero oxygen inside the reaction chamber, back diffusion of oxygen is $<$ 4 pmol s^{-1} mL^{-1} according to manufacturer. Each chamber has a volume of 2 mL and is equipped with a magnetic stirrer (set to 750 rpm). Oxygen levels were determined continuously. All experiments were performed at 37 °C. DMEM supplemented as described above (without FBS) was used as reaction medium and for standard instrumental calibration procedures with the Datlab software (Oroboros Instruments).

In cell-free experiments CORMs or iCORMs were injected into one reaction chamber and the respective solvent into the other. Final concentrations of compounds were 10, 50 and 100 μM. Oxygen levels were recorded for at least 20 min after injection and oxygen flux per volume was calculated. Area under the curve (AUC) values were calculated from the first 20 min after injection of the oxygen flux curves using the software Prism 8 (GraphPad). The oxygen flux value at time of injection was used for background subtraction of individual curves. AUC values of solvent controls were subtracted from the corresponding CORM and iCORM AUC values to determine the amount of oxygen loss within the first 20 min after injection. Two additional experiments were performed to proof the gas tightness of the reaction chambers. First, after calibration of medium, dithionite was sequentially added to the reaction chamber until complete depletion of oxygen. Seconds, the Oroboros O2k was placed in a H35 hypoxia chamber (Don Whitley Scientific, Bingley, UK) and calibration procedures were performed at 21% oxygen concentration inside the hypoxia chamber. During the experiment oxygen levels in the hypoxia chamber were lowered to 0.1%.

For cellular experiments 600,000 MEFs per reaction chamber were used and incubated until oxygen flux levels reached an equilibrium. Then CORM-401 or iCORM-401 were injected into one reaction chamber to a final concentration of 1 mM, while solvent control (PBS) was injected into the other reaction chamber; measurements were performed for a period of 4h.

2.7. Extracellular flux analyses

Extracellular flux (XF) analyses were performed with a XFe96 analyzer (Agilent Technologies, Santa Clara, CA, USA). This system is based on a 96 well plate format with free oxygen diffusion between medium and atmosphere. All XF analyses were performed in a DMEM-based assay medium (D5030, Sigma-Aldrich, Deisenhofen, Germany) containing all supplements as normal cell culture medium, except FBS, antibiotics and phenol red. For cell-free experiments a XFe96 well plate was loaded with 180 µL assay medium per well and placed in a non-CO_2 incubator at 37 °C for 1 h prior to the experiment. A XFe96 sensor cartridge was loaded with 20 µL CORM or iCORM solutions or respective solvent controls as indicated. Final concentrations of compounds in the wells were 10, 50 or 100 µM. During the experiment oxygen consumption rate (OCR) was determined in consecutive measurement cycles. One measurement cycle consisted of 3 min mixing and 3 min measuring. For cell-based experiments 7500 MEFs per well were seeded in a XFe96 well plate and were incubated for 24h in normal cell culture medium at 37 °C and 5% CO_2. Cells were washed 1h prior to the experiment with assay medium. Then 180 µL assay medium per well were added and the plate was placed in a non-CO_2 incubator at 37 °C until analysis, which was performed as stated above.

2.8. Statistical analysis

If not stated otherwise, data is given as mean of three independent experiments (n = 3) and error bars represent standard deviation (SD). Data was analyzed using one-way ANOVA with Dunnett's multiple comparisons test (control vs. treatment) or unpaired Student's t-test (CORM vs. iCORM) with $p \leq 0.05$ being considered a statistically significant difference.

3. Results

3.1. CO release characteristics and stability of CORMs

CORM-2, CORM-3 and CORM-401 (Fig. 1A–C) and the respective inactive CORMs (iCORMs) were tested for their CO-releasing properties in the Mb binding assay [18]. In the Mb assay formation of MbCO over time is used as a marker for CO release by CORMs. Each compound was added to a final concentration of 30 µM and the amount of formed MbCO in the reaction was quantified. CO release from CORM-2 reached an equilibrium within 4.5 min and 15 µM MbCO were formed. Upon incubation with iCORM-2 still 5 µM MbCO were detected (Fig. 1D). 20 µM MbCO were formed within 4.5 min in the reaction of CORM-3 with Mb. Here no reaction of iCORM-3 with Mb was determined (Fig. 1E). In the reaction of CORM-401 with Mb, formation of MbCO was still ongoing after 45 min of incubation. At this time point about 50 µM MbCO had been generated. No MbCO was detected upon incubation of iCORM-401 with Mb (Fig. 1F). To test the stability of the compounds, CORM stock solutions were stored for 7d at either −20 °C or room temperature (RT) and were subjected to the Mb assay. CO releasing capacity of CORM-2 decreased when stored at −20 °C or RT to about 12 and 8 µM formed MbCO, respectively (Fig. 1G). CO release from CORM-3 was also lowered after storage at −20 °C (15 µM MbCO) and even not detectable after storage at RT (Fig. 1H). CORM-401, however, showed no loss of activity when stored at −20 °C and only slightly less CO release (about 40 µM MbCO) when stored at RT (Fig. 1I).

3.2. Inhibition of CYP activity by CORMs

Cytochrome P450-dependent monooxygenases (CYPs) are known to be inhibited by CO. Ethoxyresorufin-*O*-deethylase (EROD) activity of recombinant CYP1A1 was assessed in the presence of CORMs and iCORMs. The assay was started directly after addition of CORMs and iCORMs to the reaction mixture. All CORMs showed a concentration dependent inhibition of EROD activity (Fig. 2). CORM-2 had the strongest inhibitory effect on EROD activity (50% inhibition at 1 µM), followed by CORM-3 (about 40% inhibition at 1 µM) and CORM-401 (about 50% inhibition at 50 µM). However, iCORM-2 inhibited EROD activity to the same extent as CORM-2. While iCORM-3 also inhibited EROD activity (about 40% inhibition at 10 µM and higher), iCORM-401 did not affect enzyme activity at any concentration tested.

3.3. High resolution respirometry

Effects of CORMs and iCORMs on cellular respiration were studied using high resolution respirometry. At first a cell-free set up was used to investigate possible interferences of the compounds with the oxygen sensing system. Directly after injection of CORM-2 and CORM-3 an apparent increase of oxygen flux was observed (Fig. 3A + B). As determined by area under the curve (AUC) analysis, about 40 nmol oxygen were consumed within the first 20 min after injection of 100 µM CORMs (Fig. 3D + E). The amount of oxygen loss is equal to about 10% of total oxygen in the reaction chamber and relates to about 20% of the injected CORM. These proportions were also found at lower dose levels. CORM-401 injection, however, did not provoke oxygen loss (Fig. 3C + F). Injection of iCORM-2, -3 and -401 increased oxygen consumption only slightly (Fig. 3A–F). To exclude the possibility of oxygen being displaced from the reaction chamber by CO, gas tightness of the system was tested. After lowering oxygen levels inside the reaction chamber with sequential dithionite injections, it was proven, that no oxygen diffused back within the next 60 min (Fig. 3G). Vice versa no oxygen was released from the reaction chamber within 60 min when a concentration gradient was applied by lowering the atmospheric oxygen levels from 21 to 0.1% using a hypoxic workstation (Fig. 3H).

Based on these data (Fig. 3A–F), only CORM-401 was suitable to study CO effects on cellular respiration in this system. After instrumental calibration, cells were added to the reaction chamber; basal oxygen flux was about 40 pmol/(s · 10^6 cells). Upon injection of CORM-401, cellular respiration was directly increased by two fold. However, over time, CORM-401 treatment decreased respiration below control level, reaching maximal inhibition at 4 h (Fig. 4A). When iCORM-401 was injected, oxygen flux also increased drastically at first, which was also found in the cell-free experiment, and was then lowered again over time to control level (Fig. 4B). However, no inhibitory effect on cellular respiration were determined.

3.4. Extracellular flux technology

Effects of CORMs and iCORMs on cellular respiration were further examined with the extracellular flux technology. Again a cell-free set up was used to exclude interferences between compounds and oxygen sensing. CORM-3, CORM-401 and their respective iCORMs showed no effects on oxygen consumption rate (OCR) (Fig. 5B + C). In contrast to this, CORM-2 and the solvent control DMSO increased OCR directly after injection (Fig. 5A), showing interferences with oxygen measurement. CORM-3 and CORM-401 were then tested in a cell-based approach. Again, CORM-3 and iCORM-3 showed no effect on OCR at the concentrations tested, compared to control (Fig. 5D). However, injection of 100 µM CORM-401 directly increased cellular OCR above control level and then decreased OCR below control level at later time points (> 60 min) (Fig. 5E), confirming our results obtained with high resolution respirometry (Fig. 4). Treatment of cells with iCORM-401 did

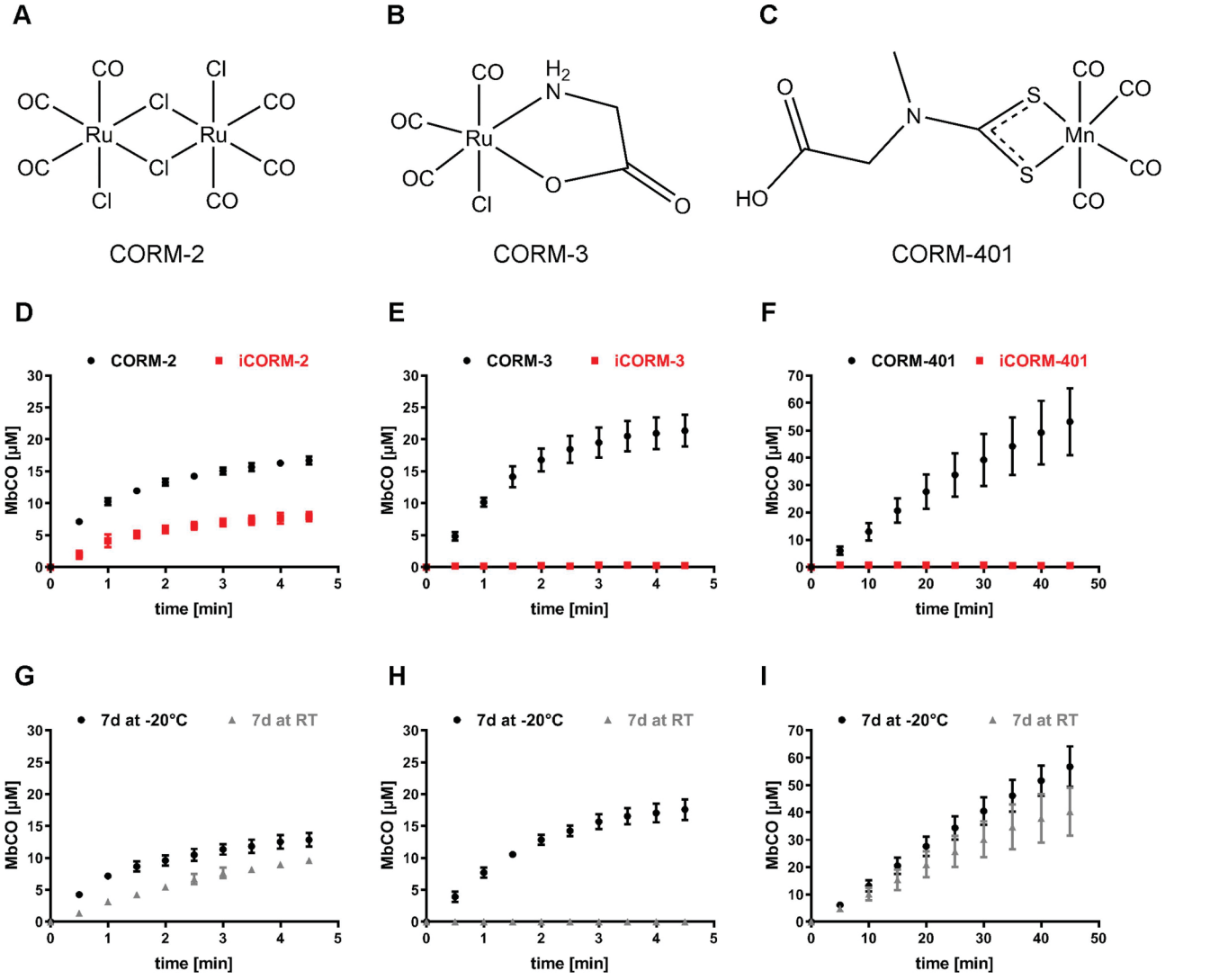

Fig. 1. Characterization of CO release from CORMs and iCORMs. Chemical structures of CORM-2 (A), CORM-3 (B) and CORM-401 (C) are provided. CO release from freshly prepared CORM and iCORM solutions (D–F) was analyzed with the Mb assay and is presented as formed MbCO. CORM solutions were also stored for seven days at either RT or −20 °C and then subjected to the Mb assay (G: CORM-2, H: CORM-3, I: CORM-401). Data is given as mean ± SD of three independent experiments. Mb = myoglobin, RT = room temperature.

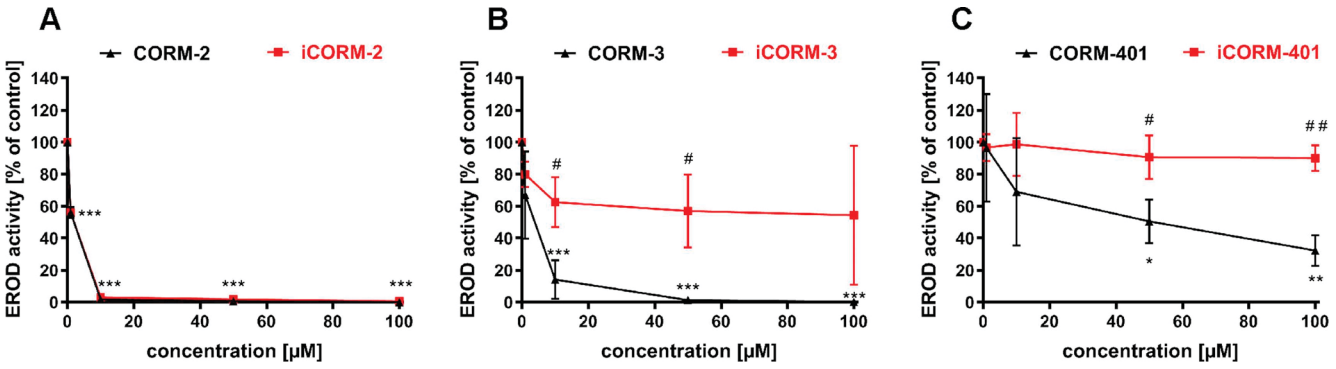

Fig. 2. Inhibition of EROD activity by CORMs and iCORMs. The non-fluorescent substrate ethoxyresorufin is converted by recombinant CYP1A1 to the fluorescent resorufin. Fluorescence (λ_{ex}:535nm/λ_{em}:590 nm) was recorded over 10 min. Activity was calculated as increase in relative fluorescence units per min. Control was set to 100%. Values are means ± SD of three independent experiments. *p < 0.05, **p < 0.01, ***p < 0.001 for ct vs CORM/iCORM; #p < 0.05, ##p < 0.01 for CORM vs iCORM.

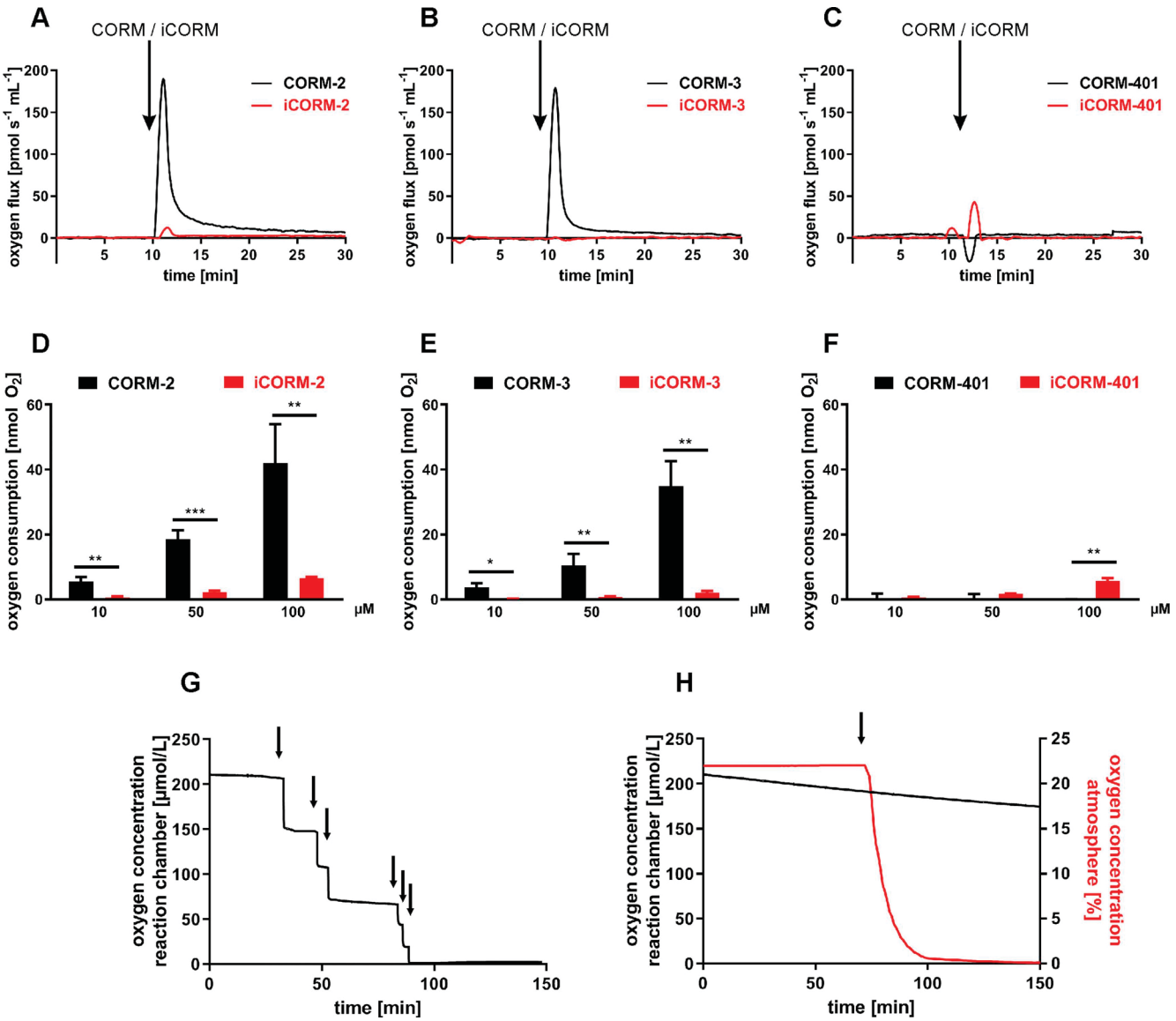

Fig. 3. Interference of CORMs with cell-free high resolution respirometry. After instrumental calibration, CORMs and iCORMs were injected into the reaction chamber and oxygen levels were monitored. Representative curves of oxygen flux after compound injection (100 μM final concentration) are shown in A-C. Arrows mark time point of injection. AUC analysis for a period of 20 min after injection was performed and is given as consumed oxygen (D–F); mean +SD; n = 3. *p < 0.05, **p < 0.01, ***p < 0.001 for CORM vs iCORM. G: oxygen concentration inside reaction chamber upon sequential dithionite injection (marked by arrows). H: oxygen concentration inside reaction chamber (black line) and of the atmosphere (red line), which was controlled by a hypoxic workstation.

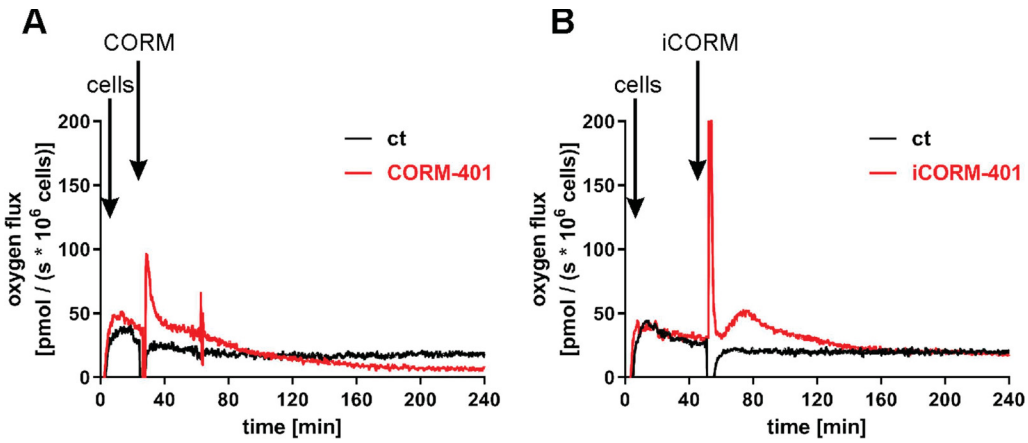

Fig. 4. CORM-401 modulates respiration of murine embryonic fibroblasts. After instrumental calibration, $6 \cdot 10^5$ cells were added per reaction chamber. CORM-401 (A) and iCORM-401 (B) were then injected to final concentrations of 1 mM and oxygen flux was monitored. Representative oxygen flux curves of three independent experiments are shown. Arrows mark time point of cell addition or compound injection, respectively.

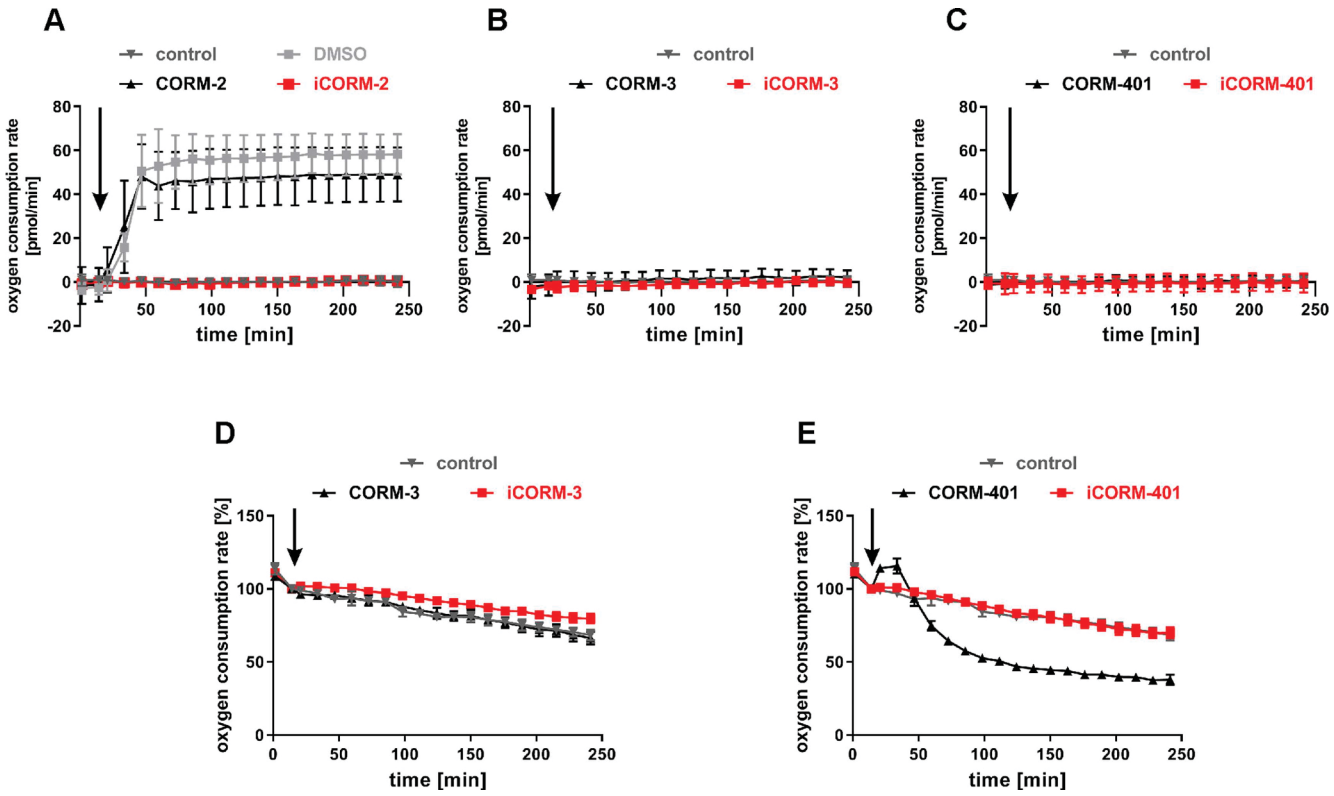

Fig. 5. Extracellular flux technology reveals modulation of cellular respiration by CORM-401 but not CORM-3. CORMs and iCORMs were injected (indicated by arrows) into reaction wells and OCR was measured over time. A–C: cell-free system; D and E: cell-based system. Final concentration of compounds: 100 μM. Three independent experiments have been performed (n = 3). Representative OCR curves are shown. Data represent mean ± SD of at least six technical replicates. OCR = oxygen consumption rate.

not affect OCR compared to control.

4. Discussion

4.1. Myoglobin binding assay – CO release and stability of CORMs

Characterization of the different CORMs with the myoglobin binding assay showed distinct differences in the kinetics of CO release, stability of the single compounds and residual activity of iCORMs. In the presence of Mb, CORM-2 and CORM-3 quickly released CO and the reaction with Mb was completed within 5 min. CORM-401 dependent CO-generation and transfer to Mb was slower and continued over a period of more than 50 min. Depending on the experimental setting, the numbers of CO molecules released from CORMs differ. In the set up tested here, the molar ratio of released CO to CORM was highest for CORM-401, followed by CORM-3 and CORM-2. Both characteristics (kinetics and amount of CO release from CORMs) are in accordance with the literature [3,13,17,22]. Thus, quite low amounts of CORM-401 are sufficient to provide a continuous supply of CO to target molecules. Both, iCORM-3 and iCORM-401 proved to be suitable controls in the myoglobin assay since no Mb-CO formation was observed. Upon incubation with iCORM-2, still some Mb-CO was generated, indicating that at least in the presence of high amounts of acceptor groups some CO releasing capacity remained. Residual CO release may impair with proper control and cannot be excluded in cell culture experiments when iCORM-2 is used as a control. Our experiments on storage stability of CORMs showed for the first time, that stock solutions of CORM-2 and CORM-3 are neither fully stable at room temperature nor at −20 °C. However, the stability of CORM-401 was not affected at −20 °C and only slightly at room temperature over a period of seven days. In this context handling of CORM-401 is easier compared to the other CORMs tested here. A reason for differences in the stability might be related to the mechanism of decomposition. While CORM-2 and CORM-3 release CO mainly under thermally controlled ligand exchange [3,13], CO release from CORM-401 mainly depends on the presence of suitable acceptor molecules [23]. The latter might also apply for the velocity of CO release from CORM-401, which most likely depends on the CO affinity of the acceptor molecule.

4.2. Inhibition of CYP activity

Cytochrome P450-dependent monooxygenases are well-known to be inhibited by the binding of CO to the prosthetic heme group at the catalytic site, when CO is present in high amounts [24]. Until now little is known about how low amounts of CO, as is the case with CO signaling, modulate CYP-mediated reactions in biological relevant systems. In the present study we measured the effects of different CORMs on the activity of recombinant CYP1A1. Both, CORM-2 and the corresponding iCORM-2 inhibited CYP1A1 activity. The latter possibly via residual CO release capacity of the iCORM sufficient to block the heme group of the enzyme. Alternatively, CO-independent inhibitory effects of CORM-2/iCORM-2 might be operative. Inhibition of CYP activity by CORM-3 was already observed at levels of 1 μM; enzyme activity was also moderately affected by the respective iCORM-3, possibly due to incomplete iCORM production. At the level of 100 μM iCORM-3 a residual CO release of 1% would be sufficient to provoke a decrease of EROD activity comparable to the 1 μM CORM-3 condition. In contrast, iCORM-401 did not inhibit CYP1A1 whereas a dose-dependent inhibition was determined with CORM-401 between 10 and 100 μM. The higher potency for CYP inhibition by CORM-3, compared to CORM-401, might be due to a faster release of CO as already demonstrated in the Mb assay.

4.3. High resolution respirometry and extracellular flux analysis

Another CO susceptible target protein is the cytochrome *c* oxidase (complex IV) of the mitochondrial respiratory chain [25,26]. Oxygen consumption of mitochondria is not only linked to ATP production, but also to maintenance of membrane potential which in turn is a main factor regulating mitochondrial quality control mechanisms such as mitophagy [27,28]. Thus, reliable research tools (CORMs), that do not influence oxygen levels or measurements, are needed to study effects of CO on these processes. Cellular respiration can be determined measuring oxygen consumption by means of high resolution respirometry. Our data indicate that such a setup is not suitable to study CO effects mimicked by CORM-2 or CORM-3. In cell free control experiments, oxygen depletion (about 20% of the added CORM amount) was observed right after addition of both CORMs. Our experiments excluded a displacement of oxygen by CO from the reaction chamber (Fig. 3G + H). Other possibilities for oxygen loss may be binding of oxygen by CORM-2 and CORM-3 as an exchange ligand for CO or consumption of oxygen by chemical reactions. Formation of hydroxyl radicals from oxygen in aqueous systems was discussed for ruthenium-based CORMs [29,30]. The latter could also be an explanation for contradictive reports on ROS generation by CORMs [31,32].

CORM-401, however, did not interfere with the setup of high resolution respirometry and proved to be suitable for cell-based experiments. This might also be related to the fact that CORM-401 only releases CO when suitable acceptor molecules are present and does not flood the system with carbon monoxide. It should be noted that inhibition of cellular respiration was only observed at a very high CORM-401 concentration (1 mM). This is most likely due to the high cell number (corresponding to high amounts of heme proteins) required for this type of experiment and is in accordance with findings from other groups [33].

The extracellular flux technology represents an alternative method to determine cellular respiration. Oxygen flux is measured in transiently formed micro chambers using a fluorogenic sensor. The overall oxygen tension in the reaction medium is hardly affected since oxygen levels are adjusted between measurement cycles by mixing of the medium. Also in this system, CORM-2 was not suitable for CO generation. DMSO, which is required as a solvent, interfered with the determination of oxygen consumption rate (OCR) with the XFe96 analyzer. However, this was not the case when injecting CORM-2 or DMSO as solvent control using XF24 technology [34]. Since both systems differ regarding volumes of the well and injection fraction, the DMSO concentrations after injection might vary between the systems.

In cell-based experiments CORM-3 showed no effect on respiration. This is probably due to a fast CO release directly after injection, with the majority of CO produced in the extracellular space. Upon application of CORM-401, OCR was transiently raised, representing an uncoupling effect of mitochondria by CO exposure as described before [33,35]. At later time points a continuous decrease of OCR was observed, as to be expected when the respiratory chain is inhibited by CO exposure. Cellular respiration was not affected by iCORM-401. We assume, that CO release from CORM-401 takes place intracellularly, since the presence of CO acceptors (heme proteins) is needed. This property seems to contribute significantly to the reported modulation of the cellular OCR by CORM-401. Although CO is a small gaseous molecule, that can easily pass membranes, the location of CO generation seems to be of high importance for modulation of biological processes [5,36]. It should also be mentioned here, that extracellular CO release from CORM-401 cannot be excluded in our study.

4.4. Conclusion

Our data show that studies with CORMs as CO generating systems to investigate CO-dependent biological effects are associated with several pitfalls. Depending on the readout system not all CORMs produce reliable, CO-related results. In the cases of CORM-2 and CORM-3 unexpected biological effects were found, probably due to non-CO related activities. Such effects have been described for CORM-2, which was found to modulate K^+ ion channel activity in a CO-independent manner [37]. CORM-2 also inhibited the anticoagulant activity of phospholipase A_2 independently of CO release, and reactive ruthenium species were discussed to play a role in this inhibition [38]. A CO-independent antimicrobial effect was described for CORM-3, with thiol-reactive Ru (II) ion being the active agent [39]. Our own data add oxygen depletion by CORM-2 and CORM-3 to the list of undesired side effects of compounds originally designed for CO delivery. These findings must be taken into account in studies on oxygen levels such as in hypoxia signaling or modulation of OXPHOS. Lack of storage stability of CORM-2 and CORM-3 is another issue that needs to be addressed in context of CO research. This characteristic potentially complicates comparisons between different experiments or studies, if not controlled properly.

In summary, of the compounds investigated in the present study CORM-2 and to a lesser extent CORM-3, although used most throughout the literature, were least suitable for the tested read outs. In contrast, CORM-401 proved to be most suitable for addressing susceptible heme proteins. It is hence recommended for research on CO signaling and could be used in future studies on regulatory effects in cellular energy metabolism and mitochondrial dynamics. All of the CORMs investigated here belong to the group of metal complexes with CO-ligands attached. It should be noted that transition metal-free CO-releasing compounds have been introduced and may offer a possible viable alternative [40–42].

Author statement

David Stucki: conceptualization, formal analysis, investigation, writing – original draft and review & editing, visualization, supervision.
Heide Krahl: investigation.
Moritz Walter: investigation.
Julia Steinhausen: investigation.
Katrin Hommel: methodology.
Peter Brenneisen: writing – review & editing.
Wilhelm Stahl: conceptualization, writing – review & editing, supervision.

Acknowledgments

This work was funded by the Deutsche Forschungsgemeinschaft (DFG, German Research Foundation) Projektnummer STA699/3-1 (WS). We are grateful to Prof. Andreas Reichert for critical comments and to the ‘Cellular Metabolism Platform’ at the Medical Faculty of the Heinrich Heine University Düsseldorf for access to the Seahorse Extracellular Flux Analyzer.

References

[1] R. Tenhunen, H.S. Marver, R. Schmid, Microsomal heme oxygenase. Characterization of the enzyme, J. Biol. Chem. 244 (1969) 6388–6394.
[2] K. Magierowska, T. Brzozowski, M. Magierowski, Emerging role of carbon monoxide in regulation of cellular pathways and in the maintenance of gastric mucosal integrity, Pharmacol. Res. 129 (2018) 56–64.
[3] R. Motterlini, J.E. Clark, R. Foresti, P. Sarathchandra, B.E. Mann, C.J. Green, Carbon monoxide-releasing molecules: characterization of biochemical and vascular activities, Circ. Res. 90 (2002) E17–E24.
[4] U. Schatzschneider, Novel lead structures and activation mechanisms for CO-releasing molecules (CORMs), Br. J. Pharmacol. 172 (2015) 1638–1650.
[5] T. Soboleva, C.R. Simons, A. Arcidiacono, A.D. Benninghoff, L.M. Berreau, Extracellular vs intracellular delivery of CO: does it matter for a stable, diffusible gasotransmitter? J. Med. Chem. 62 (2019) 9990–9995.
[6] S.W. Ryter, L.E. Otterbein, Carbon monoxide in biology and medicine, Bioessays 26 (2004) 270–280.
[7] R. Motterlini, R. Foresti, Biological signaling by carbon monoxide and carbon monoxide-releasing molecules, Am. J. Physiol. Cell Physiol. 312 (2017) C302–c313.
[8] L. Braud, M. Pini, L. Muchova, S. Manin, H. Kitagishi, D. Sawaki, G. Czibik, J. Ternacle, G. Derumeaux, R. Foresti, R. Motterlini, Carbon monoxide-induced

metabolic switch in adipocytes improves insulin resistance in obese mice, JCI Insight 3 (2018).
[9] M. Walter, W. Stahl, P. Brenneisen, A.S. Reichert, D. Stucki, Carbon monoxide releasing molecule 401 (CORM-401) modulates phase I metabolism of xenobiotics, Toxicol. Vitro 59 (2019) 215–220.
[10] T. Niwa, N. Murayama, Y. Imagawa, H. Yamazaki, Regioselective hydroxylation of steroid hormones by human cytochromes P450, Drug Metab. Rev. 47 (2015) 89–110.
[11] I. Fleming, Cytochrome P450-dependent eicosanoid production and crosstalk, Curr. Opin. Lipidol. 22 (2011) 403–409.
[12] D. Bishop-Bailey, S. Thomson, A. Askari, A. Faulkner, C. Wheeler-Jones, Lipid-metabolizing CYPs in the regulation and dysregulation of metabolism, Annu. Rev. Nutr. 34 (2014) 261–279.
[13] J.E. Clark, P. Naughton, S. Shurey, C.J. Green, T.R. Johnson, B.E. Mann, R. Foresti, R. Motterlini, Cardioprotective actions by a water-soluble carbon monoxide-releasing molecule, Circ. Res. 93 (2003) e2–8.
[14] B. Sun, Z. Sun, Q. Jin, X. Chen, CO-releasing molecules (CORM-2)-liberated CO attenuates leukocytes infiltration in the renal tissue of thermally injured mice, Int. J. Biol. Sci. 4 (2008) 176–183.
[15] P. Kaczara, B. Proniewski, C. Lovejoy, K. Kus, R. Motterlini, A.Y. Abramov, S. Chlopicki, CORM-401 induces calcium signalling, NO increase and activation of pentose phosphate pathway in endothelial cells, FEBS J. 285 (2018) 1346–1358.
[16] D. Babu, G. Leclercq, R. Motterlini, R.A. Lefebvre, Differential effects of CORM-2 and CORM-401 in murine intestinal epithelial MODE-K cells under oxidative stress, Front. Pharmacol. 8 (2017) 31.
[17] S. Fayad-Kobeissi, J. Ratovonantenaina, H. Dabire, J.L. Wilson, A.M. Rodriguez, A. Berdeaux, J.L. Dubois-Rande, B.E. Mann, R. Motterlini, R. Foresti, Vascular and angiogenic activities of CORM-401, an oxidant-sensitive CO-releasing molecule, Biochem. Pharmacol. 102 (2016) 64–77.
[18] A.J. Atkin, J.M. Lynam, B.E. Moulton, P. Sawle, R. Motterlini, N.M. Boyle, M.T. Pryce, I.J. Fairlamb, Modification of the deoxy-myoglobin/carbonmonoxy-myoglobin UV-vis assay for reliable determination of CO-release rates from organometallic carbonyl complexes, Dalton Trans. 40 (2011) 5755–5761.
[19] W.J. Bowen, The absorption spectra and extinction coefficients of myoglobin, J. Biol. Chem. 179 (1949) 235–245.
[20] M.D. Burke, R.T. Mayer, Ethoxyresorufin: direct fluorimetric assay of a microsomal O-dealkylation which is preferentially inducible by 3-methylcholanthrene, Drug Metab. Dispos. 2 (1974) 583–588.
[21] N. Ishihara, M. Nomura, A. Jofuku, H. Kato, S.O. Suzuki, K. Masuda, H. Otera, Y. Nakanishi, I. Nonaka, Y. Goto, N. Taguchi, H. Morinaga, M. Maeda, R. Takayanagi, S. Yokota, K. Mihara, Mitochondrial fission factor Drp1 is essential for embryonic development and synapse formation in mice, Nat. Cell Biol. 11 (2009) 958–966.
[22] X. Ji, K. Damera, Y. Zheng, B. Yu, L.E. Otterbein, B. Wang, Toward carbon monoxide-based therapeutics: critical drug delivery and developability issues, J. Pharmacol. Sci. 105 (2016) 406–416.
[23] S.H. Crook, B.E. Mann, A.J. Meijer, H. Adams, P. Sawle, D. Scapens, R. Motterlini, [Mn(CO)4{S2CNMe(CH2CO2H)}], a new water-soluble CO-releasing molecule, Dalton Trans. 40 (2011) 4230–4235.
[24] T. Leemann, P. Bonnabry, P. Dayer, Selective inhibition of major drug metabolizing cytochrome P450 isozymes in human liver microsomes by carbon monoxide, Life Sci. 54 (1994) 951–956.
[25] L.C. Petersen, The effect of inhibitors on the oxygen kinetics of cytochrome c oxidase, Biochim. Biophys. Acta 460 (1977) 299–307.
[26] D. Pankow, W. Ponsold, Effect of carbon monoxide exposure on heart cytochrome c oxidase activity of rats, Biomed. Biochim. Acta 43 (1984) 1185–1189.
[27] S.R. Chowdhury, J. Djordjevic, B.C. Albensi, P. Fernyhough, Simultaneous evaluation of substrate-dependent oxygen consumption rates and mitochondrial membrane potential by TMRM and safranin in cortical mitochondria, Biosci. Rep. 36 (2015) e00286.
[28] M. Zimmermann, A.S. Reichert, How to get rid of mitochondria: crosstalk and regulation of multiple mitophagy pathways, Biol. Chem. 399 (2017) 29–45.
[29] A.F. Tavares, M. Teixeira, C.C. Romao, J.D. Seixas, L.S. Nobre, L.M. Saraiva, Reactive oxygen species mediate bactericidal killing elicited by carbon monoxide-releasing molecules, J. Biol. Chem. 286 (2011) 26708–26717.
[30] J.D. Seixas, M.F. Santos, A. Mukhopadhyay, A.C. Coelho, P.M. Reis, L.F. Veiros, A.R. Marques, N. Penacho, A.M. Goncalves, M.J. Romao, G.J. Bernardes, T. Santos-Silva, C.C. Romao, A contribution to the rational design of Ru(CO)3Cl2L complexes for in vivo delivery of CO, Dalton Trans. 44 (2015) 5058–5075.
[31] P. Kaczara, R. Motterlini, K. Kus, A. Zakrzewska, A.Y. Abramov, S. Chlopicki, Carbon monoxide shifts energetic metabolism from glycolysis to oxidative phosphorylation in endothelial cells, FEBS Lett. 590 (2016) 3469–3480.
[32] C.C. Lin, L.D. Hsiao, R.L. Cho, C.M. Yang, Carbon monoxide releasing molecule-2-upregulated ROS-dependent heme oxygenase-1 Axis suppresses lipopolysaccharide-induced airway inflammation, Int. J. Mol. Sci. 20 (2019).
[33] P. Kaczara, R. Motterlini, G.M. Rosen, B. Augustynek, P. Bednarczyk, A. Szewczyk, R. Foresti, S. Chlopicki, Carbon monoxide released by CORM-401 uncouples mitochondrial respiration and inhibits glycolysis in endothelial cells: a role for mitoBKCa channels, Biochim. Biophys. Acta 1847 (2015) 1297–1309.
[34] C.E.N. Reiter, A.I. Alayash, Effects of carbon monoxide (CO) delivery by a CO donor or hemoglobin on vascular hypoxia inducible factor 1α and mitochondrial respiration, FEBS Open Bio 2 (2012) 113–118.
[35] J.L. Wilson, F. Bouillaud, A.S. Almeida, H.L. Vieira, M.O. Ouidja, J.L. Dubois-Rande, R. Foresti, R. Motterlini, Carbon monoxide reverses the metabolic adaptation of microglia cells to an inflammatory stimulus, Free Radic. Biol. Med. 104 (2017) 311–323.
[36] T. Soboleva, H.J. Esquer, S.N. Anderson, L.M. Berreau, A.D. Benninghoff, Mitochondrial-localized versus cytosolic intracellular CO-releasing organic PhotoCORMs: evaluation of CO effects using bioenergetics, ACS Chem. Biol. 13 (2018) 2220–2228.
[37] G. Gessner, N. Sahoo, S.M. Swain, G. Hirth, R. Schonherr, R. Mede, M. Westerhausen, H.H. Brewitz, P. Heimer, D. Imhof, T. Hoshi, S.H. Heinemann, CO-independent modification of K(+) channels by tricarbonyldichlororuthenium (II) dimer (CORM-2), Eur. J. Pharmacol. 815 (2017) 33–41.
[38] V.G. Nielsen, The anticoagulant effect of Apis mellifera phospholipase A2 is inhibited by CORM-2 via a carbon monoxide-independent mechanism, J. Thromb. Thrombolysis 49 (2020) 100–107.
[39] H.M. Southam, T.W. Smith, R.L. Lyon, C. Liao, C.R. Trevitt, L.A. Middlemiss, F.L. Cox, J.A. Chapman, S.F. El-Khamisy, M. Hippler, M.P. Williamson, P.J.F. Henderson, R.K. Poole, A thiol-reactive Ru(II) ion, not CO release, underlies the potent antimicrobial and cytotoxic properties of CO-releasing molecule-3, Redox Biol 18 (2018) 114–123.
[40] T. Soboleva, L.M. Berreau, 3-Hydroxyflavones and 3-Hydroxy-4-oxoquinolines as carbon monoxide-releasing molecules, Molecules 24 (2019).
[41] E. Palao, T. Slanina, L. Muchova, T. Solomek, L. Vitek, P. Klan, Transition-metal-free CO-releasing BODIPY derivatives activatable by visible to NIR light as promising bioactive molecules, J. Am. Chem. Soc. 138 (2016) 126–133.
[42] Z. Pan, V. Chittavong, W. Li, J. Zhang, K. Ji, M. Zhu, X. Ji, B. Wang, Organic CO prodrugs: structure-CO-release rate relationship studies, Chemistry 23 (2017) 9838–9845.

2.2 Cell viability testing after CORM-401 exposure

According to the findings presented in *Manuscript* 2, CORM-401 was selected as a suitable CO delivering system and used in all further studies. For toxicity testing and dose finding the sulforhodamine B (SRB) assay was applied on MEFs using different concentrations and treatment durations with CORM-401, iCORM-401 or medium only for control. In the SRB assay the protein amount of living (adherent) cells is determined and the assay was performed as described elsewhere (Stucki et al., 2018). In brief, cells were treated as indicated and fixed with 10 % TCA (w/v) for 1 h at 4 °C after 30, 90 or 240 min of exposure, respectively. Staining of total protein amount per well was performed using SRB dye solved in 1 % acetic acid. Fixed samples were then washed with 1 % acetic acid and SRB extraction was performed with 10 mM Tris. Next, absorbance at $\lambda = 492$ nm was measured with a plate reader (Tecan, Infinite M200). Values of positive control (0.1 % Triton X-100) were used for background subtraction. Cell viability was calculated relative to untreated control, which was set to 100 %.

Upon CORM-401 treatment (10 – 100 µM), viability of cells was not affected after 30 or 90 min of exposure, respectively (Fig. 3A). At an incubation time of 240 min, cell viability was about 90 % of control at the 50 µM level and significantly decreased to about 80 % at 100 µM CORM-401. Treatment of cells with iCORM-401 for 240 min had no effect on cell viability (Fig. 3B). Hence, 50 µM was selected as a non-cytotoxic CORM-401 concentration to be used in further experiments with MEFs in a time frame of 0 to 240 min.

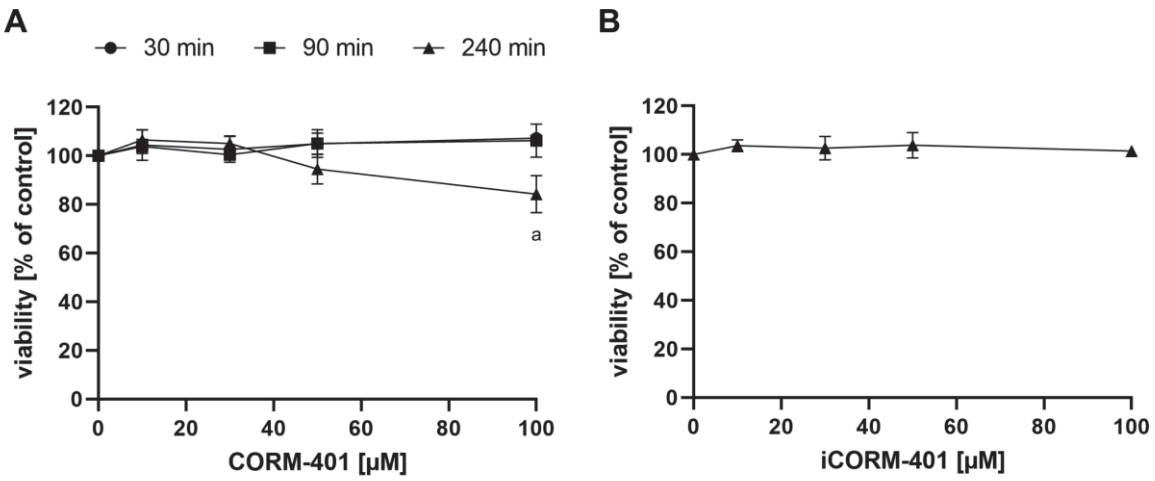

Figure 3: Effects of CORM-401 and iCORM-401 on cell viability of MEFs. Cellular viability of MEFs was determined with the SRB assay. Different concentrations of CORM-401 (A) and iCORM-401 (B) were tested. Control was set to 100% cell viability; positive control (0.1 % Triton X-100) was used for background subtraction. Data is given as mean of three independent experiments ± SD. Statistical analysis was performed using one-way ANOVA with a: control vs CORM-401 with $p \leq 0.05$.

2.3 *Manuscript 3*: Endogenous Carbon Monoxide Signaling Modulates Mitochondrial Function and Intracellular Glucose Utilization: Impact of the Heme Oxygenase Substrate Hemin

David Stucki[1], Julia Steinhausen[1], Philipp Westhoff[3], Heide Krahl[1], Dominik Brilhaus[3], Annika Massenberg[1], Andreas PM Weber[2], Andreas S Reichert[1], Peter Brenneisen[1] and Wilhelm Stahl[1]

[1] Institute of Biochemistry and Molecular Biology I, Medical Faculty, Heinrich Heine University Düsseldorf, D-40001 Düsseldorf, Germany.
[2] Institute of Plant Biochemistry, Cluster of Excellence on Plant Sciences (CEPLAS), Heinrich Heine University Düsseldorf, D-40001 Düsseldorf, Germany.
[3] Plant Metabolism and Metabolomics Laboratory, Cluster of Excellence on Plant Sciences (CEPLAS), Heinrich Heine University Düsseldorf, D-40001 Düsseldorf, Germany.

Received: 5th June 2020; Accepted: 17th July 2020; Published: 23rd July 2020

Published in: *Antioxidants*, **9**: 652.

DOI: 10.3390/antiox9080652

Contribution statement:
D.S. contributed to conceptualization and supervision of the study, performed all experiments except of metabolome analysis and extracellular flux analysis with MCF-7 cells. D.S. analyzed and visualized all experiments, wrote the main part of the original draft and contributed to review & editing of the manuscript.

Graphical abstract:

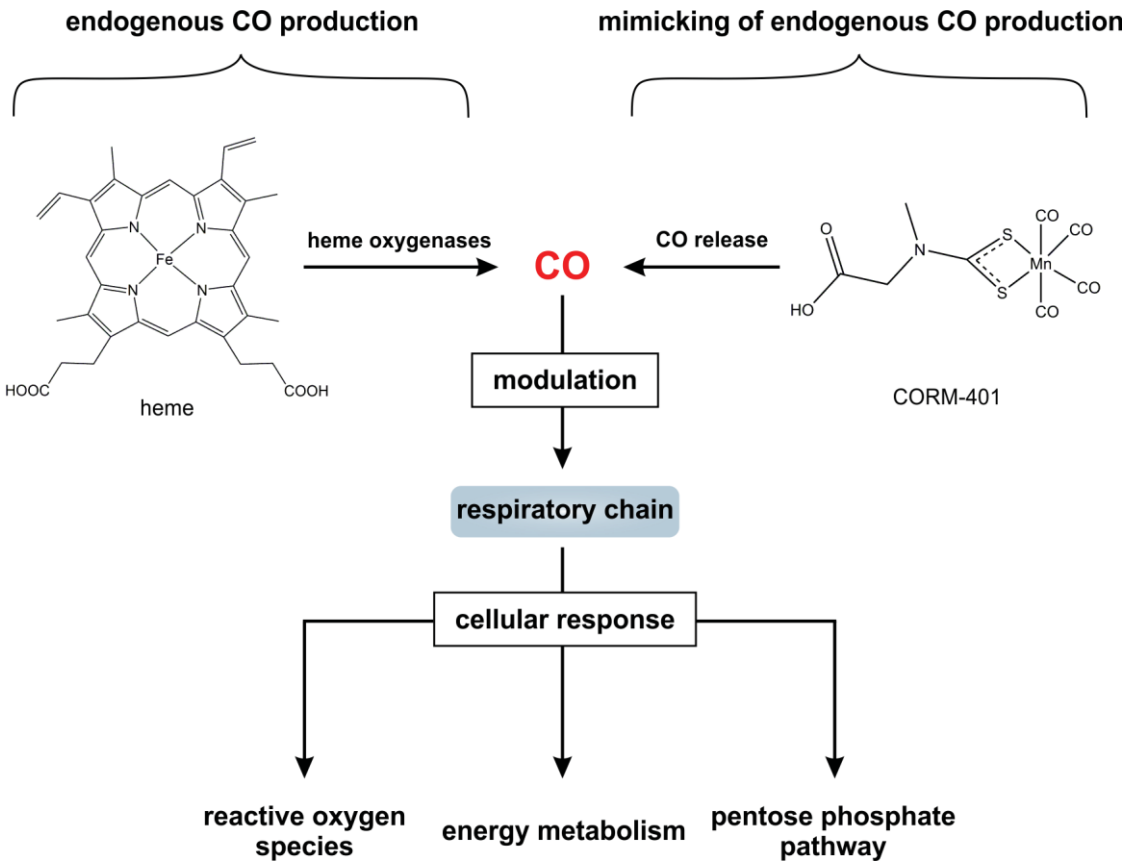

antioxidants

MDPI

Article

Endogenous Carbon Monoxide Signaling Modulates Mitochondrial Function and Intracellular Glucose Utilization: Impact of the Heme Oxygenase Substrate Hemin

David Stucki [1], Julia Steinhausen [1], Philipp Westhoff [2], Heide Krahl [1], Dominik Brilhaus [2], Annika Massenberg [1], Andreas P. M. Weber [3], Andreas S. Reichert [1], Peter Brenneisen [1] and Wilhelm Stahl [1,*]

1 Institute of Biochemistry and Molecular Biology I, Medical Faculty, Heinrich Heine University Düsseldorf, D-40001 Düsseldorf, Germany; david.stucki@hhu.de (D.S.); julia.steinhausen@hhu.de (J.S.); heide.krahl@hhu.de (H.K.); anmas104@hhu.de (A.M.); reichert@hhu.de (A.S.R.); peter.brenneisen@hhu.de (P.B.)

2 Plant Metabolism and Metabolomics Laboratory, Cluster of Excellence on Plant Sciences (CEPLAS), Heinrich Heine University Düsseldorf, D-40001 Düsseldorf, Germany; philipp.westhoff@hhu.de (P.W.); dominik.brilhaus@hhu.de (D.B.)

3 Institute of Plant Biochemistry, Cluster of Excellence on Plant Sciences (CEPLAS), Heinrich Heine University Düsseldorf, D-40001 Düsseldorf, Germany; andreas.weber@uni-duesseldorf.de

* Correspondence: wilhelm.stahl@hhu.de; Tel.: +49-211-811-2711

Received: 5 June 2020; Accepted: 19 July 2020; Published: 23 July 2020

Abstract: Stress-inducible heme oxygenase-1 (HO-1) catalyzes the oxidative cleavage of heme yielding biliverdin, ferrous iron, and carbon monoxide (CO). Heme oxygenase activity has been attributed to antioxidant defense via the redox cycling system of biliverdin and bilirubin. There is increasing evidence that CO is a gaseous signaling molecule and plays a role in the regulation of energy metabolism. Inhibitory effects of CO on the respiratory chain are well established, but the implication of such a process on the cellular stress response is not well understood. By means of extracellular flux analyses and isotopic tracing, we studied the effects of CO, either released from the CO donor CORM-401 or endogenously produced by heme oxygenases, on the respiratory chain and glucose metabolism. CORM-401 was thereby used as a tool to mimic endogenous CO production by heme oxygenases. In the long term (>60 min), CORM-401-derived CO exposure inhibited mitochondrial respiration, which was compensated by increased glycolysis accompanied by a loss of the ATP production rate and an increase in proton leakage. This effect pattern was likewise observed after endogenous CO production by heme oxygenases. However, in the present setting, these effects were only observed when sufficient substrate for heme oxygenases (hemin) was provided. Modulation of the HO-1 protein level was less important. The long-term influence of CO on glucose metabolism via glycolysis was preceded by a short-term response (<30 min) of the cells to CO. Stable isotope-labeling experiments and metabolic flux analysis revealed a short-term shift of glucose consumption from glycolysis to the pentose phosphate pathway (PPP) along with an increase in reactive oxygen species (ROS) generation. Overall, we suggest that signaling by endogenous CO stimulates the rapid formation of reduction equivalents (NADPH) via the PPP, and plays an additional role in antioxidant defense, e.g., via feed-forward stimulation of the bilirubin/biliverdin redox cycling system.

Keywords: heme; heme oxygenase; substrate; respiratory chain; metabolism

1. Introduction

Heme oxygenases (HOs) catalyze the oxidative cleavage of heme to yield biliverdin, ferrous iron, and carbon monoxide (CO). Biliverdin is then further degraded to bilirubin via biliverdin reductase [1]. In mammalian cells, two major isoforms of heme oxygenases, HO-1 and HO-2, are present and located mainly at the endoplasmatic reticulum [2]. While HO-2 is constitutively expressed, the expression of HO-1 is triggered by the nuclear factor (erythroid derived-2)-like 2 (Nrf2)/kelch-like ECH-associated protein 1 (Keap1) system and responds to numerous exogenous and endogenous stressors, including electrophilic compounds or prooxidative stimuli. Among them are several reactive oxygen species (ROS), such as superoxide, hydrogenperoxide, and lipidperoxides, but also transition metals, ultraviolet light, secondary plant constituents, and the natural substrate of HOs, namely heme molecules [3–5]. In this context, an induction of HO-1 expression has been associated with the cellular stress response, in particular as an adaptive mechanism of antioxidant defense [6]. Scavenging of ROS has been attributed to the redoxcycling system of biliverdin and bilirubin, which comprises oxidation of bilirubin by ROS to yield biliverdin and enzymatically catalyzed reduction of biliverdin to bilirubin with nicotinamide adenine dinucleotide phosphate (NADPH) as an electron donor [7].

CO is a highly toxic gas, which binds after inhalation strongly to the heme moiety of hemoglobin and thus impairs oxygen transport and delivery throughout the organism [8]. However, a new aspect of research on CO covers the concept that CO acts as an endogenously produced signaling molecule in line with other gaseous compounds, such as nitric oxide or hydrogen sulfide [9]. Over the past decades, evidence has accumulated that beyond the direct antioxidant system of biliverdin/bilirubin, CO signaling contributes significantly to the HO-mediated cytoprotective effects and coordinates cellular defense. In this context, CO signaling is thought to exert protective effects for organisms and cells under conditions of sepsis, myocardial injury, and fibrosis or inflammation [10–13]. Furthermore, beneficial CO effects have been demonstrated in experimental models of multiple sclerosis [14–16], type I diabetes [17], and systemic lupus erythematosus [18]. Although the mechanisms of action are far from understood, protective properties of low CO doses are widely accepted. Obviously, control of endogenous CO synthesis depends on the enzyme activity of HOs and/or provision of substrate (heme), but these relations are poorly understood.

Intracellular target structures of CO are likely ferrous iron-containing proteins, in particular heme proteins, such as constituents of the respiratory chain or cytochrome P450-dependent monooxygenases [19,20]. Inhibitory effects of CO on the respiratory chain are well established; however, the implication of such a process on the stress response and on altering the energy metabolism of a cell is not well understood. The interplay of CO with the major ATP generating system and resulting shifts in the use and metabolism of energy carriers like glucose and thus the energy status of the cell likely represents a key regulatory hub.

For studying the effects of low CO amounts on cellular processes, CO-releasing molecules (CORMs) have been introduced as valuable research tools [21,22]. CORMs provide a continuous exposure of cells to standardized amounts of CO (in contrast to the application of gaseous CO). From the number of different CORMs, CORM-401 was already shown to be a suitable CO delivery system, especially for studies on the impact of CO on energy metabolism [23]. CORM-401 releases CO only in the close presence of suitable CO acceptors (heme proteins) [24] and therefore ensures controlled intracellular availability of the signaling molecule. In this study, we used CORM-401 as a CO delivery system to mimic effects on cellular energy metabolism and related processes by endogenously generated CO.

2. Materials and Methods

2.1. Chemicals

Tetracarbonyl[N-(dithiocarboxy-κS,κS')-N-methylglycine]manganite(CORM-401), Dulbecco's Modified Eagle's Medium (DMEM, low glucose), manganese sulfate monohydrate, hemin, DMSO, hemin, [U-^{13}C]-glucose, and PBS were from Sigma-Aldrich (Deisenhofen, Germany); methanol

and acetonitrile from Merck (Darmstadt, Germany); trifluoroacetic acid and chloroform were from VWR (Langenfeld, Germany); sodium dodecyl sulfate (SDS) and Tris-(hydroxymethyl)-aminomethan from Roth (Karlsruhe, Germany); and sarcosine-N-dithiocarbamate was obtained from 3B Scientific Corporation (Wuhan, China). All compounds used in the mito stress test or glycolytic rate assay were from Agilent Technologies (Santa Clara, CA, USA).

2.2. Handling of CORM-401 and iCORM-401

CORM-401 was freshly dissolved in PBS (5 mM) and aliquots were stored at −20 °C. The compound is stable under these conditions [23]. CO release from CORM-401 occurs only in the presence of CO acceptors, such as heme proteins [24,25]. In accordance with the literature, an equimolar mixture of sarcosine-N-dithiocarbamate and $MnSO_4$ was used as iCORM-401, the inactive form of CORM-401, as a control for non-CO related effects of CORM-401 [24,26,27]. CORM-401 and iCORM-401 were protected from light at all times.

2.3. Cell Culture

Murine embryonic fibroblasts (MEFs) (a kind gift from Dr. Ishihara [28]), human hepatocellular carcinoma (HepG2) cells (85011430, Sigma-Aldrich, Deisenhofen, Germany), normal human dermal fibroblasts (NHDFs) (C-12300, Promocell, Heidelberg, Germany), and human mammary gland breast cancer (MCF-7) cells (HTB-22, ATCC, Wesel, Germany) were cultured in DMEM (low glucose), supplemented with 10% fetal bovine serum (FBS, PAN-Biotech, Aidenbach, Germany), penicillin (100 U/mL), streptomycin (100 µg/mL), and GlutaMAX™ (2 mM) at 37 °C and 5% CO_2 in a humidified atmosphere.

All cells were washed and supplied with XF assay medium (see next paragraph) for 1 h prior to treatment. Cell confluency was about 70–90% before the start of experiments. If not stated otherwise, treatment was also performed using XF assay medium.

2.4. Extracellular Flux Analyses

Extracellular flux (XF) analyses were performed with an XFe96 analyzer (Agilent Technologies, Santa Clara, CA, USA). All XF analyses were performed in a DMEM-based XF assay medium (103575-100, Agilent Technologies, Santa Clara, CA, USA) supplemented with glucose (1 g/L), GlutaMAX™ (2 mM) and sodium pyruvate (1 mM), but without FBS, antibiotics, and phenol red. For experiments 7500 MEFs, 12,000 NHDFs, 15,000 HepG2 or 50,000 MCF-7 cells per well were plated in XFe96 well plates and incubated for 24 h in normal cell culture medium at 37 °C and 5% CO_2. After culture medium was changed, cells were placed in a non-CO_2 incubator (37 °C) for 1 h prior to experiments. A XFe96 sensor cartridge was loaded with 20 µL of CORM-401 or iCORM-401 solutions or medium (control). Final concentrations of compounds in the wells were 50 µM. During the experiment, the oxygen consumption rate (OCR) and extracellular acidification rate (ECAR) were determined in consecutive measurement cycles. One measurement cycle consisted of 3 min mixing and 3 min measuring.

Next to the basic XF analyses described above, the so-called "mito stress test" was performed for further characterization of the effects on cellular respiration. In the mito stress test, modulators of the respiratory chain are injected in the order: oligomycin (MEF and NHDF: 1 µM; HepG2 and MCF-7: 2 µM), carbonyl cyanide-*p*-trifluoromethoxyphenylhydrazone (FCCP) (MEF, NHDF and HepG2: 1 µM; MCF-7: 0.5 µM), rotenone + antimycin A (0.5 µM each). Differences in OCR levels between injections give the parameters maximal respiration, ATP production, proton leak (here the term "proton leak" is used to describe the process of protons moving from the mitochondrial intermembrane space into the matrix independently of ATP synthase), and non-mitochondrial respiration. Maximal respiration is defined as the highest OCR value after FCCP injection minus non-mitochondrial respiration (OCR after rotenone + antimycin A injection). ATP production is defined as the difference of the last OCR value before oligomycin injection and the lowest OCR value after oligomycin injection but before FCCP injection. Proton leak is defined as the lowest OCR value after oligomycin but before FCCP injection

minus non-mitochondrial respiration. The mito stress test was either performed after acute injection of CORM-401/iCORM-401 or acute KCN injection or after 4 h of pre-incubation with the heme oxygenase substrate hemin. Upon dilution in aqueous solutions, hemin decomposes to Cl^- and heme, the natural substrate of heme oxygenases. Cells were then stained for DNA amount with SYBR™ green according to the manufacturer's instructions (ThermoFisher) and fluorescence signal (λ_{ex}: 492 nm/λ_{em}: 520 nm) was measured with a plate reader (Tecan, Infinite M200). Data achieved after pre-incubation of cells with hemin was normalized to SYBR™ green fluorescence. In another set of experiments using MEFs, first oligomycin was added to reaction wells and then 50 μM CORM-401/iCORM-401 or medium for control. OCR and ECAR levels were then monitored over time.

Another assay performed with XF technology is the glycolytic rate assay. The glycolytic rate assay provides information about basal glycolytic rates as well as glycolytic compensatory capacities upon inhibition of the mitochondrial respiratory chain. Extracellular acidification after acute injection of CORM-401/iCORM-401 or medium only (control) gives the induced glycolysis. Following this, rotenone + antimycin A (0.5 μM each) were injected, provoking a glycolytic compensation for inhibition of mitochondrial respiration (compensatory glycolysis). Addition of 2-deoxyglucose (55 mM) inhibits hexokinase and was used to verify that extracellular acidification is glycolysis-based.

2.5. Transfection of Cells and Gene Silencing

MEFs were transfected 24 h prior to experiments via reverse transfection. For overexpression experiments, 1 μg pCMV3-Hmox1 or the corresponding empty vector (MG52753-UT and CV011, Sino Biological, Eschborn, Germany) and Lipofectamine™ 2000 transfection reagent (ThermoFisher, Schwerte, Germany) were mixed in a reaction tube for 10 min to form transfection complexes. Transfection complexes were then gently mixed with a cell suspension of 100,000 MEFs per mL and cells were subsequently plated on appropriate dishes and plates.

For gene silencing experiments, RNAiMAX transfection reagent (ThermoFisher) was mixed with Hmox1 siRNA mix (GS15368) or negative siRNA (SI03650318, Qiagen, Hilden, Germany) in a reaction tube (final concentration of siRNA: 20 nM), and incubated for 10 min to allow formation of reaction complexes. Transfection complexes were then gently mixed with an MEF cell suspension (100,000 cells/mL) and cells were plated on appropriate dishes and plates.

2.6. SDS PAGE and Western Blot Analysis

For Western blot analysis, cells were lysed with 1% SDS, supplemented with a protease inhibitor cocktail (Roche, Grenzach, Germany). Protein determination was performed using the DC™ protein assay kit from Biorad (Munich, Germany). Equal amounts of total protein (~30 μg) were subjected to SDS-PAGE (12% gels), followed by electro blotting of proteins onto polyvinylidene difluoride (PVDF) membranes (pore size 0.45 μm, GE Healthcare, Solingen, Germany). Blots were developed with the ECL system provided by Cell Signaling Technology (Frankfurt a. Main, Germany) and chemiluminescence signals were monitored using the Fusion SL Advance gel documentation device (Peqlab, Erlangen, Germany). Primary antibodies from rabbits were used: Anti-heme oxygenase-1 (ab52947) was from Abcam (Cambridge, UK); anti-β-tubulin (9F3), anti-hexokinase I (C64G5), anti-GAPDH (D16H11), and anti-pyruvatedehydrogenase (PDH; C54G1) from Cell Signaling (Leiden, Netherlands). Secondary antibodies were horseradish peroxidase (HRP)-coupled goat anti-rabbit IgG (111-035-144) from Dianova (Hamburg, Germany). Equal loading of gels was confirmed using signals from β-tubulin or coomassie blue staining.

2.7. Metabolomics

About 1.8×10^6 MEFs per dish were plated on 10-cm dishes 48 h prior to the experiment. Cells were then supplied with XF assay medium for 1 h containing 1 g/L [U-^{12}C]-glucose. Treatment of cells with 50 μM CORM-401/iCORM-401 or medium only (control) was then performed in XF assay medium containing 1 g/L [U-^{13}C]-glucose. Before the start of the incubation (0 min) and at time points of

30, 90 and 240 min, cells were washed with ice cold PBS, resuspended in PBS, and transferred to reaction tubes. Samples were then centrifuged at 800 *g* and 4 °C for 5 min. The supernatant was discarded, and the cell pellet resuspended in 500 µL 22% water, 22% chloroform, and 46% methanol (*v*/*v*/*v*) for lysis of cells. Samples were then centrifuged at 14,000 *g* at 4 °C for 10 min and 100 µL of the supernatant (extract) were transferred to a glass inlet and dried by lyophilization for ion chromatography—mass spectrometry (IC-MS) analysis. The residual 400 µL were stored at −80 °C as a sample backup. For IC-MS measurements, a combination of a Dionex ICS-6000 HPIC and a Thermo Fisher Scientific Q Exactive Plus mass spectrometer was used according to a method described by others previously [29] with slight modifications. In brief, the dried sample was reconstituted in 100 µL of deionized water of which 5 µL were injected via a Dionex AS-AP autosampler. For the anion exchange chromatography, a Dionex IonPac AS11-HC column (2 mm × 250 mm, 4 µm particle size, Thermo Fisher Scientific) equipped with a Dionex IonPac AG11-HC guard column (2 mm × 50 mm, 4 µm, Thermo Fisher Scientific) was used and the mobile phase was generated using an eluent generator with a potassium hydroxide cartridge starting at 10 mM KOH. The mass spectrometer operated in negative mode with a combination of full mass scan and a data-dependent Top5 MS2 (ddMS2) experiment with a resolution of 140,000 and 17,500 respectively. Data analysis was conducted using Compound Discoverer (version 3.1, Thermo Fisher Scientific). The standard workflow for stable isotope labeling from Compound Discoverer was chosen and the default settings were used, which are 5 ppm mass tolerance, 30% intensity tolerance, and 0.1% intensity threshold for isotope pattern matching. As an additional level of validation, an in-house database for retention times and MS^2 spectra was created using mzVault (Thermo Fisher Scientific) and implemented in the annotation workflow.

2.8. Analysis of 2-Hydroxyethidium Formation via HPLC

About 2×10^5 MEFs per dish were plated on 6 cm dishes 24 h prior to the experiment. Cells were then washed with Hank's Balanced Salt Solution (HBSS) and loaded with 20 µM dihydroethidium (DHE) in HBSS for 30 min. Cells were washed again and treated with 50 µM CORM-401 or iCORM-401 in HBSS or HBSS only (control) for 30 min. Subsequently, cells were washed with ice-cold PBS and resuspended in 1 mL of PBS. Samples were centrifuged at 800 *g* for 3 min at 4 °C. The supernatant was discarded and the pellet resuspended in 200 µL of methanol/acetonitrile/water/TFA (40/40/20/0.1; *v*/*v*/*v*/*v*) for lysis of cells, and centrifuged at 14,000 *g* for 10 min at 4 °C. Cell pellets were kept for protein determination as described previously with slight modifications [30]. Briefly, cell pellets were air dried, resuspended in 63 mM Tris/HCl buffer (pH 6.8) containing 2% SDS, and stored at −20 °C until further use. Samples were then sonicated, and the total protein amount was determined as described above. The HPLC system consisted of a Merck-Hitachi L-7100 pump connected with a fluorescence detector (Merck-Hitachi L-7480) and a data registration system. HPLC was performed with a mobile phase of 21% acetonitrile, 79% water, and 0.1% TFA (*v*/*v*/*v*) at a flow rate of 2.0 mL/min. A Suplex™ pKb-100 column (250 × 4.6 mm, 5 µm) from Sigma-Aldrich was used as the stationary phase. Cellular extracts were diluted 1:2 with the mobile phase and directly injected into the HPLC system. 2-Hydroxyethidium (2-OH-E^+) was measured at λ_{ex} = 480 nm/λ_{em} = 580 nm and a retention time of about 9 min. Signal areas were normalized to the total protein amount and the control, which was set to 1.

2.9. Statistical Analysis

If not stated otherwise, data is given as the mean of three independent experiments (n = 3) and error bars represent the standard deviation (SD). Data were analyzed either using unpaired Student's t-test or one-way ANOVA, with $p \leq 0.05$ being considered a statistically significant difference.

3. Results

3.1. Extracellular Flux Analysis Shows a Distinct Modulation of Cellular Respiration and Glycolysis by CO

CO is known to inhibit cellular respiration via binding to heme proteins of the mitochondrial electron transport chain. Thus, we first examined in MEFs the effects of CORM-401 and inactive CORM-401 (iCORM-401) on cellular respiration and extracellular acidification (as a marker for glycolysis) by means of extracellular flux technology. Cellular response to CORM-401 administration followed a time-dependent two-phase profile. In the first phase (<60 min), directly after the application of 50 μM CORM-401, a moderate and transient increase of the cellular oxygen consumption rate (OCR) (third measurement point in Figure 1A) occurred. In the second phase (>60 min), a continuous decrease of OCR was observed as expected upon inhibition of mitochondrial respiration by CO (Figure 1A), confirming the validity of the experimental setting for MEFs. Concomitantly, the extracellular acidification rate (ECAR) transiently decreased within the first 30 min after CORM-401 injection and only increased above the control at later time points (>60 min) (Figure 1B). Treatment of cells with iCORM-401 did not affect OCR and ECAR compared to the control.

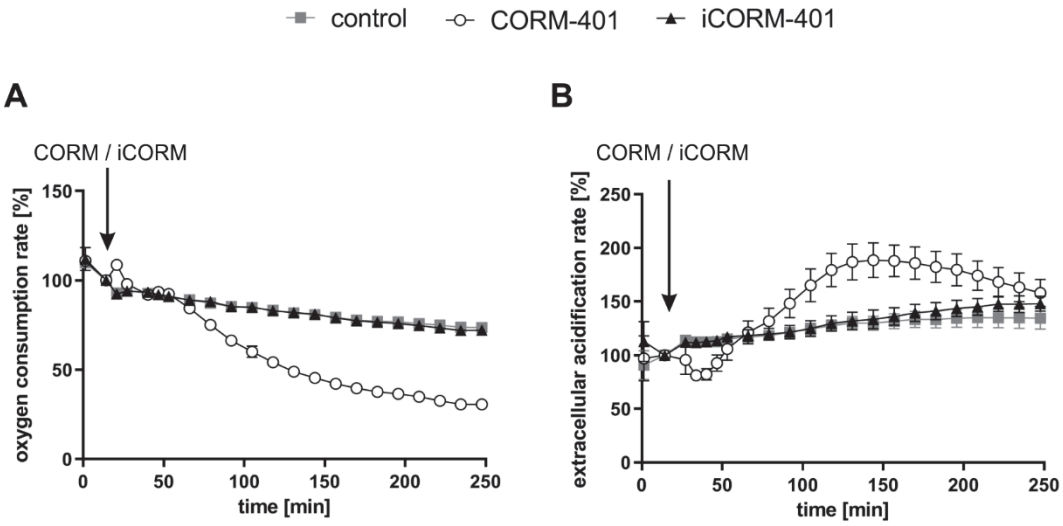

Figure 1. Extracellular flux technology reveals CO-dependent modulation of cellular respiration and extracellular acidification by CORM-401. CORM-401 and iCORM-401 were injected (indicated by arrows) into reaction wells and OCR (**A**) and ECAR (**B**) were measured over time. Final concentration of compounds: 50 μM. Three independent experiments were performed (n = 3). Representative OCR and ECAR curves are shown. Data represent mean ± SD of at least six technical replicates. OCR = oxygen consumption rate, ECAR = extracellular acidification rate.

3.2. The Mito Stress Test Reveals a CO-Specific Effect Pattern after Treatment of Different Cell Types with CORM-401

Modulation of mitochondrial function by CORM-401 during the first phase (<60 min) after the start of exposure was further analyzed with the mito stress test. In this assay, modulators of the mitochondrial electron transport chain are sequentially added to cells and the parameters ATP production, maximal respiration, or proton leakage (for details, see the materials and methods section) can be calculated from the differences in OCR levels before and after the addition of the compounds. CORM-401, iCORM-401, or medium (control) were injected into the reaction wells directly before the mito stress test was started. Directly after the application of CORM-401 (50 μM), cellular OCR was slightly increased (Figure 2A), confirming the results from experiments shown in Figure 1A. Subsequent inhibition of the ATP synthase by oligomycin only led to a moderate drop of cellular OCR, according to a decreased mitochondrial ATP production in the CORM-401 treatment group,

as compared to the control. Addition of the uncoupling agent FCCP to the test system increased OCR and the increase is a measure for maximal respiration of cells. In comparison to iCORM-401 and control, maximal respiration was lower in cells treated with CORM-401. With the final application of rotenone and antimycin A, inhibitors of complex I and III, respectively, the electron transport chain is completely inhibited. The remaining OCR reflects only oxygen-consuming processes not related to the mitochondrial respiratory chain. Here, no major differences were found between treatment groups.

Coupling of substrate oxidation and ATP synthesis is usually not complete, as protons move from the mitochondrial intermembrane space into the matrix independently of ATP synthase. Such proton transfer processes are collectively termed "proton leak" and can be calculated in the present setting from the difference of OCR after oligomycin injection and after rotenone and antimycin A injection. Proton leak in cells treated with CORM-401 was dramatically increased whereas iCORM-401 treatment had no effect (Figure 2D). A schematic depiction of the OCR curves from Figure 2A and the resulting parameters is given in Figure S1.

The quantification and dose dependency of the parameters described above are summarized in Figure 2B–D and statistically significant differences are given in Table S1. None of the parameters were affected by the lowest concentration of CORM-401, indicating 10 μM as a threshold concentration for CO activity of the compound. At higher levels (30–100 μM), CORM-401 significantly decreased maximal respiration in a dose-dependent manner, to a residual activity of about 30% of the control at 100 μM (Figure 2B). ATP production also concentration dependently decreased upon CORM-401 treatment. After the treatment of cells with 50 μM CORM-401, ATP production was lowered by 50%; however, no further decrease was found at the 100 μM level (Figure 2C). Opposing this, proton leak was significantly increased following CO exposure (Figure 2D). At 50 μM CORM-401, proton leak was about 4-fold higher compared to the control, but this effect was not enhanced at 100 μM. A CO-dependent induction of proton leakage by CORM-401 was also demonstrated in another experimental setting. First, ATP synthase was inhibited by oligomycin injection, leading to a direct decrease of cellular OCR (Figure 2E) and a compensatory increase of ECAR (glycolysis) (Figure 2F). Next, CORM-401, iCORM-401, or medium only (control) were added to the reaction wells. While no further change of OCR and ECAR was observed under control and iCORM-401 conditions, CORM-401 led to an increase of OCR levels. Since this increase of respiration is independent of ATP synthase activity, an induction of proton leakage by CO is suggested. Simultaneously, CORM-401 exposure lowered ECAR levels, which were elevated as a compensatory mechanism for the oligomycin-mediated inhibition of ATP synthase.

To demonstrate the general validity of the observed CO effects on parameters of mitochondrial respiration, three more cell types (NHDFs, HepG2 and MCF-7 cells) were subjected to the mito stress test with CORM-401 under the same conditions and almost similar results were observed (Figure S2). For further control, MEFs were subjected to the mito stress test after acute KCN injection. Comparable to CO, cyanide is known to inhibit mitochondrial respiration via binding to the heme moiety of cytochrome *c* oxidase [31]. Increasing concentrations of cyanide decreased maximal respiration and mitochondrial ATP production. However, no effect on proton leakage was found (Figure S3), even if the respiratory chain was not completely inhibited.

In summary, our results demonstrate that modulation of mitochondrial function by CO occurs very fast and presents both inhibitory (decrease of maximal respiration and ATP production) and stimulating (increase of proton leak) effects with respect to cellular respiration. In the first phase after CORM-401 exposure (<60 min), inhibitory and stimulating effects likely counteract each other and no major effects on basal OCR are found, whereas in the second phase (>60 min), inhibitory effects are predominating and total cellular OCR is lowered.

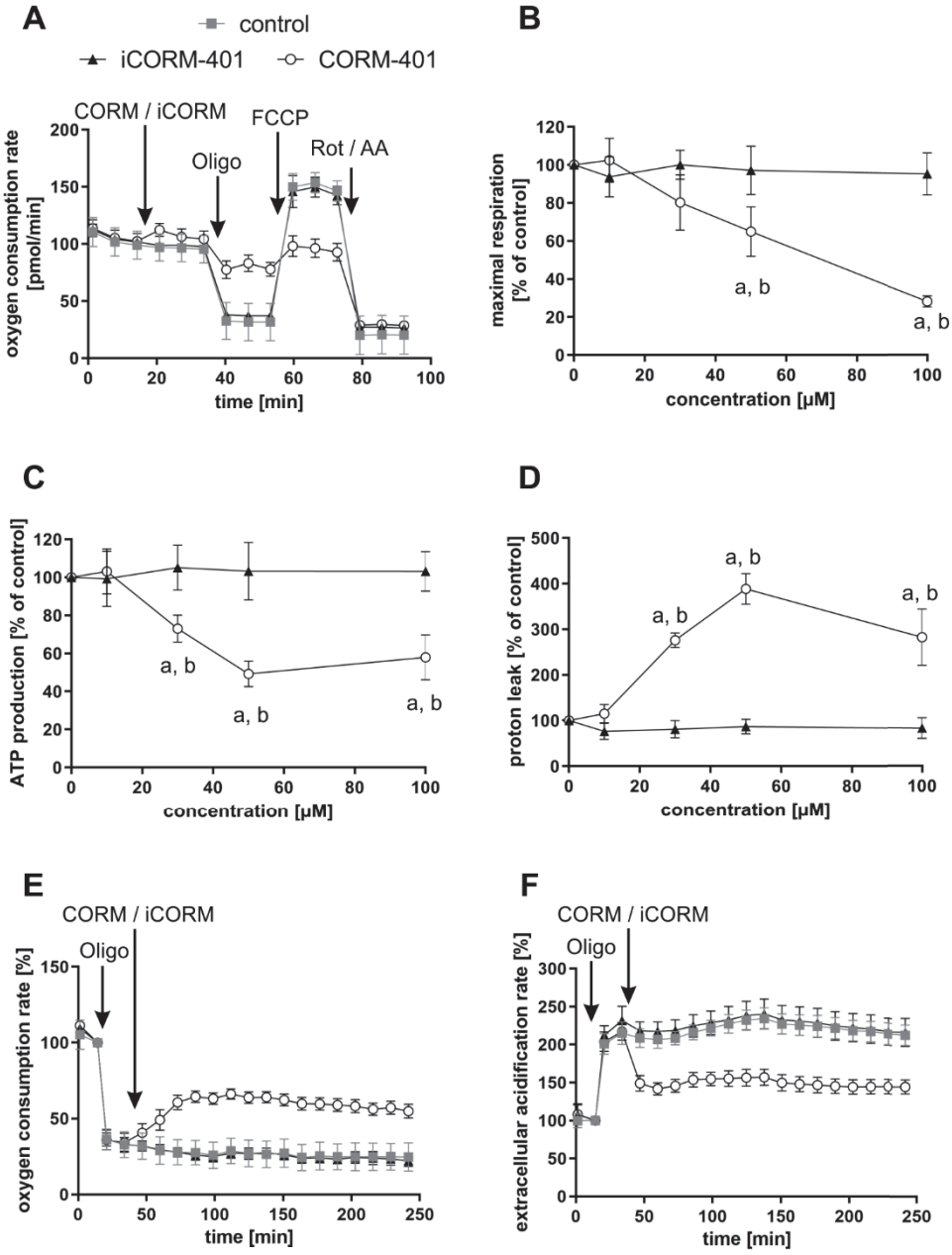

Figure 2. Modulation of mitochondrial respiratory parameters by CO results in a specific effect pattern. CORM-401 and iCORM-401 were injected into reaction wells and the mito stress test (sequential injection of oligomycin, FCCP, and rotenone + antimycin A) was performed. Injections are indicated by arrows. Representative OCR curves are given (**A**) with the final concentration of CORM-401/iCORM-401: 50 µM. Data represent mean ± SD of at least six technical replicates. Quantification of the mitochondrial respiratory parameters maximal respiration (**B**), ATP production (**C**), and proton leak (**D**) is shown for 10–100 µM CORM-401/iCORM-401. Data represent mean ± SD of three independent experiments (n = 3). In a modified experimental setting, first oligomycin and then 50 µM CORM-401 or iCORM-401 were applied and OCR (**E**) and ECAR (**F**) were monitored over time. Representative OCR and ECAR curves of three independent experiments are shown. Data represent mean ± SD of at least six technical replicates. OCR = oxygen consumption rate, ECAR = extracellular acidification rate, Oligo = oligomycin, Rot/AA = rotenone + antimycin A. Statistical analysis was performed using one-way ANOVA and detailed results are given in Table S1. a: control vs. CORM-401, b: CORM-401 vs. iCORM-401 with $p \leq 0.05$.

3.3. Substrate Availability is Involved in the Regulation of Endogenous CO Production

Endogenously, CO is produced upon degradation of heme by heme oxygenases, with HO-1 as a stress-inducible form. To test whether CO-dependent effects observed after CORM-401 treatment can be recapitulated with endogenously generated CO, MEFs were transfected with a plasmid encoding for the *Hmox1* gene (HO-1 group) or an empty vector for the control. HO-1 protein levels were elevated in the HO-1 group compared to the control as confirmed by Western blot analysis (Figure S4A). Transfected cells were then preincubated with different concentrations of hemin (substrate of heme oxygenases) or medium with 0.1% DMSO (control) for a period of 4 h and then subjected to the mito stress test (Figure 3A–C). In accordance with the previous results obtained with the CO donor CORM-401, maximal respiration and ATP production were decreased, and proton leak increased in a concentration-dependent manner between 5 and 20 μM of hemin. At low concentrations of hemin (2 μM), maximal respiration slightly increased in both groups (Figure 3A). While no major effect on ATP production of cells was found at 2 μM hemin, treatment with higher concentrations (10 and 20 μM) led to a significant decrease of about 50% compared to the untreated control (Figure 3B). Proton leak was found to be elevated at 2 μM hemin to about 160–200% of the control, but this effect was hardly increased at higher concentrations of hemin (Figure 3C). The effects in response to hemin treatment were similar in both groups (empty vector and HO-1).

In the following experiment, cells were transfected with siRNA against *Hmox1* encoded mRNAs or negative siRNA. Depletion of the HO-1 protein amount was confirmed by Western blot analysis, with β-tubulin as the loading control (Figure S4B). Cellular maximal respiration was significantly increased with 2 μM hemin (140–160% of control), but concentration-dependently decreased below the control level at 5–20 μM hemin (Figure 3D). No effect on ATP production was found after incubation of cells with 2 μM hemin, while a decrease to about 60% of the control level was observed at the 5 μM level, which was further decreased to about 45% at concentrations above 10 μM hemin (Figure 3E). The proton leak of cells was significantly increased after treatment with 2 μM hemin to about 200–250% and moderately further increased to about 270% at the 20 μM level (Figure 3F). No major difference was found between both groups (negative siRNA and *Hmox1* siRNA) upon hemin treatment.

In summary, the CO-derived effect pattern in the mito stress test after exposure of cells to the model substance CORM-401 was also observed when cells were supplied with the HO substrate hemin, suggesting endogenous CO production. While HO-1 enzyme levels were not limiting under these conditions, sufficient provision of the substrate was demanded to obtain CO effects.

We thereby demonstrated the suitability of CORM-401 to mimic endogenous CO production by heme oxygenases and hence decided to use CORM-401 in the following experiments as a model compound for further analysis of the CO effects on cellular metabolism.

3.4. CO Lowers Compensatory Glycolysis of Cells

Upon inhibition of the mitochondrial respiratory chain, less ATP is produced, which is usually accompanied by a compensatory stimulation of glycolysis. In accordance with the inhibitory effect on mitochondrial respiration (Figure 1A, >60 min), we determined a decreased mitochondrial ATP production after CORM-401 treatment (Figure 2 and Figure S2). In the long term (>60 min), we also observed a compensatory increase in ECAR a marker for glycolytic flux (Figure 1B). However, in the first phase (about 30 min) after CORM-401 addition, ECAR was transiently decreased, an observation made in numerous experiments with different cells.

To further study this early effect, a glycolytic rate assay was performed applying CORM-401, iCORM-401, or medium (control) directly before the start of the test. Upon application of CORM-401 (50 μM), ECAR directly decreased below the control level (Figure 4A), which confirms the results of an acute response (<30 min) mentioned above. Such an acute response is termed "induced glycolysis" and this parameter was significantly lowered by CORM-401 treatment in a concentration-dependent manner. While 10 μM CORM-401 had no effect, about 60% residual activity compared to the control was found at the 100 μM level (Figure 4B). Next, rotenone and antimycin A were injected to abolish electron

transfer in the mitochondrial respiratory chain. This treatment induces a compensatory increase of glycolysis accompanied by elevated ECAR levels. However, this compensatory effect was less pronounced in CORM-401-treated cells (Figure 4A) and dose-dependently decreased at concentrations of CORM-401 above 10 µM (Figure 4C). Since the application of iCORM-401 did not affect parameters of the glycolytic rate assay compared to the control, this modulation of glucose metabolism is triggered by CO, which was also reflected in the statistical analysis of the data (Table S3), showing significant differences between the CORM-401 and iCORM-401 treatment groups.

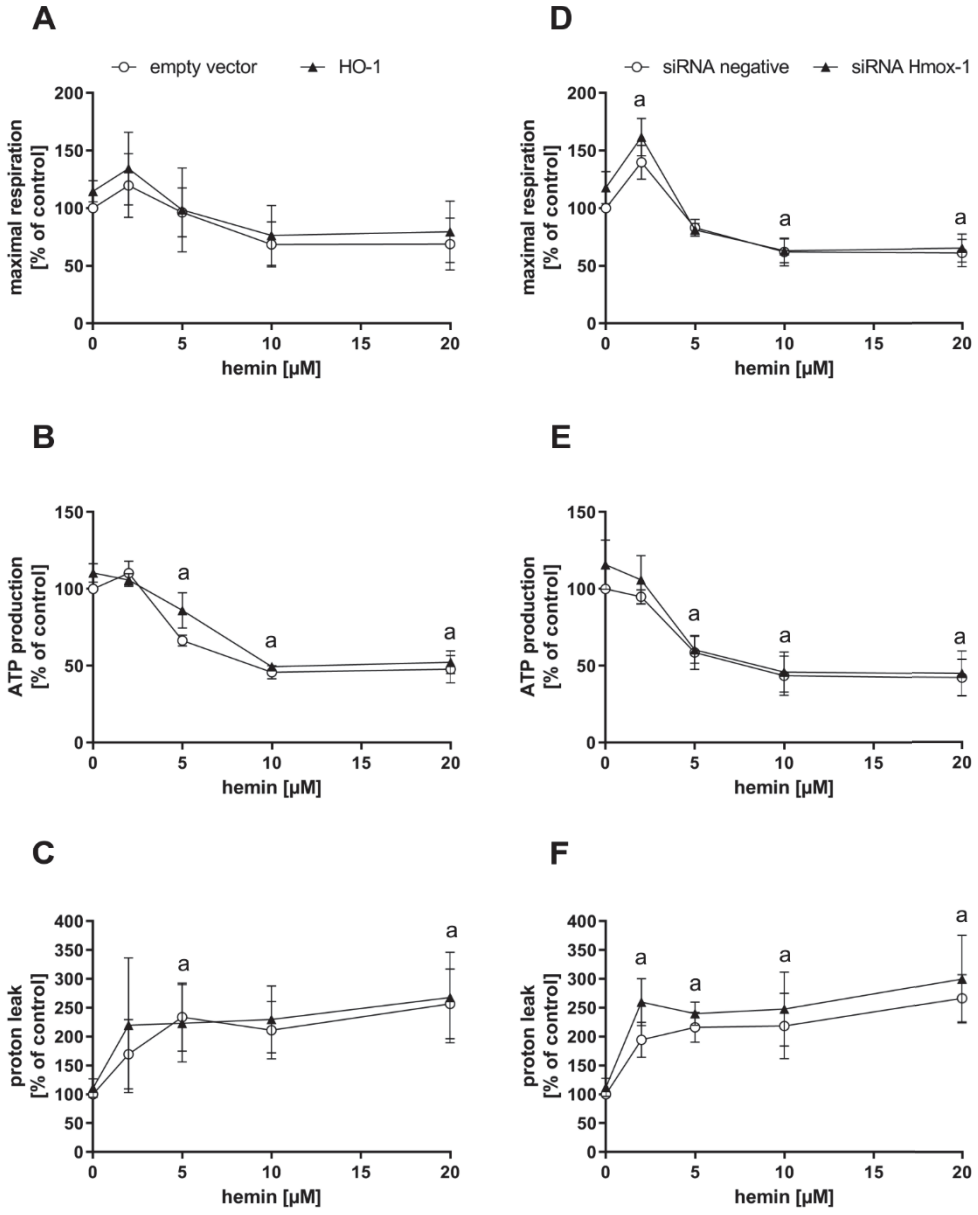

Figure 3. Hemin treatment of cells leads to an effect pattern of mitochondrial respiratory parameters comparable to CO. Heme oxygenase-1 protein levels of MEFs were genetically modified by either overexpression (left panel) or knockdown using siRNA (right panel). Cells were then treated with 2–20 µM hemin for 4 h and subjected to the mito stress test. Quantifications of the mitochondrial respiratory parameters maximal respiration (**A**,**D**), ATP production (**B**,**E**), and proton leak (**C**,**F**) are given. Data represent the mean ± SD of three independent experiments (n = 3). Statistical analysis was performed using one-way ANOVA and detailed results are given in Table S2. a: control vs. treatment with $p \leq 0.05$.

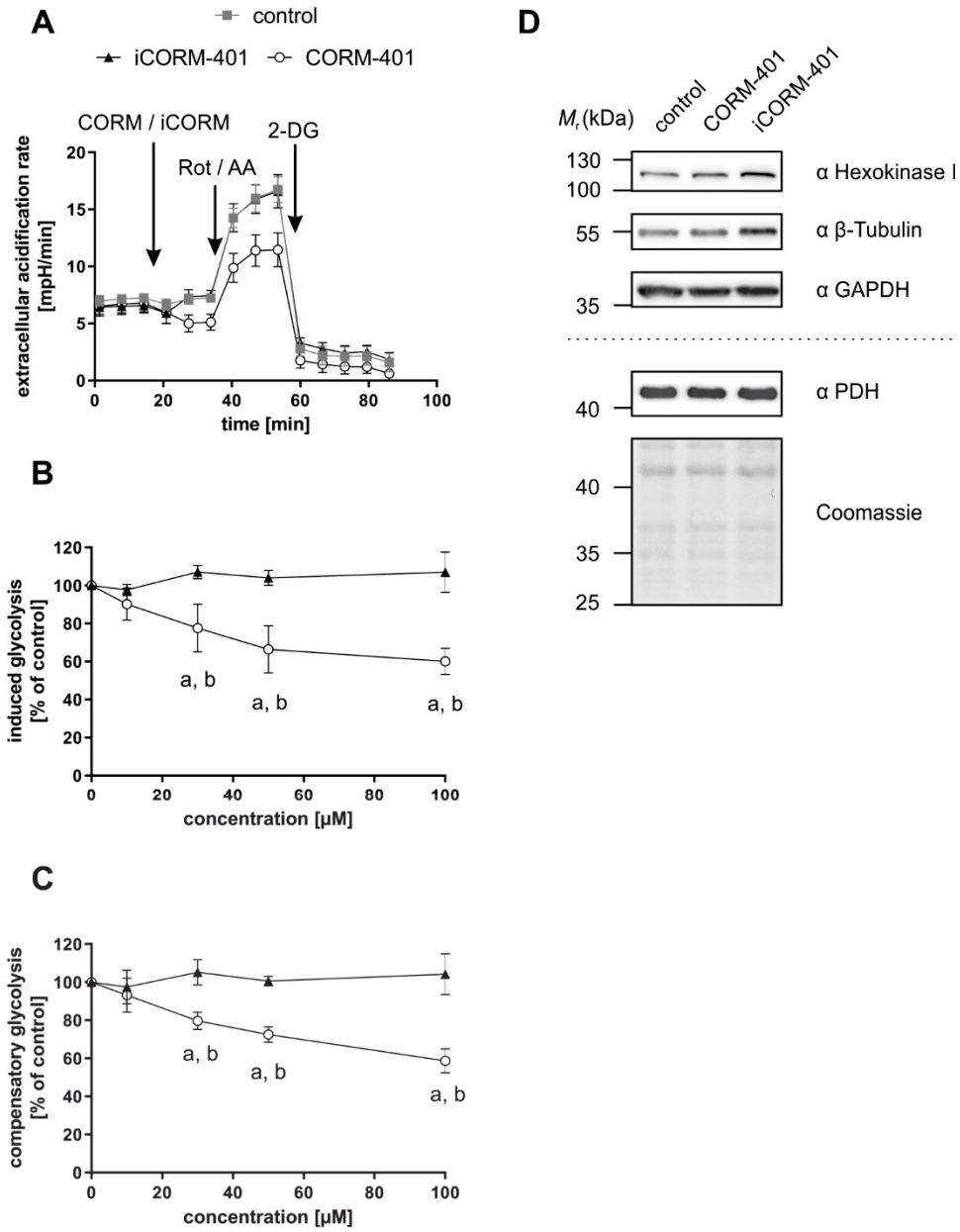

Figure 4. CO-dependent decrease of glycolytic parameters is independent of glycolysis enzyme protein levels. CORM-401 and iCORM-401 were injected into reaction wells and the glycolytic rate assay (sequential injection of rotenone + antimycin A and 2-DG) was performed. Injections are indicated by arrows. Representative ECAR curves are given (**A**) with a final concentration of CORM-401/iCORM-401: 50 µM. Data represent mean ± SD of at least six technical replicates. Quantifications of the glycolytic parameters compensatory glycolysis (**B**) and induced glycolysis (**C**) are shown for 10–100 µM CORM-401/iCORM-401. Data represent mean ± SD of three independent experiments (n = 3). Representative Western blot analyses of glycolysis enzymes after treatment of MEFs with 50 µM CORM-401/iCORM-401 or medium only for 30 min are shown (**D**). The dashed line separates results of two different gels, loaded with the same samples (n = 3). ECAR = extracellular acidification rate, Rot/AA = rotenone + antimycin A, 2-DG = 2-deoxyglucose, PDH = pyruvate dehydrogenase. Statistical analysis was performed using one-way ANOVA and detailed results are given in Table S3. a: control vs. CORM-401, b: CORM-401 vs. iCORM-401 with $p \leq 0.05$.

Changes in the protein levels of glycolytic enzymes do not play a role in this context. Following incubation of cells with 50 μM CORM-401 or iCORM-401, no change in the protein levels of hexokinase I, GAPDH, or PDH were observed by Western blot analysis (Figure 4D). Equal loading of the gels was controlled via β-tubulin analysis or coomassie blue staining, respectively.

Thus, this short-term decrease in glycolysis implies other limiting factors.

3.5. CO Causes a Transient Metabolic Shift from Glycolysis to Pentose Phosphate Pathway

Since the CO-mediated fluctuations of ECAR could not be explained by changes of the protein level, glycolytic activity was assessed by isotopic tracing with [U-^{13}C]-glucose. Cells were loaded with labeled glucose and then treated with 50 μM CORM-401, iCORM-401, or medium only (control). The metabolic pattern was analyzed by means of IC-MS, 30, 90 and 240 min after the addition of CORM-401. Relative exchange rates of uniformly labeled metabolites are shown in Figure 5 and statistical analysis of the data using one-way ANOVA is given in Table S4.

The extracellular acidification rate (ECAR) as a marker for glycolytic flux is a read out related to the final steps of glycolysis. Among the metabolites analyzed by isotopic tracing, phosphoenolpyruvate (PEP) is most downstream in glycolysis. After 30 min of CORM-401 treatment, cells exhibited significantly less labeled PEP (M + 3), compared to control, showing a decreased flux through glycolysis within the first 30 min of CO exposure. Although at later time points (240 min), PEP (M + 3) levels are the same for control and CORM-401 treated cells, the flux is nevertheless increased, indicated by a steeper slope of the CORM-401 curve (dashed line), substantiating the observation from Figure 1B.

Upstream of PEP, this effect is less pronounced. The relative exchange rate of 1,3-bisphosphoglycerate (1,3BPG) M + 3 at 30 min is similar for the treatment and control but is significantly higher upon CORM-401 treatment at later time points (90 or 240 min). Again, the CORM-401 curve exhibits a steeper slope, indicating an increased flux at the late time points.

The ^{13}C label pattern of metabolites in the preparatory phase of glycolysis, such as fructose-1,6-bisphosphate (F1,6BP) or glucose-6-phosphate (G6P), differs from that observed in the pay-off phase. For both metabolites, higher exchange rates are measured already within 30 min of incubation with CORM-401 compared to the control. At later time points, this effect is persistent but not further enhanced as all curves (treatments and control) run in parallel between 30 and 240 min.

Taken together, these findings suggest that glycolytic flux within the first 30 min of incubation with CORM-401 is lower in the pay-off phase and higher in the preparatory phase. Beyond 30 min, the glycolytic flux is elevated upon CO exposure.

It is conspicuous that the labeling of glyceraldehyde-3-phosphate (G3P) does not fit into this pattern. Already at an early time point (30 min) of treatment with CORM-401, a relative exchange rate of about 90% was determined for G3P M + 3 whereas the exchange rate was only 60% for F1,6BP M+6. Since G3P can also be generated in the pentose phosphate pathway (PPP), it is suggested that both pathways (glycolysis and PPP) contribute to the formation of labeled G3P M + 3. The assumption is fostered by the analysis of other metabolites of the PPP.

Typical metabolites, such as 6-phosphogluconate (6PG), ribulose-5-phosphate (Ru5P), sedoheptulose-7-phosphate (S7P), or erythrose-4-phosphate (E4P), exhibit an increased labeling after CORM-401 exposure (30 min), compared to the control. Again, this effect is persistent but not further enhanced as the curves (treatment and control) extend parallel between 30 and 240 min.

In summary, the data provide evidence that upon application of CORM-401, CO immediately causes a transient increase of glucose flux through the PPP, redirecting labeled fragments towards glycolysis via G3P.

It is noteworthy that the relative exchange rates for M + 5 of phosphoribosyl pyrophosphate (PRPP) do not differ between the treatment and control at time points up to 90 min. This suggests that the quick physiological response of the PPP triggered by CO mainly aims to enhance the regeneration or production of NADPH. This is often observed as a compensatory mechanism in defense

of oxidative stress, providing NADPH as a cofactor for glutathione reductase for the maintenance of reduced glutathione.

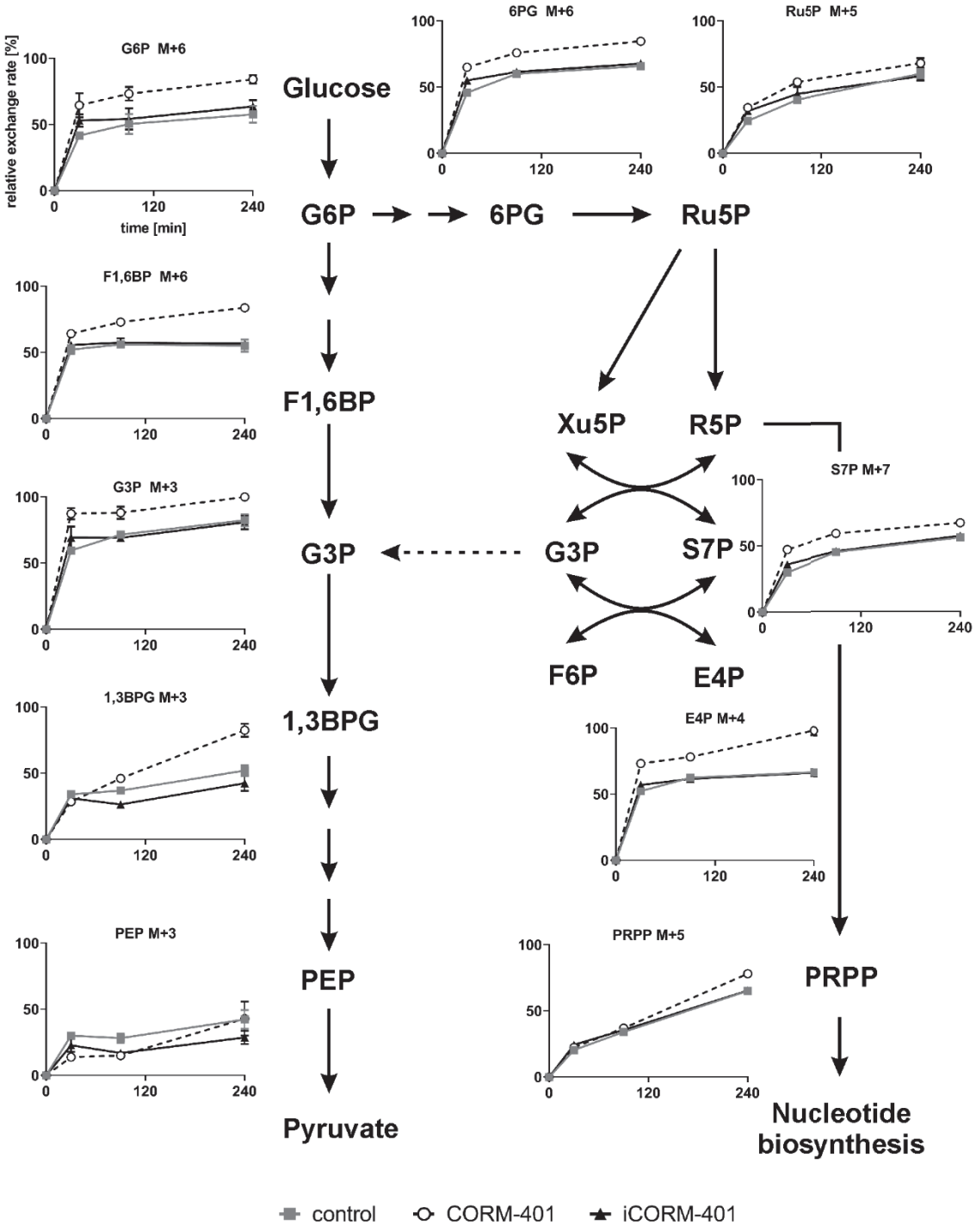

Figure 5. Scheme of the glycolysis and pentose phosphate pathway and the uniform metabolite labeling after simultaneous incubation of cells with [U-^{13}C]-glucose and CORM-401/iCORM-401. MEFs were simultaneously treated with [U-^{13}C]-glucose and 50 μM CORM-401/iCORM-401 or medium only (control), for 30, 90 or 240 min. Cells were then lysed and extracts analyzed via IC-MS analysis. Relative exchange rates of uniformly labeled metabolites are shown as mean ± SD (n = 4). Statistical analysis was performed using one-way ANOVA and results are given in Table S4.

3.6. Exposure of Cells to CORM-401/CO is Associated with a Moderate Increase of Reactive Oxygen Species

Electron leakage of the respiratory chain is a major endogenous source of reactive oxygen species, such as superoxide and hydrogen peroxide. It has been described that the inhibition of mitochondrial respiration by CO is associated with an increased production of ROS [19]. ROS in turn are known inducers of the PPP [32] in order to address the NADPH demand for antioxidant defense systems. Therefore, we investigated whether in the present setting, CORM-401 application leads to an increase in ROS levels. As a measure of ROS formation, oxidation of dihydroethidium (DHE) to 2-hydroxyethidium (2-OH-E^+) was determined by means of HPLC. As shown in Figure 6, about 50% more 2-OH-E^+ was found, in cells treated for 30 min with 50 µM CORM-401, compared to the control and iCORM-401 treatment group.

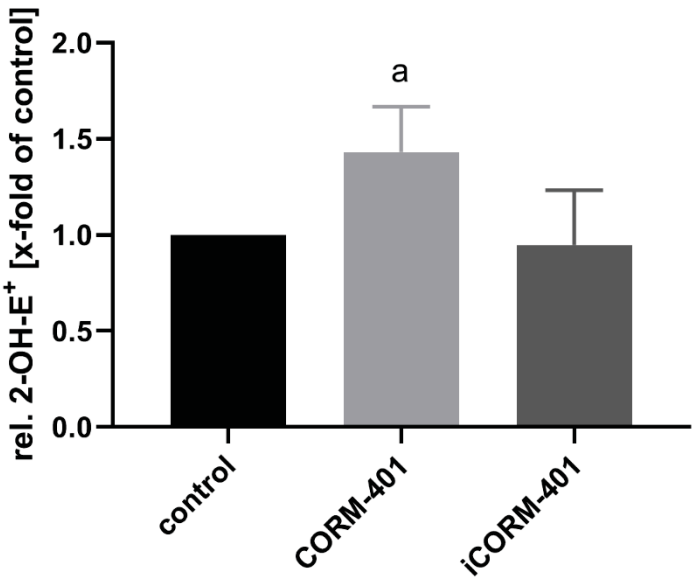

Figure 6. CO from CORM-401 produces a mild oxidative stress. Cells were pre-incubated with 20 µM DHE for 30 min and then treated with 50 µM CORM-401/iCORM-401 for 30 min. Formation of 2-OH-E+ as a marker for superoxide production was monitored using HPLC analysis, quantified via the signal area, and normalized to the total protein amount of cells. Data is given as the relative amount of 2-OH-E+ (control was set to 1) and represents the mean ± SD of three independent experiments (n = 3). Statistically significant differences were evaluated using Student's t-test with a: control vs. CORM-401 and $p \leq 0.05$. DHE = dihydroethidium.

4. Discussion

Induction of HO-1 is mediated by numerous prooxidative stressors from different sources. Among them are physical noxae (radiation), secondary plant constituents, drugs, or pollutants, but also endogenous oxidative challenges related to cell or tissue responses following, e.g., lesions or infections [10,12]. Therefore, this stress-dependent stimulation of HO-1 expression is considered to be a component of the antioxidant network, with redox cycling between biliverdin and bilirubin as a mechanism for scavenging of ROS, such as lipophilic peroxyl radicals [7].

Upon degradation of the HO-1 substrate heme, CO is also generated. It is generally assumed that CO is a gaseous signaling molecule, which may play a role in the stress response and is involved in the cytoprotective events related to HO-1 activation in addition or alternatively to biliverdin/bilirubin redox cycling. One of the main intracellular targets of CO is the mitochondrial respiratory chain, which is in particular inhibited by the binding of CO to the heme moiety of cytochrome *c* oxidase [33,34]. Inhibition is accompanied by an elevated generation of ROS, especially superoxide formation via

one-electron transfer to oxygen [19,35]. At low levels, deliberately generated ROS are also considered to be signaling molecules activating downstream proteins by targeted oxidation [36].

Early events of CO signaling aimed at the respiratory chain can be studied by means of extracellular flux technology and the use of CO-generating systems. These CO-releasing molecules (CORMs) are suitable tools to ensure a continuous supply of intracellular CO and can thus be used to mimic endogenous CO production. As determined with this methodology, the expected inhibition of the respiratory chain after exposure of cells to the CO donor CORM-401 was observed at time points later than 60 min (Figure 1A).

A more detailed analysis of CO-mediated modulation of cellular respiration in the mito stress test revealed a specific pattern of CO-dependent effects comprising a decreased maximal respiration, lowered ATP production, together with an increased proton leakage (Figure 2). These characteristics were found to be very similar in different cell types (Figure S2) and are in accordance with the literature. CORM-401 was found to decrease mitochondrial ATP turnover and maximal respiration while increasing proton leakage in endothelial EA.hy926 cells and 3T3-L1 adipocytes as determined with extracellular flux technology [37,38]. Taken together, the present results underline the validity of our test system, which was further used in the study to investigate the role of HO-1 expression and substrate dependency on endogenous CO production.

In order to study the impact of endogenous CO formation on mitochondrial respiration, we modulated HO-1 protein levels via overexpression and gene silencing. Hemin was applied as a substrate for heme oxygenases and cells were subjected to the mito stress test. Very similar to the observations made with CORM-401 treatment, a decrease in maximal respiration and ATP production was found whereas proton leakage was increased (Figure 3), which is in accordance with the literature [39], thus indicating that HO-dependent production of endogenous CO modulates mitochondrial respiration. Under the conditions applied here, the modulation of mitochondrial respiration was dependent on the amount of the substrate hemin but not on the expression level of HO-1. Therefore, we suggest that availability of the substrate plays a role in the regulation of heme oxygenase-mediated CO signaling.

Hemin was also recently described to exert neuroprotective effects via abrogation of sevoflurane-induced activation of the mitochondrial intrinsic pathway of apoptosis [40]. This was discussed to be mediated via induction of neuroglobin levels; however, CO signaling following hemin degradation by heme oxygenases was not excluded as the mode of action. Interestingly, another metabolite of heme degradation (bilirubin) was also found to modulate mitochondrial function [41]. The authors showed that after long exposure (24 h) of murine adipose tissue to bilirubin, OCR levels were increased. This was discussed to be mediated via binding of bilirubin to peroxisome proliferator-activated receptor-α (PPARα) and subsequently an increased mitochondrial biogenesis. Such a long-term effect probably complements the quicker and more direct regulation of mitochondrial function by CO signaling demonstrated here.

Typically, an inhibition of respiration is associated with less ATP production and a subsequent compensation via increased glycolytic flux, which we also observed as an elevated acidification rate at later time points (>60 min) following treatment with CORM-401 (Figure 1B). However, directly after treatment with CORM-401 (up to 30 min), glycolysis was decreased and stayed below the control level (Figure 1B), suggesting a direct regulatory effect of CO on intracellular glucose utilization, which was further confirmed by the glycolytic rate assay (Figure 4A). Here, compensatory glycolysis was also less pronounced upon CORM-401 exposure (Figure 4C). Glycolysis enzyme levels were excluded as the limiting factor.

We therefore followed the metabolic fate of glucose after CORM-401 administration using [U-^{13}C]-glucose for isotopic tracing (Figure 5). The labeling pattern basically confirmed the extracellular flux data, providing evidence for a transient decrease of glycolysis at early time points (<30 min) followed by an increased flux at later time points (>60 min).

The transient decrease of glycolysis directly after CO exposure is accompanied by a short prominent burst of a flux through the PPP, redirecting metabolites back towards glycolysis via G3P. Such an induction of the PPP by CO has been reported [26,42]; however, we highlight here the dynamic nature of this effect and its interplay with energy-providing glucose metabolism, which has not been described so far. Redirection of PPP metabolites indicates that the major goal of this shift is related to the provision of the reduction equivalent NADPH as an essential element of antioxidant defense. It is interesting to note that this also includes the redox cycling system provided by biliverdin and bilirubin, suggesting that endogenous CO generated by heme oxygenases can mediate a rapid feed-forward stimulation for this pathway. Concomitantly, ROS generation was shown to be elevated after CORM-401 exposure. These observations may shed light on contradictory reports about pro- and antioxidative properties of CO [13,43] and suggest an additional role for heme oxygenases as part of a complex antioxidant network.

5. Conclusions

The present data add further evidence that endogenously generated CO plays a role in cellular stress response. Upon regulation of glucose metabolism by CO, reduction equivalents (NADPH) for antioxidant defense are provided on short term, whereas inhibition of mitochondrial respiration and shift to glycolysis is a later effect. CO signaling mediated by HO activity is in part substrate-regulated and likely complements antioxidant defense, provided by the HO-dependent biliverdin/bilirubin redox cycling system.

Supplementary Materials: The following are available online at http://www.mdpi.com/2076-3921/9/8/652/s1, Figure S1: Schematic depiction of OCR curves from Figure 2A and the resulting calculated parameters, Figure S2: CO-derived effect pattern of mitochondrial respiratory parameters is similar in different cell types, Figure S3: Cyanide application leads to an inhibition of maximal respiration and ATP production, but no increase of proton leakage, Figure S4: Genetical modification of HO-1 protein levels in MEFs, Table S1: Statistical analysis belonging to Figure 2B–D, Table S2: Statistical analysis belonging to Figure 3, Table S3: Statistical analysis belonging to Figure 4B,C, Table S4: Statistical analysis belonging to Figure 5.

Author Contributions: Conceptualization, D.S., P.B. and W.S.; methodology, D.S., J.S., P.W. and D.B.; investigation, D.S., J.S., P.W., H.K. and A.M.; formal analysis, D.S. and P.W.; writing–original draft preparation, D.S. and W.S.; writing–review and editing, D.S., P.W., A.S.R., P.B. and W.S.; funding acquisition, W.S. and A.P.M.W. All authors have read and agreed to the published version of the manuscript.

Funding: This work was funded by the Deutsche Forschungsgemeinschaft (DFG, German Research Foundation) project STA699/3-1 (WS) and additionally funded by the Deutsche Forschungsgemeinschaft (DFG, German Research Foundation) under Germany's Excellence Strategy–EXC-2048/1–project ID 390686111. We are grateful to the 'Cellular Metabolism Platform' at the Medical Faculty of the Heinrich Heine University Düsseldorf for access to the Seahorse Extracellular Flux Analyzer.

Conflicts of Interest: The authors declare no conflict of interest. The funders had no role in the design of the study; in the collection, analyses, or interpretation of data; in the writing of the manuscript, or in the decision to publish the results.

References

1. Tenhunen, R.; Marver, H.S.; Schmid, R. The enzymatic conversion of heme to bilirubin by microsomal heme oxygenase. *Proc. Natl. Acad. Sci. USA* **1968**, *61*, 748–755. [CrossRef] [PubMed]
2. Applegate, L.A.; Noël, A.; Vile, G.; Frenk, E.; Tyrrell, R.M. Two genes contribute to different extents to the heme oxygenase enzyme activity measured in cultured human skin fibroblasts and keratinocytes: Implications for protection against oxidant stress. *Photochem. Photobiol.* **1995**, *61*, 285–291. [CrossRef] [PubMed]
3. Furfaro, A.L.; Traverso, N.; Domenicotti, C.; Piras, S.; Moretta, L.; Marinari, U.M.; Pronzato, M.A.; Nitti, M. The Nrf2/HO-1 Axis in Cancer Cell Growth and Chemoresistance. *Oxidative Med. Cell. Longev.* **2016**, *2016*, 1958174. [CrossRef]
4. Sun, J.; Brand, M.; Zenke, Y.; Tashiro, S.; Groudine, M.; Igarashi, K. Heme regulates the dynamic exchange of Bach1 and NF-E2-related factors in the Maf transcription factor network. *Proc. Natl. Acad. Sci. USA* **2004**, *101*, 1461–1466. [CrossRef] [PubMed]

5. Holland, R.; Fishbein, J.C. Chemistry of the cysteine sensors in Kelch-like ECH-associated protein 1. *Antioxid. Redox Signal.* **2010**, *13*, 1749–1761. [CrossRef] [PubMed]
6. Medina, M.V.; Sapochnik, D.; Garcia Solá, M.; Coso, O. Regulation of the Expression of Heme Oxygenase-1: Signal Transduction, Gene Promoter Activation, and Beyond. *Antioxid. Redox Signal.* **2020**, *32*, 1033–1044. [CrossRef]
7. Stocker, R.; Yamamoto, Y.; McDonagh, A.F.; Glazer, A.N.; Ames, B.N. Bilirubin is an antioxidant of possible physiological importance. *Science* **1987**, *235*, 1043–1046. [CrossRef]
8. Veronesi, A.; Pecoraro, V.; Zauli, S.; Ottone, M.; Leonardi, G.; Lauriola, P.; Trenti, T. Use of carboxyhemoglobin as a biomarker of environmental CO exposure: Critical evaluation of the literature. *Environ. Sci. Pollut Res. Int.* **2017**, *24*, 25798–25809. [CrossRef]
9. Motterlini, R.; Foresti, R. Biological signaling by carbon monoxide and carbon monoxide-releasing molecules. *Am. J. Physiol. Cell Physiol.* **2017**, *312*, C302–C313. [CrossRef]
10. Lancel, S.; Hassoun, S.M.; Favory, R.; Decoster, B.; Motterlini, R.; Neviere, R. Carbon monoxide rescues mice from lethal sepsis by supporting mitochondrial energetic metabolism and activating mitochondrial biogenesis. *J. Pharmacol. Exp. Ther.* **2009**, *329*, 641–648. [CrossRef]
11. Segersvard, H.; Lakkisto, P.; Hanninen, M.; Forsten, H.; Siren, J.; Immonen, K.; Kosonen, R.; Sarparanta, M.; Laine, M.; Tikkanen, I. Carbon monoxide releasing molecule improves structural and functional cardiac recovery after myocardial injury. *Eur. J. Pharmacol.* **2017**, *818*, 57–66. [CrossRef]
12. Suliman, H.B.; Keenan, J.E.; Piantadosi, C.A. Mitochondrial quality-control dysregulation in conditional HO-1-/- mice. *JCI Insight* **2017**, *2*, e89676. [CrossRef]
13. Lin, C.C.; Hsiao, L.D.; Cho, R.L.; Yang, C.M. Carbon Monoxide Releasing Molecule-2-Upregulated ROS-Dependent Heme Oxygenase-1 Axis Suppresses Lipopolysaccharide-Induced Airway Inflammation. *Int. J. Mol. Sci.* **2019**, *20*, 3157. [CrossRef]
14. Chora, A.A.; Fontoura, P.; Cunha, A.; Pais, T.F.; Cardoso, S.; Ho, P.P.; Lee, L.Y.; Sobel, R.A.; Steinman, L.; Soares, M.P. Heme oxygenase-1 and carbon monoxide suppress autoimmune neuroinflammation. *J. Clin. Investig.* **2007**, *117*, 438–447. [CrossRef]
15. Fagone, P.; Mangano, K.; Quattrocchi, C.; Motterlini, R.; Di Marco, R.; Magro, G.; Penacho, N.; Romao, C.C.; Nicoletti, F. Prevention of clinical and histological signs of proteolipid protein (PLP)-induced experimental allergic encephalomyelitis (EAE) in mice by the water-soluble carbon monoxide-releasing molecule (CORM)-A1. *Clin. Exp. Immunol.* **2011**, *163*, 368–374. [CrossRef]
16. Fagone, P.; Mangano, K.; Coco, M.; Perciavalle, V.; Garotta, G.; Romao, C.C.; Nicoletti, F. Therapeutic potential of carbon monoxide in multiple sclerosis. *Clin. Exp. Immunol.* **2012**, *167*, 179–187. [CrossRef]
17. Nikolic, I.; Saksida, T.; Mangano, K.; Vujicic, M.; Stojanovic, I.; Nicoletti, F.; Stosic-Grujicic, S. Pharmacological application of carbon monoxide ameliorates islet-directed autoimmunity in mice via anti-inflammatory and anti-apoptotic effects. *Diabetologia* **2014**, *57*, 980–990. [CrossRef]
18. Mackern-Oberti, J.P.; Llanos, C.; Carreño, L.J.; Riquelme, S.A.; Jacobelli, S.H.; Anegon, I.; Kalergis, A.M. Carbon monoxide exposure improves immune function in lupus-prone mice. *Immunology* **2013**, *140*, 123–132. [CrossRef]
19. Queiroga, C.S.; Almeida, A.S.; Vieira, H.L. Carbon monoxide targeting mitochondria. *Biochem. Res. Int.* **2012**, *2012*, 749845. [CrossRef]
20. Walter, M.; Stahl, W.; Brenneisen, P.; Reichert, A.S.; Stucki, D. Carbon monoxide releasing molecule 401 (CORM-401) modulates phase I metabolism of xenobiotics. *Toxicol. Vitro* **2019**, *59*, 215–220. [CrossRef]
21. Motterlini, R.; Clark, J.E.; Foresti, R.; Sarathchandra, P.; Mann, B.E.; Green, C.J. Carbon monoxide-releasing molecules: Characterization of biochemical and vascular activities. *Circ. Res.* **2002**, *90*, E17–E24. [CrossRef]
22. Schatzschneider, U. Novel lead structures and activation mechanisms for CO-releasing molecules (CORMs). *Br. J. Pharmacol.* **2015**, *172*, 1638–1650. [CrossRef] [PubMed]
23. Stucki, D.; Krahl, H.; Walter, M.; Steinhausen, J.; Hommel, K.; Brenneisen, P.; Stahl, W. Effects of frequently applied carbon monoxide releasing molecules (CORMs) in typical CO-sensitive model systems—A comparative in vitro study. *Arch. Biochem. Biophys.* **2020**, *687*, 108383. [CrossRef] [PubMed]

24. Fayad-Kobeissi, S.; Ratovonantenaina, J.; Dabire, H.; Wilson, J.L.; Rodriguez, A.M.; Berdeaux, A.; Dubois-Rande, J.L.; Mann, B.E.; Motterlini, R.; Foresti, R. Vascular and angiogenic activities of CORM-401, an oxidant-sensitive CO-releasing molecule. *Biochem. Pharmacol.* **2016**, *102*, 64–77. [CrossRef] [PubMed]
25. Crook, S.H.; Mann, B.E.; Meijer, A.J.; Adams, H.; Sawle, P.; Scapens, D.; Motterlini, R. [Mn(CO)4{S2CNMe(CH2CO2H)}], a new water-soluble CO-releasing molecule. *Dalton Trans.* **2011**, *40*, 4230–4235. [CrossRef]
26. Kaczara, P.; Proniewski, B.; Lovejoy, C.; Kus, K.; Motterlini, R.; Abramov, A.Y.; Chlopicki, S. CORM-401 induces calcium signalling, NO increase and activation of pentose phosphate pathway in endothelial cells. *FEBS J.* **2018**, *285*, 1346–1358. [CrossRef]
27. Babu, D.; Leclercq, G.; Motterlini, R.; Lefebvre, R.A. Differential Effects of CORM-2 and CORM-401 in Murine Intestinal Epithelial MODE-K Cells under Oxidative Stress. *Front. Pharmacol.* **2017**, *8*, 31. [CrossRef]
28. Ishihara, N.; Nomura, M.; Jofuku, A.; Kato, H.; Suzuki, S.O.; Masuda, K.; Otera, H.; Nakanishi, Y.; Nonaka, I.; Goto, Y.; et al. Mitochondrial fission factor Drp1 is essential for embryonic development and synapse formation in mice. *Nat. Cell Biol.* **2009**, *11*, 958–966. [CrossRef]
29. Schwaiger, M.; Rampler, E.; Hermann, G.; Miklos, W.; Berger, W.; Koellensperger, G. Anion-Exchange Chromatography Coupled to High-Resolution Mass Spectrometry: A Powerful Tool for Merging Targeted and Non-targeted Metabolomics. *Anal. Chem.* **2017**, *89*, 7667–7674. [CrossRef]
30. Stucki, D.; Brenneisen, P.; Reichert, A.S.; Stahl, W. The BH3 mimetic compound BH3I-1 impairs mitochondrial dynamics and promotes stress response in addition to its pro-apoptotic key function. *Toxicol. Lett.* **2018**, *295*, 369–378. [CrossRef]
31. Yano, N.; Muramoto, K.; Mochizuki, M.; Shinzawa-Itoh, K.; Yamashita, E.; Yoshikawa, S.; Tsukihara, T. X-ray structure of cyanide-bound bovine heart cytochrome c oxidase in the fully oxidized state at 2.0 Å resolution. *Acta Cryst. F Struct Biol. Commun.* **2015**, *71*, 726–730. [CrossRef]
32. Kuehne, A.; Emmert, H.; Soehle, J.; Winnefeld, M.; Fischer, F.; Wenck, H.; Gallinat, S.; Terstegen, L.; Lucius, R.; Hildebrand, J.; et al. Acute Activation of Oxidative Pentose Phosphate Pathway as First-Line Response to Oxidative Stress in Human Skin Cells. *Mol. Cell* **2015**, *59*, 359–371. [CrossRef] [PubMed]
33. Petersen, L.C. The effect of inhibitors on the oxygen kinetics of cytochrome c oxidase. *Biochim. Biophys. Acta* **1977**, *460*, 299–307. [CrossRef]
34. Pankow, D.; Ponsold, W. Effect of carbon monoxide exposure on heart cytochrome c oxidase activity of rats. *Biomed. Biochim. Acta* **1984**, *43*, 1185–1189. [PubMed]
35. Bilban, M.; Bach, F.H.; Otterbein, S.L.; Ifedigbo, E.; d'Avila, J.C.; Esterbauer, H.; Chin, B.Y.; Usheva, A.; Robson, S.C.; Wagner, O.; et al. Carbon monoxide orchestrates a protective response through PPARgamma. *Immunity* **2006**, *24*, 601–610. [CrossRef] [PubMed]
36. Sies, H.; Jones, D.P. Reactive oxygen species (ROS) as pleiotropic physiological signalling agents. *Nat. Rev. Mol. Cell Biol.* **2020**, 1–21. [CrossRef]
37. Kaczara, P.; Motterlini, R.; Rosen, G.M.; Augustynek, B.; Bednarczyk, P.; Szewczyk, A.; Foresti, R.; Chlopicki, S. Carbon monoxide released by CORM-401 uncouples mitochondrial respiration and inhibits glycolysis in endothelial cells: A role for mitoBKCa channels. *Biochim. Biophys. Acta* **2015**, *1847*, 1297–1309. [CrossRef]
38. Braud, L.; Pini, M.; Muchova, L.; Manin, S.; Kitagishi, H.; Sawaki, D.; Czibik, G.; Ternacle, J.; Derumeaux, G.; Foresti, R.; et al. Carbon monoxide-induced metabolic switch in adipocytes improves insulin resistance in obese mice. *JCI Insight* **2018**, *3*, e123485. [CrossRef]
39. Higdon, A.N.; Benavides, G.A.; Chacko, B.K.; Ouyang, X.; Johnson, M.S.; Landar, A.; Zhang, J.; Darley-Usmar, V.M. Hemin causes mitochondrial dysfunction in endothelial cells through promoting lipid peroxidation: The protective role of autophagy. *Am. J. Physiol. Heart Circ. Physiol.* **2012**, *302*, H1394–H1409. [CrossRef]
40. Yang, F.; Shan, Y.; Tang, Z.; Wu, X.; Bi, C.; Zhang, Y.; Gao, Y.; Liu, H. The Neuroprotective Effect of Hemin and the Related Mechanism in Sevoflurane Exposed Neonatal Rats. *Front. Neurosci.* **2019**, *13*, 537. [CrossRef]
41. Gordon, D.M.; Neifer, K.L.; Hamoud, A.A.; Hawk, C.F.; Nestor-Kalinoski, A.L.; Miruzzi, S.A.; Morran, M.P.; Adeosun, S.O.; Sarver, J.G.; Erhardt, P.W.; et al. Bilirubin remodels murine white adipose tissue by reshaping mitochondrial activity and the coregulator profile of peroxisome proliferator-activated receptor α. *J. Biol. Chem.* **2020**, jbc-RA120. [CrossRef]

42. Yamamoto, T.; Takano, N.; Ishiwata, K.; Ohmura, M.; Nagahata, Y.; Matsuura, T.; Kamata, A.; Sakamoto, K.; Nakanishi, T.; Kubo, A.; et al. Reduced methylation of PFKFB3 in cancer cells shunts glucose towards the pentose phosphate pathway. *Nat. Commun.* **2014**, *5*, 3480. [CrossRef] [PubMed]
43. Kaczara, P.; Motterlini, R.; Kus, K.; Zakrzewska, A.; Abramov, A.Y.; Chlopicki, S. Carbon monoxide shifts energetic metabolism from glycolysis to oxidative phosphorylation in endothelial cells. *FEBS Lett.* **2016**, *590*, 3469–3480. [CrossRef] [PubMed]

Supplementary material of:

Endogenous carbon monoxide signaling modulates mitochondrial function and intracellular glucose utilization: impact of the heme oxygenase substrate hemin.

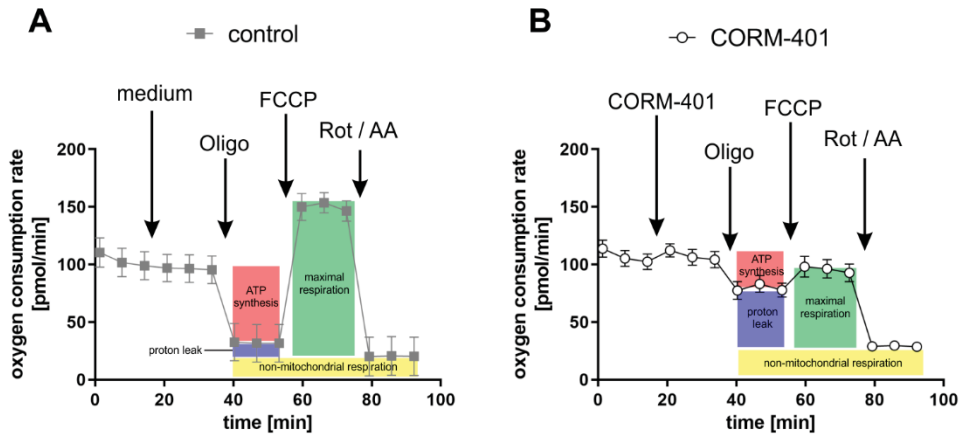

Figure S1: Schematic depiction of OCR curves from Fig 2A and the resulting calculated parameters. Red: ATP synthesis, blue: proton leak, green: maximal respiration, yellow: non-mitochondrial respiration.

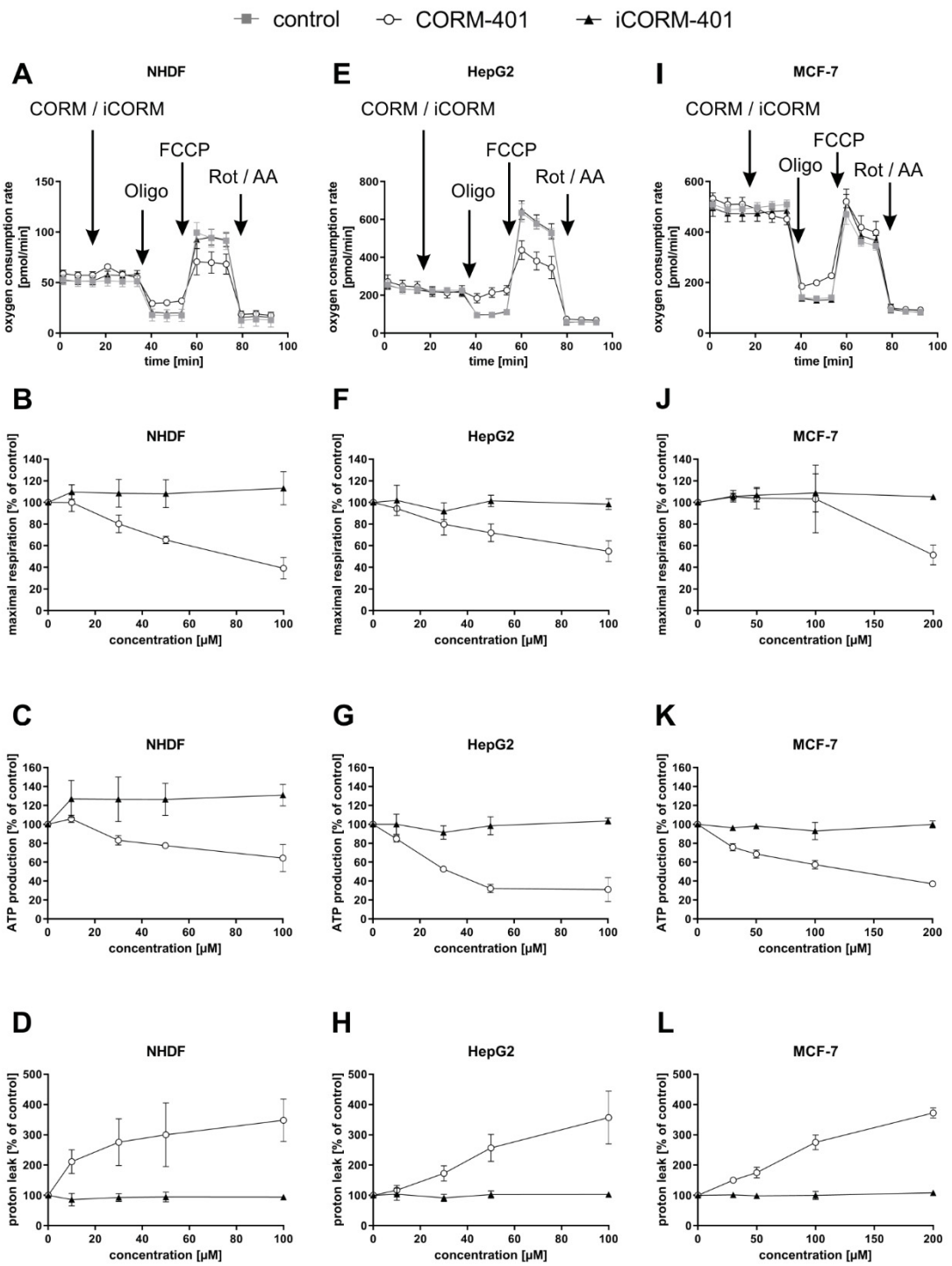

Figure S2: CO-derived effect pattern of mitochondrial respiratory parameters is similar in different cell types. CORM-401 and iCORM-401, were injected into reaction wells and the mito stress test (sequential injection of oligomycin, FCCP and rotenone + antimycin A) was performed. Representative OCR curves at the level of 50 µM CORM-401/iCORM-401 are given for NHDF (A), HepG2 (E) and MCF-7 (I) cells. Quantifications of the mitochondrial respiratory parameters (maximal respiration, ATP production and proton leak) for the different cell types are given: NHDF (B-D), HepG2 (F-H), MCF-7 (J-L). Data represent mean ± SD of three independent experiments (n = 3). OCR = oxygen consumption rate, NHDF = normal human dermal fibroblasts, HepG2 = human hepatocellular carcinoma cells, MCF-7 = human mammary gland breast cancer cells.

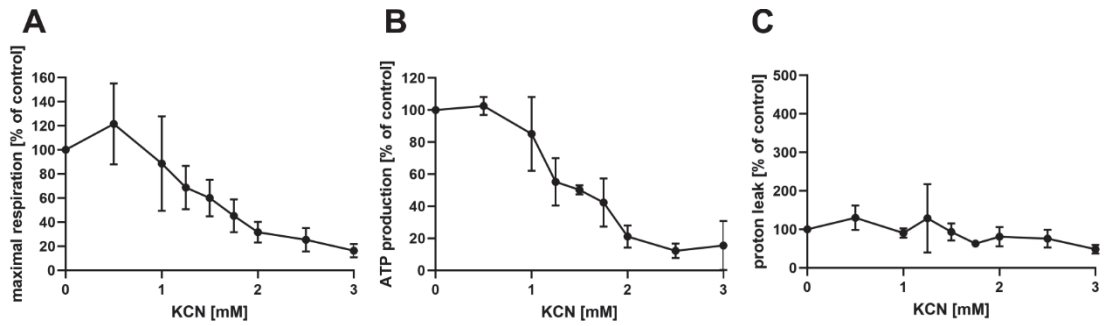

Figure S3: Cyanide application leads to an inhibition of maximal respiration and ATP production, but no increase of proton leakage. KCN was injected into reaction wells and the mito stress test (sequential injection of oligomycin, FCCP and rotenone + antimycin A) was performed. Quantifications of the mitochondrial respiratory parameters (maximal respiration (A), ATP production (B) and proton leak(C)) are given. Data represent mean ± SD of three independent experiments (n = 3).

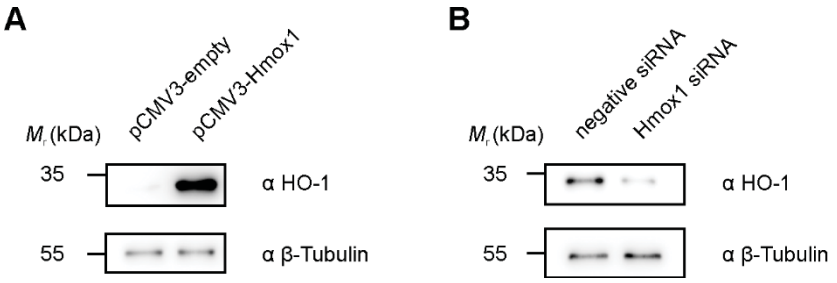

Figure S4: Genetical modification of HO-1 protein levels in MEFs. Representative Western blot analyses of HO-1 protein levels of MEFs (n = 3). Overexpression of HO-1 was achieved by transfecting cells with pCMV3-Hmox1 (A). As control pCMV3-empty (empty vector) was used. Knock down of HO-1 was achieved by transfecting cells with siRNA directed against Hmox1 (B). As control negative siRNA was used.

Table S1: Statistical analysis belonging to figure 2B-D. For statistical analysis one-way ANOVA was used with Sidak's multiple comparisons test. *p<0.05, **p<0.01, ***p<0.001, n.s. = not significant, ct = control.

parameter	ct vs CORM-401				ct vs iCORM-401				CORM-401 vs iCORM-401				µM
	10	30	50	100	10	30	50	100	10	30	50	100	
maximal respiration	n.s.	n.s.	**	***	n.s.	n.s.	n.s.	n.s.	n.s.	n.s.	*	***	
ATP production	n.s.	*	***	***	n.s.	n.s.	n.s.	n.s.	n.s.	*	***	***	
proton leak	n.s.	***	***	***	n.s.	n.s.	n.s.	n.s.	n.s.	***	***	***	

Table S2: Statistical analysis belonging to figure 3. For statistical analysis one-way ANOVA was used with Sidak's multiple comparisons test. Untreated (0 µM hemin) empty vector group was used as reference. *p<0.05, **p<0.01, ***p<0.001, n.s. = not significant, ct = control, ref = reference.

group	hemin [µM]	maximal respiration	ATP production	proton leak	group	hemin [µM]	maximal respiration	ATP production	proton leak
empty vector	0	ref	ref	ref	negative siRNA	0	ref	ref	ref
	2	n.s.	n.s.	n.s.		2	**	n.s.	*
	5	n.s.	***	*		5	n.s.	**	**
	10	n.s.	***	n.s.		10	**	***	**
	20	n.s.	***	*		20	**	***	***
HO-1	0	n.s.	n.s.	n.s.	*Hmox1* siRNA	0	n.s.	n.s.	n.s.
	2	n.s.	n.s.	n.s.		2	***	n.s.	**
	5	n.s.	n.s.	n.s.		5	n.s.	**	*
	10	n.s.	***	n.s.		10	**	***	**
	20	n.s.	***	*		20	**	***	***

Table S3: Statistical analysis belonging to figure 4B+C. For statistical analysis one-way ANOVA was used with Sidak's multiple comparisons test. *p<0.05, **p<0.01, ***p<0.001, n.s. = not significant, ct = control.

parameter	ct vs CORM-401				ct vs iCORM-401				CORM-401 vs iCORM-401				µM
	10	30	50	100	10	30	50	100	10	30	50	100	
induced glycolysis	n.s.	*	**	**	n.s.	n.s.	n.s.	n.s.	n.s.	**	***	***	
compensatory glycolysis	n.s.	**	***	***	n.s.	n.s.	n.s.	n.s.	n.s.	**	***	***	

Table S4: Statistical analysis belonging to figure 5. For statistical analysis one-way ANOVA was used with Sidak's multiple comparisons test. *p<0.05, **p<0.01, ***p<0.001, n.s. = not significant, ct = control.

parameter	ct vs CORM-401			ct vs iCORM-401			CORM-401 vs iCORM-401			min
	30	90	240	30	90	240	30	90	240	
G6P M+6	***	***	***	*	n.s.	n.s.	*	**	***	
F1,6BP M+6	***	***	***	n.s.	n.s.	n.s.	***	***	***	
G3P M+3	***	***	***	*	n.s.	n.s.	***	***	***	
1,3BPG M+3	n.s.	**	***	n.s.	**	**	n.s.	***	***	
PEP M+3	**	*	n.s.	n.s.	**	**	n.s.	n.s.	*	
6PG M+6	***	***	***	***	n.s.	n.s.	***	***	***	
Ru5P M+5	***	***	**	**	n.s.	n.s.	n.s.	**	**	
S7P M+7	***	***	***	***	n.s.	n.s.	***	***	***	
E4P M+4	***	***	***	*	n.s.	n.s.	***	***	***	
PRPP M+5	n.s.	n.s.	***	**	n.s.	n.s.	n.s.	n.s.	***	

2.4 CO induces adenine nucleotide signaling

2.4.1 CORM-401 exposure leads to decreased mitochondrial ATP production and increased ADP and AMP levels

In *Manuscript 3* extracellular flux technology was used to evaluate effects of CORM-401 on energy providing pathways of cells. Compared to control, a lowered ATP-linked mitochondrial respiration and a decreased induced glycolysis were determined directly after CORM-401 application to MEFs (Fig 2+4 of *Manuscript 3*). However, oxygen consumption and extracellular acidification rates are only indirect measures for ATP production. A modified approach of these experiments, the ATP rate assay, was applied next to convert OCR and ECAR measures to mitochondrial and glycolytic ATP production rates, respectively (Eq 2 – 4).

(Eq 2) $$mitoATP\ production\ rate = \left(OCR_{basal} - OCR_{Oligo}\right) * Koxy\ * P/O$$

(Eq 3) $$glycoATP\ production\ rate = PER - ((OCR_{basal} - OCR_{Rot/AA}) *\ CCF)$$

(Eq 4) $$PER = ECAR * BF *\ Vol_{microchamber} * Kvol$$

OCR = oxygen consumption rate (pmol O_2/min)
Koxy = 2 pmol O/pmol O_2
P/O = 2.75 pmol ATP/pmol O
PER = proton efflux rate (pmol H^+/min)
CCF = CO_2 contribution factor = 0.61 pmol H^+/pmol O_2
ECAR = extracellular acidification rate (mpH/min)
BF = buffer factor = 2.4 mmol H^+/L/pH
$Vol_{microchamber}$ = 2.8 µL
Kvol = volume scaling factor = 1.6

For details on extracellular flux analysis conduction see *Manuscript 3*, chapter 2.4. In the ATP rate assay a direct injection of 50 µM CORM-401/iCORM-401 or medium only (control) was followed by sequential injections of oligomycin (inhibitor of ATP synthase) and a mixture of rotenone and antimycin A (inhibitors of complex I and III, respectively). Representative OCR and proton efflux rate (PER) curves are given in Fig 4A+B. Compared to control, injection of CORM-401 directly led to a slight increase of OCR (comparable to *Manuscript 2*, Fig 5E and *Manuscript 3* Fig 1A and 2A) and the expected decrease in OCR values following oligomycin

injection was less pronounced in the CORM-401 group. Injection of rotenone and antimycin A completely inhibited mitochondrial respiration and OCR values observed afterwards are only linked to non-mitochondrial oxygen consuming processes. Here no differences between treatment groups were found. Upon CORM-401 injection also a slight decrease of PER values was determined, indicating a lowered glycolytic flux directly after administration of the compound. Inhibition of ATP synthase by oligomycin induced a compensatory increase in glycolysis, but this compensation was less pronounced in the CORM-401 treatment group compared to control. The final injection of rotenone and antimycin A is needed to analyze the mitochondria-derived PER (($OCR_{basal} - OCR_{Rot/AA}$) * CCF). Treatment of cells with iCORM-401 did not affect OCR and PER values under the present settings. Using Eq 2-4, mitochondrial and glycolytic ATP production rates were calculated for control and iCORM-401 conditions. For both groups values about 200 and 80 pmol/min, for mitochondrial and glycolytic ATP production rate, respectively, were found (Fig 4C). Upon exposure of cells to CORM-401, the mitochondrial ATP production rate was significantly decreased to about 100 pmol/min, while the glycolytic ATP production rate was only slightly lowered (about 70 pmol/min). This is also reflected in the ATP rate index (Fig 4D), which was decreased by CORM-401 compared to control and iCORM-401, demonstrating a less OXPHOS-driven ATP production phenotype of cells after exposure to CO. Finally, total ATP production rate of cells was decreased from about 280 pmol/min for control and iCORM-401 to about 170 pmol/min after CORM-401 treatment (Fig 4E). Summed up these data demonstrate, that the inhibitory effect of CORM-401 derived CO on cellular ATP production rates, address mitochondria as the primary target.

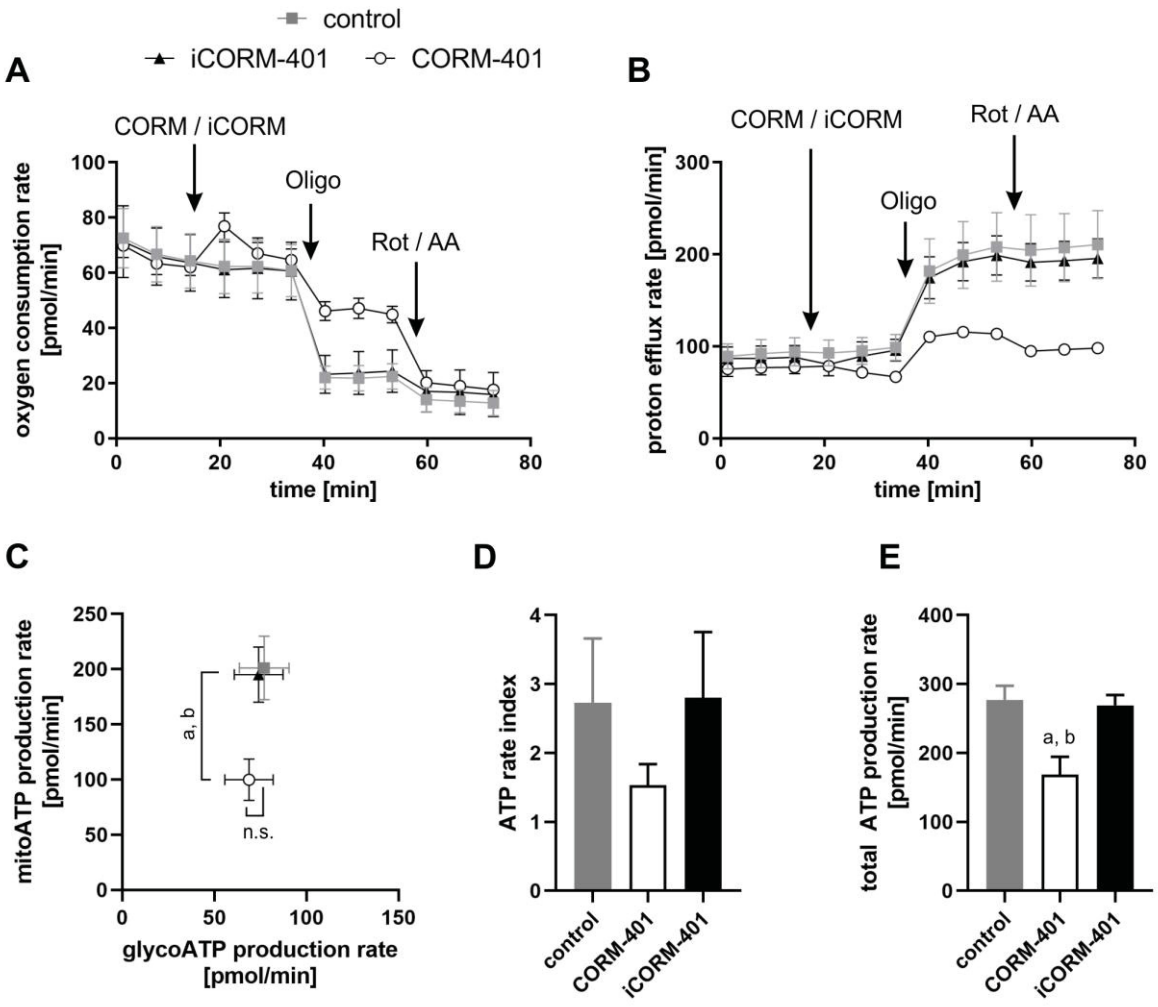

Figure 4: CO from CORM-401 affects mainly mitochondrial ATP production rate. CORM-401 and iCORM-401, were injected into reaction wells and the ATP rate assay (sequential injection of oligomycin and rotenone + antimycin A) was performed using extracellular flux technology. Injections are indicated by arrows. Representative OCR and PER curves are given (A+B) with final concentration of CORM-401/iCORM-401: 50 µM. Data represent mean ± SD of at least six technical replicates. Quantification of the mitochondrial and glycolytic ATP production rate (C), ATP rate index (D) and total ATP production rate (E) are shown. Data represent mean ± SD of three independent experiments (n = 3). OCR = oxygen consumption rate, PER = proton efflux rate, Oligo = oligomycin, Rot / AA = rotenone + antimycin A. Statistical analysis was performed using unpaired Student's t-Test with a: control vs CORM-401 and b: CORM-401 vs iCORM-401 with $p \leq 0.05$.

To further investigate the effect of CO on cellular energy metabolism, levels of ATP, ADP, AMP and succinate were analyzed by means of IC-MS (Fig 5). The data shown in Fig 5 are part of the data set described in Fig 5 of *Manuscript 3*. The experiment was performed as described in *Manuscript 3*, chapter 2.7. For further sample preparation, cell pellets were dried *in vacuo*, resuspended in 63 mM Tris/HCl buffer (pH 6.8) containing 2 % SDS (w/v) and stored at –80 °C until further use. Samples were sonicated and the total protein amount was determined with the DC™ protein assay kit (Biorad, Munich, Germany) for data normalization. Although

CORM-401 exposure significantly decreased mitochondrial ATP production rate of cells (Fig 4C), total ATP levels were not affected after 30 and 90 min of incubation compared to control (Fig 5A). Only after 240 min of incubation, ATP was decreased below control level. In contrast, iCORM-401 application, which did not affect ATP production rate (Fig 4C), led to a slight drop of ATP levels below control (Fig 5A). However, the levels of ADP and AMP were elevated upon CORM-401 exposure (90 and 240 min) to about two- and four-fold of control, respectively (Fig 5B+C). Here, iCORM-401 treatment showed no effect. Additionally, succinate levels were also determined by IC-MS analysis. Succinate is a substrate of the succinate dehydrogenase (SDH), a constituent of complex II of the mitochondrial respiratory chain (Beach et al., 2020). Succinate levels were also increased by about two-fold, 90 and 240 min after CORM-401 application compared to control and iCORM-401 treated cells (Fig 5D). Succinate accumulation indicates a decreased enzymatic activity of SDH (Beach et al., 2020), which can most likely be attributed to the inhibitory effect of CO on mitochondrial respiration already described in Fig 5 of *Manuscript 2* and Fig 1 of *Manuscript 3*.

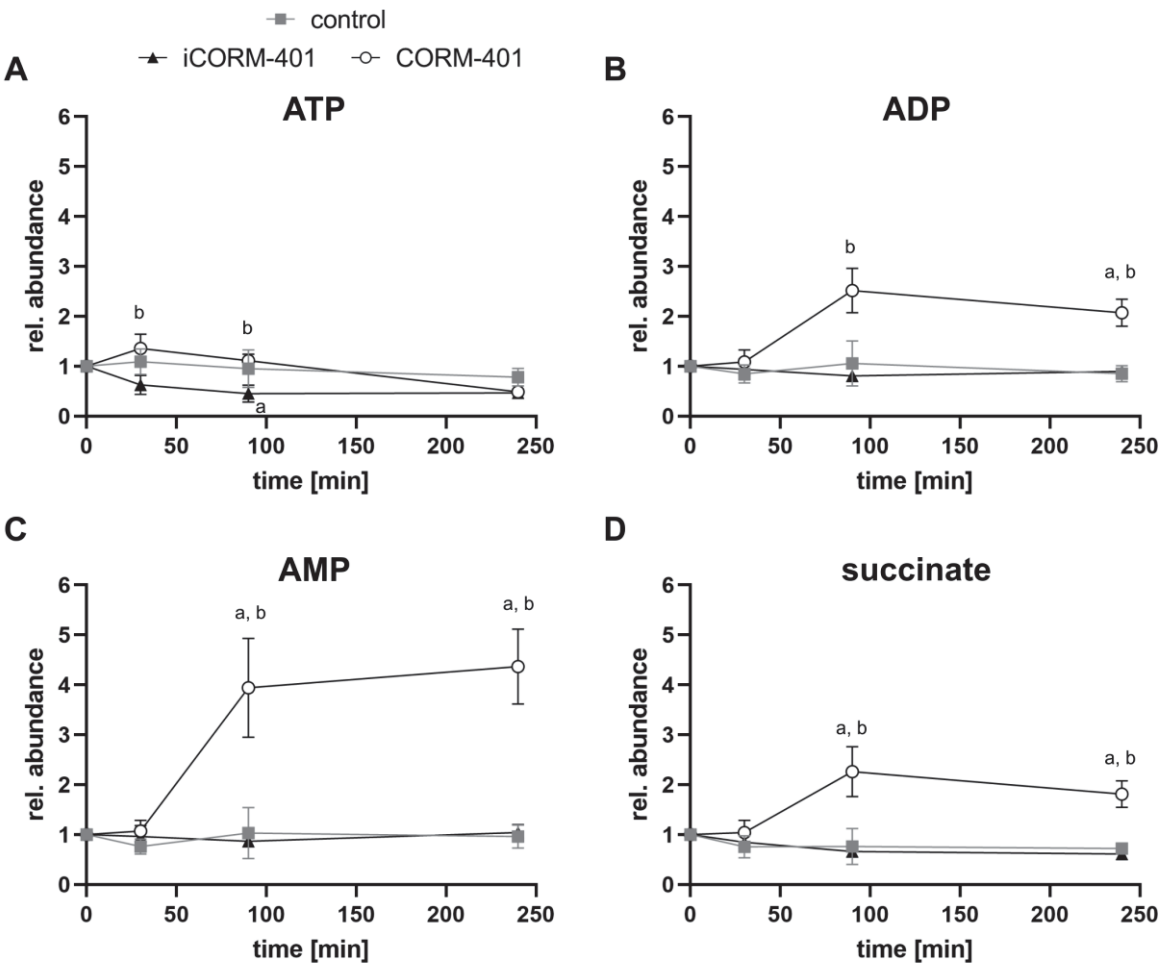

Figure 5: Effects of CO on cellular energy metabolism. MEFs were treated with 50 µM CORM-401/iCORM-401 or medium only (control), for 30, 90 or 240 min. Cells were then lyzed and extracts analysed via IC-MS analysis for the abundance of ATP (A), ADP (B), AMP (C) and succinate (D). Signal areas were normalized by total protein amounts of cell pellets and are given as relative abundance. Control (0 min) was set to 1. Data is given as mean ± SD (n = 4). Statistical analysis was performed using two-way ANOVA with a: control vs CORM-401/iCORM-401 and b: CORM-401 vs iCORM-401 with $p \leq 0.05$.

2.4.2 CO from CORM-401 activates AMP-activated protein kinase (AMPK) and Unc-51 like autophagy activating kinase 1 (ULK1)

Since increased AMP levels were found after CORM-401 exposure, the effects of CO on a major AMP-sensing protein, AMPK, were studied next. AMP can directly bind to the γ-subunit of AMPK, thereby activating the protein complex, which can be monitored by analyzing the phosphorylation status of Thr172 of the α-subunit (Herzig and Shaw, 2018). Here Western blot analysis was used to investigate the effects of 50 µM CORM-401/iCORM-401 or medium for control after 0.5, 1.5 and 4 h of treatment on total and p-AMPKα^{Thr172} protein levels. Oligomycin (2 µM, 1.5 h) which is known to efficiently inhibit ATP synthesis and hence

increase AMP levels was used as a positive control. After treatment, cells were lysed with 1 % SDS, supplemented with a protease inhibitor cocktail (Roche, Grenzach, Germany) and a phosphatase inhibitor cocktail (Sigma-Aldrich, Deisenhofen, Germany). Protein determination was performed using the DC™ protein assay kit from Biorad (Munich, Germany) and about 30 µg of total protein per sample were subjected to SDS-PAGE (12 % gels), followed by electro blotting of proteins onto PVDF membranes (pore size 0.45 µm, GE Healthcare, Solingen, Germany). Blots were developed with the ECL-system provided by Cell Signaling Technology (Frankfurt am Main, Germany) and chemiluminescence signals were monitored using the Fusion SL Advance gel documentation device (Peqlab, Erlangen, Germany). Primary antibodies from rabbits were used: anti-AMPKα (2532S), anti-p-AMPKα^{Thr172} (40H9), anti-GAPDH (D16H11), anti-ULK1 (D8H5) and anti-p-ULK1^{Ser555} (D1H4) were from Cell Signaling (Leiden, Netherlands). Secondary antibody was: horseradish peroxidase (HRP)-coupled goat anti-rabbit IgG (111-035-144) from Dianova (Hamburg, Germany).

As shown in Fig 6A, similar amounts of total AMPKα were found at the tested conditions. However, the p-AMPKα^{Thr172} to total AMPKα ratio was higher in the CORM-401 treatment group compared to control and iCORM-401. After 0.5 h of CORM-401 exposure, only a slight increase of p-AMPKα^{Thr172}/AMPKα was observed (Fig 6B), however, after 1.5 and 4 h a 15- and 20-fold increase, respectively, was found. The phosphorylation status of AMPKα at Thr172 was not altered by iCORM-401 treatment. With the same samples, also the phosphorylation of ULK1 at Ser555 was analyzed. ULK1 is a known target of AMPK and phosphorylation at Ser555 indicates an activation of the protein (Kim et al., 2011). Activated ULK1 can translocate to the outer mitochondrial membrane and phosphorylate mitophagy receptors such as FUNDC1 (Wu et al., 2014). Thus, it can be used as a marker for mitophagy induction. After CORM-401 treatment, an increased ratio of p-ULK1^{Ser555} to total ULK1 was found at time points 1.5 (2.5-fold) and 4 h (4-fold) compared to control and iCORM-401 (Fig 6C). It should also be noted, that while total ULK1 levels were not affected at the tested conditions, this was not the case for the 4 h CORM-401 treatment. Here total ULK1 was slightly decreased (Fig 6A), which might indicate a proceeding digestion of the mitochondria-localized protein via ongoing mitophagy.

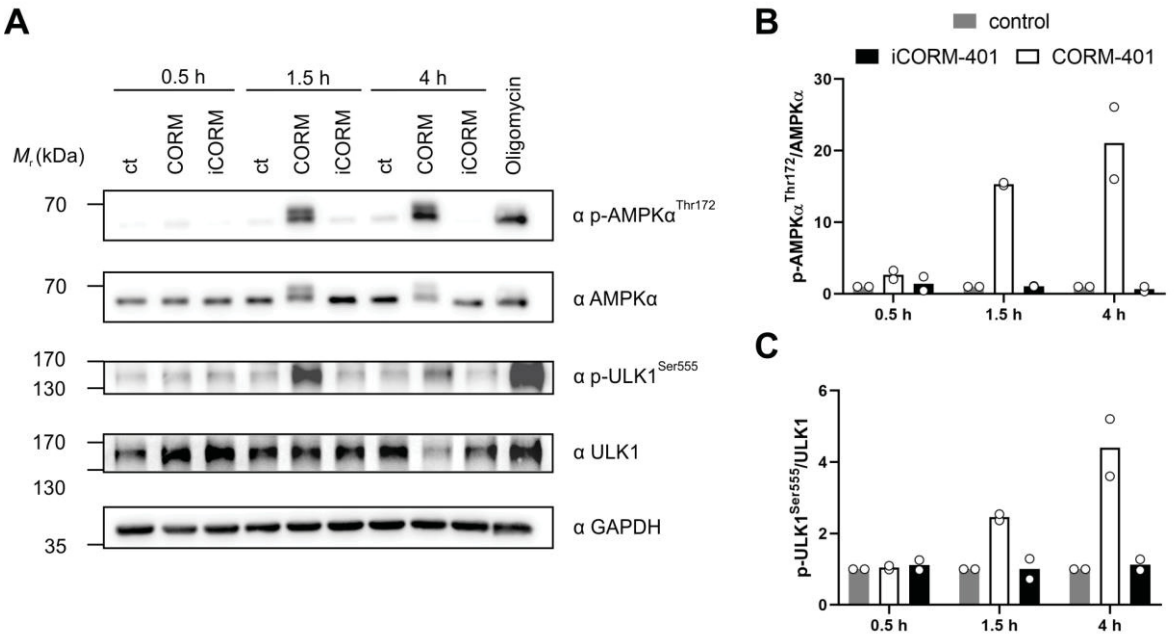

Figure 6: CO induces activating phosphorylation of AMPKα and ULK1. MEFs were treated with 50 µM CORM-401/iCORM-401 or medium for control. At indicated time points cells were lyzed and subjected to Western blot analysis. Oligomycin (2 µM, 1.5 h) was used as a positive control for the activation of AMPK. A representative Western blot is shown (A) as well as the densitometric quantification of p-AMPKα^{Thr172}/AMPKα (B) and p-ULK1^{Ser555}/ULK1 (C). Control of the respective time point was set to 1. Data is given as mean of two independent experiments and values of each experiment are shown as circles.

Taken together, these data suggest, that CO derived from CORM-401 decreases the mitochondrial ATP production rate via inhibition of the mitochondrial respiratory chain, while total ATP levels and therefore the cellular energy status are only affected at late time points. Increasing amounts of AMP were found already after 90 min of exposure, likely responsible for the activation of AMPK-mediated signaling and phosphorylation of the downstream target protein ULK1 at Ser555, suggesting an induction of mitophagy by CO via this pathway.

2.5 *Manuscript 4*: Carbon monoxide releasing molecule 401 (CORM-401) modulates phase I metabolism of xenobiotics

Moritz Walter[1], Wilhelm Stahl[1], Peter Brenneisen[1], Andreas S Reichert[1] and David Stucki[1]

[1] Institute of Biochemistry and Molecular Biology I, Medical Faculty, Heinrich Heine University Düsseldorf, D-40001 Düsseldorf, Germany.

Received: 21st January 2019; Accepted: 16th April 2019; Published: 17th April 2019

Published in: *Toxicology in Vitro*, **59**: 215-220.

DOI: 10.1016/j.tiv.2019.04.018

Contribution statement:
D.S. contributed to conceptualization and supervision of the study as well as data visualization. D.S. performed the statistical analyses, wrote the original draft and contributed to review & editing of the manuscript.

Graphical abstract:

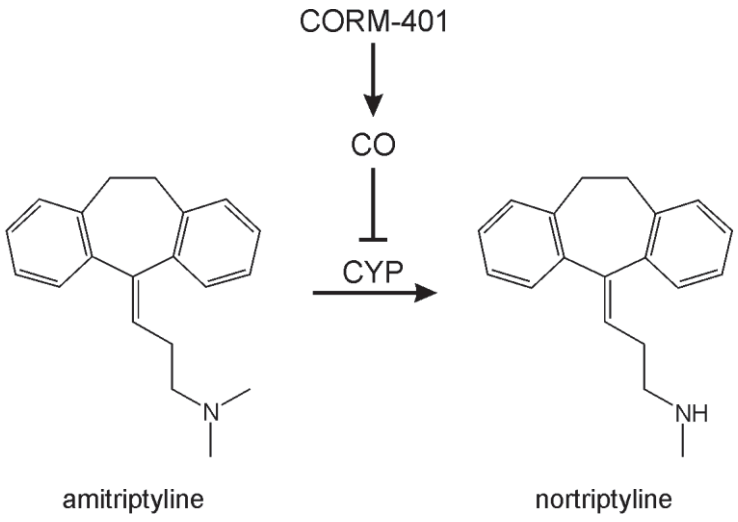

Toxicology in Vitro 59 (2019) 215–220

Contents lists available at ScienceDirect

Toxicology in Vitro

journal homepage: www.elsevier.com/locate/toxinvit

Carbon monoxide releasing molecule 401 (CORM-401) modulates phase I metabolism of xenobiotics

Moritz Walter, Wilhelm Stahl*, Peter Brenneisen, Andreas S. Reichert, David Stucki

Institute of Biochemistry and Molecular Biology I, Medical Faculty, Heinrich Heine University Düsseldorf, Postfach 10 10 07, D-40001 Düsseldorf, Germany

ARTICLE INFO

Keywords:
Carbon monoxide
CORM
CYP
Xenobiotic metabolism

ABSTRACT

Next to its well-studied toxicity, carbon monoxide (CO) is recognized as a signalling molecule in various cellular processes. Thus, CO-releasing molecules (CORMs) are of considerable interest for basic research and drug development. Aim of the present study was to investigate if CO, released from CORMs, inhibits cytochrome P450-dependent monooxygenase (CYP) activity and modulates xenobiotic metabolism. CORM-401 was used as a model CO delivering compound; inactive CORM-401 (iCORM-401), unable to release CO, served as control compound. CO release from CORM-401, but not from iCORM-401, was validated using the cell free myoglobin assay. CO-dependent inhibition of CYP activity was shown by 7-ethoxyresorufin-*O*-deethylation (EROD) with recombinant CYP and HepG2 cells. Upon CORM-401 exposure EROD activity of recombinant CYP decreased concentration dependently, while iCORM-401 had no effect. Treatment with CORM-401 decreased EROD activity in HepG2 cells at concentrations higher than 50 µM CORM-401, while iCORM-401 showed no effect. At the given concentrations cell viability was not affected. Amitriptyline was selected as a model xenobiotic and formation of its metabolite nortriptyline by recombinant CYP was determined by HPLC. CORM-401 treatment inhibited the formation of nortriptyline whereas iCORM-401 treatment did not. Overall, we demonstrate CO-mediated inhibitory effects on CYP activity when applying CORMs. Since CORMs are currently under drug development, the findings emphasize the importance to take into account that this class of compounds may interfere with xenobiotic metabolism.

1. Introduction

Carbon monoxide (CO) is a gaseous molecule which forms stable complexes with heme moieties of proteins and modulates their biological function. It is well known as a toxic gas, but also endogenously produced by the enzyme heme oxygenase. There is increasing evidence, that CO is a small signalling molecule such as nitric oxide or hydrogensulfide. CO-dependent signalling has been linked to the regulation of vital processes including modulation of inflammation, apoptosis, vascular tone and general stress response (Ling et al., 2018). CO-releasing molecules (CORMs) have been developed for research purposes to deliver CO directly and at low concentrations at target sites to provide CO for intracellular signalling (Motterlini et al., 2002). This kind of compounds attracted attention as basic research tools, but also in drug development (Hopper et al., 2018; Garcia-Gallego and Bernardes, 2014; Motterlini and Foresti, 2017). CORMs are investigated in experimental studies based on their effects on mitochondrial function. Application of CORM-401 to obese mice was shown to uncouple mitochondrial respiration in adipocytes and to promote a switch to glycolysis accompanied by an improved insulin sensitivity (Braud et al., 2018). In a model of doxorubicin-induced cardiomyopathy in rats it was shown that treatment of isolated hearts with CORM-3 reveals a positive inotropic effect compared to a classical inotropic compound (Musameh et al., 2010). Furthermore, CORMs are tested in clinical studies on patients with sickle cell anemia and delayed cerebral ischemia (Keipert, 2016; Dhar et al., 2017; Misra et al., 2017).

Cytochrome P450-dependent monooxygenases (CYP) represent a major part of the xenobiotic metabolizing system in the organism. It is well established, that CO inhibits the activity of CYP enzymes via binding to its prosthetic heme group. Inhibition has been demonstrated e.g. in liver microsomal fractions which were purged with CO gas prior or throughout CYP activity assays (Leemann et al., 1994). However, potential inhibition of CYPs by CORMs and thus modulation of CYP-dependent metabolism of xenobiotics has not been analyzed, yet.

In the present study we address the question, whether CO delivered by CORMs inhibits CYP activity and is capable to modulate xenobiotic metabolism of model compounds.

* Corresponding author.
E-mail address: wilhelm.stahl@hhu.de (W. Stahl).

https://doi.org/10.1016/j.tiv.2019.04.018
Received 21 January 2019; Received in revised form 5 April 2019; Accepted 16 April 2019
Available online 17 April 2019

2. Materials and methods

2.1. Chemicals

Tetracarbonyl[N-(dithiocarboxy-κ*S*,κ*S*')-*N*-methylglycine]manganite (CORM-401), Dulbecco's Modified Eagle's Medium (DMEM), 3-(4,5-dimethylthiazol-2-yl)-2,5-diphenyltetrazolium bromide (MTT), manganese sulfate monohydrate, 3-methylcholanthrene, dicoumarol, amitriptyline, nortriptyline, ethoxyresorufin, sodium dithionite, myoglobin (from equine skeletal muscle), NADPH, H_2O_2 (30%) and PBS were from Sigma-Aldrich (Deisenhofen, Germany), acetonitrile (HPLC grade) and trifluoroacetic acid from VWR (Langenfeld, Germany), trichloroacetic acid from Merck (Darmstadt, Germany), DMSO from Roth (Karlsruhe, Germany) and sarcosine-N-dithiocarbamate was obtained from 3B Scientific Corporation (Wuhan, China).

CORM-401 was dissolved in PBS and aliquots were stored at −20 °C. The compound is stable under these conditions and releases CO (2–3 mol CO per mol CORM-401) only in the presence of CO acceptors such as heme proteins (Crook et al., 2011; Fayad-Kobeissi et al., 2016). An equimolar mixture of sarcosine-N-dithiocarbamate and $MnSO_4$ was used as inactive CORM-401 (iCORM-401). The mixture does not release CO and is regularly applied as control to mimic effects of the CORM-401 backbone (Kaczara et al., 2018; Babu et al., 2017; Fayad-Kobeissi et al., 2016). CORM-401 and iCORM-401 were protected from light at all times.

2.2. Myoglobin assay

Release of CO from CORM-401 and iCORM-401 was assessed with the myoglobin (Mb) assay. In the Mb assay the conversion of deoxymyoglobin (deoxy-Mb) to carboxymyoglobin (Mb-CO) is determined spectrophotometrically in the range of 500–600 nm (Motterlini et al., 2002). Myoglobin (70 μM) was dissolved in PBS and sodium dithionite was added to a final concentration of 0.2% (w/v), for complete oxygen depletion. An absorbance spectrum was recorded at the beginning of the experiment (deoxy-Mb). Then CORM-401 or iCORM-401 were added to a final concentration of 20 μM, the solution was covered with N_2 gas and further absorbance spectra were recorded every 5 min for 30 min.

2.3. Cell culture

Human hepatocellular carcinoma (HepG2) cells (Sigma, 85011430) were chosen as a model system to study CYP enzyme activity and were cultured in DMEM (low glucose), supplemented with 10% fetal bovine serum (FBS, PAN-Biotech, Aidenbach, Germany), penicillin (100 U/mL), streptomycin (100 μg/mL) and GlutaMAX™ (2 mM) (growth medium) at 37 °C and 5% CO_2 in a humidified atmosphere. For all experiments cells were grown for 48 h on 48-well plates; seeding density was 30,000 cells per well. Cell confluency was about 60% at the beginning of the studies. Treatment was performed in serum-free DMEM (same supplements as stated above), if not stated otherwise.

2.4. Ethoxyresorufin-O-deethylase activity assay

The ethoxyresorufin-*O*-deethylase (EROD) assay was used as a measure for the activity of CYP1A enzymes. The assay is based on the deethylation of the non-fluorescent substrate ethoxyresorufin to the fluorescent product resorufin (Burke and Mayer, 1974). The EROD assay was performed as a cell-free and a cellular variant, both in 48 well plates.

For the cell-free approach the reaction mixture (250 μL per well) consisted of 0.125 pmol recombinant human CYP1A1 enzyme with cytochrome P450 reductase (Sigma, C3735) and 2.5 μM ethoxyresorufin in a 0.1 M potassium phosphate buffer (pH 7.2). CORM-401 or iCORM-401 were added to final concentrations of 1–300 μM and the reaction was directly started by adding NADPH to a final concentration of 200 μM. The reaction was recorded for 10 min at 37 °C by measuring the fluorescence of the newly formed resorufin (λ_{ex}: 535 nm/λ_{em}: 590 nm) every 2 min with a plate reader (Tecan, Infinite M200). EROD activity was calculated as increase of relative fluorescence units (RFU) per min. For comparison solvent control (PBS) was set to 100%.

For the cellular EROD assay, HepG2 cells were cultured in 48 well plates (48 h) and were then treated with 1 μM 3-methylcholanthrene (3-MC) for 24 h (in growth medium) to induce CYP1A expression. Afterwards cells were washed with PBS and treated with different concentrations of CORM-401, iCORM-401 or medium (control) for 2 h. Then EROD assay medium was added (2.5 μM ethoxyresorufin, 10 μM dicoumarol in serum-free DMEM). Dicoumarol was used as an inhibitor of NAD(P)H quinone oxidoreductase 1 (NQO1) to prevent degradation of resorufin (Lubet et al., 1985). For 30 min EROD activity was followed as described above.

2.5. Viability testing

For dose finding, the MTT assay was applied with CORM-401, iCORM-401, H_2O_2 (positive control) or medium (control) at different concentrations and treatment periods. The assay was performed on 48 well plates. After treatment, cells were washed with PBS and 250 μL MTT solution (0.5 mg/mL) was added per well. Cells were incubated for another 0.5 h. MTT solution was removed and cells were washed with PBS. In the MTT assay yellow 3-(4,5-dimethylthiazol-2-yl)-2,5-diphenyltetrazolium bromide is reduced to the purple 1-(4,5-dimethylthiazol-2-yl)-3,5-diphenylformazan, by mainly mitochondrial reductases of living cells. The formazan was extracted with 250 μL DMSO per well. Absorbance was measured with a plate reader (Tecan, Infinite M200) at λ = 570 nm. Control was set to 100% viability; values of positive control were used for background subtraction.

2.6. HPLC analyses of amitriptyline and nortriptyline

Reaction tubes containing 0.1 M potassium phosphate buffer (pH 7.2), 5 pmol recombinant human CYP1A2 enzyme with cytochrome P450 reductase (Sigma; C5614), 100 μM amitriptyline and different concentrations CORM-401, iCORM-401 or solvent were incubated in a water bath at 37 °C. The total volume of the mixture was 0.5 mL. The reaction was started by adding NADPH to a final concentration of 200 μM and stopped after 1 h of incubation with 25 μL TCA (30%). Samples were centrifuged at 10,000*g* for 5 min at 4 °C. The aqueous supernatants were directly analyzed with HPLC, and the concentrations of amitriptyline and nortriptyline were quantified with the external standard method. The HPLC system consisted of a Merck–Hitachi L-7100 pump connected with a Merck-Hitachi UV-VIS detector (Merck-Hitachi L-4250) and a data registration system. Detection wavelength was 240 nm. Mobile phase was 30% acetonitrile, 70% water and 0.1% TFA (v/v/v); flow rate was 1.5 mL/min. A Cortecs C-18 column (150 mm × 4.6 mm, 2.7 μm) from Waters (Eschborn, Germany) was used as stationary phase. The column temperature was set to 40 °C. Retention times of amitriptyline and nortriptyline were about 9.6 and 8.8 min, respectively.

2.7. Statistical analysis

Means were calculated from at least three independent experiments. Error bars represent standard error of the mean (S.E.M.). Statistical analysis was performed by using one-way ANOVA with Dunnett's or Bonferroni's post-hoc test, with $p \leq .05$ considered to be significant.

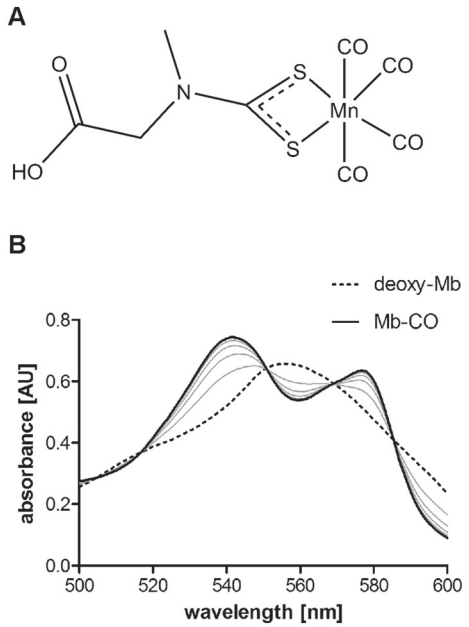

Fig. 1. CORM-401 is a CO delivering substance. A) Chemical structure of CORM-401. B) CO delivering property of CORM-401 was analyzed with the myoglobin (Mb) assay. The shift of the absorption spectrum of deoxy-Mb (dashed line; $t = 0$ min) to Mb-CO (black, solid line; $t = 30$ min) overtime is indicative for proceeding CO release from CORM-401. Mixed spectra (grey, solid lines) were also recorded at $t = 5$, 10, 15, 20 and 25 min. Shown is a representative result of three independent experiments.

3. Results

3.1. CORM-401 is a CO delivering compound

CORM-401 (Fig. 1A) was chosen as a model compound for CO delivery. Its capability to release CO was examined spectrophotometrically using the Myoglobin (Mb) assay (Fig. 1B). Therefore, CORM-401 was added to a solution of deoxy-Mb (start spectrum; dashed line) and the conversion of deoxy-Mb to Mb-CO (end spectrum; black, solid line) was determined over a period of 30 min. Every 5 min additional spectra were recorded (mixed spectra; grey, solid lines), showing a time-dependent CO release of CORM-401. After 30 min of incubation most of the CO bound to CORM-401 was released. These data are in accordance with earlier reported half-live values ($t_{1/2}$: 12–14 min) for CO release from CORM-401 in the Mb assay (Fayad-Kobeissi et al., 2016). Incubation of deoxy-Mb with iCORM-401 did not provoke a change of the deoxy-Mb spectrum confirming that this compound is not able to release CO or interferes with the Mb assay (data not shown).

3.2. CO from CORM-401 inhibits EROD activity of recombinant cytochrome P450

The non-fluorescent substrate ethoxyresorufin is deethylated by enzymes of the CYP1A subfamily to form the fluorescent resorufin, a reaction suitable to determine CYP1A activity. Effects of CORM-401 and iCORM-401 on EROD activity were assessed in a cell-free system with recombinant human CYP1A1 (Fig. 2). Upon incubation with CORM-401, EROD activity was inhibited in a concentration dependent manner. The lowest concentration (1 μM CORM-401) had no effect, however, EROD activity was decreased to about 55% of control at 10 μM CORM-401 and was further decreased at higher concentrations of CORM-401 (50–300 μM). 50–300 μM CORM-401 values were all significantly lower compared to control and the respective iCORM-401 values. Incubation with iCORM-401 did not affect EROD activity at

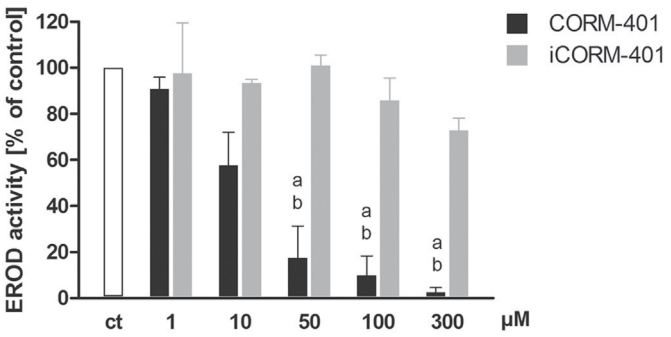

Fig. 2. CO from CORM-401 inhibits EROD activity of recombinant CYP1A1. Assay mixture consisted of 2.5 μM ethoxyresorufin, 0.125 pmol CYP1A1, 200 μM NADPH and CORM-401, iCORM-401 or PBS (solvent control, ct), respectively in a 0.1 M potassium phosphate buffer (pH 7.2). Fluorescence (λ_{ex}: 535 nm/λ_{em}: 590 nm) of the newly formed resorufin was recorded over 10 min. Activity was calculated as increase in relative fluorescence units per min. Control was set to 100%. Values are means ± SEM of three independent experiments. ANOVA analysis with Bonferroni's post-hoc test was performed for determination of statistical significances. (a) treatment vs. ct with $p \leq .05$; (b) CORM-401 vs. respective iCORM-401 with $p \leq .05$. ct = control.

concentrations between 1 and 100 μM. At the highest concentration (300 μM), a moderate decrease of EROD activity to about 80% was observed. Taken together the data demonstrate, that inhibition of EROD activity is due to CORM-401-mediated CO release.

3.3. CORM-401 derived CO inhibits EROD activity in HepG2 cells while cellular viability is not affected

To test whether CO can inhibit enzymes of the CYP1A protein family in living cells we chose HepG2 cells as model system and determined the effects of CORM-401 derived CO on EROD activity. The influence of CORM-401 and iCORM-401 on cell viability was tested in the MTT assay (Fig. 3). Upon CORM-401 treatment, viability of cells was decreased in a concentration- and time-dependent manner (Fig. 3A). Estimated IC_{50} values for CORM-401 were 150 μM and 100 μM for 6 and 24 h, respectively. At an incubation time of 2 h, cell viability was only slightly decreased to about 80% at 100 μM and to about 70% at 250 μM CORM-401. Treatment of cells with iCORM-401 had no major effects on cell viability. Only after 24 h of incubation and concentrations above 100 μM, a minor decrease of viability was determined (Fig. 3B).

Based on viability data, HepG2 cells (pre-stimulated with 3-MC) were treated with CORM-401 and iCORM-401 at concentrations of 25–100 μM for 2 h and CYP enzyme activity was measured with the EROD assay. Comparable to results from the cell-free EROD assay, CORM-401, but not iCORM-401 decreased EROD activity in HepG2 cells in a concentration dependent manner (Fig. 4). While the lowest concentration (25 μM CORM-401) had no effect, EROD activity was decreased to about 80% at 50 μM CORM-401 and even further at higher concentrations. At the 100 μM level only 40% of EROD activity remained as compared to the control. The 75 and 100 μM CORM-401 values were significantly lower compared to control and the respective iCORM-401 treatments.

3.4. CYP-dependent metabolism of the tricyclic antidepressant amitriptyline is inhibited in-vitro by CORM-401

To study CORM-401 related drug interactions we decided to use the tricyclic antidepressant amitriptyline as a model drug because it is known to be subjected to CYP1A dependent metabolism. A major CYP-derived metabolite of amitriptyline is nortriptyline, formed via *N*-demethylation (Venkatakrishnan et al., 1998). By means of HPLC analyses, effects of CORM-401 on the formation of nortriptyline from amitriptyline were studied in a cell-free approach using recombinant

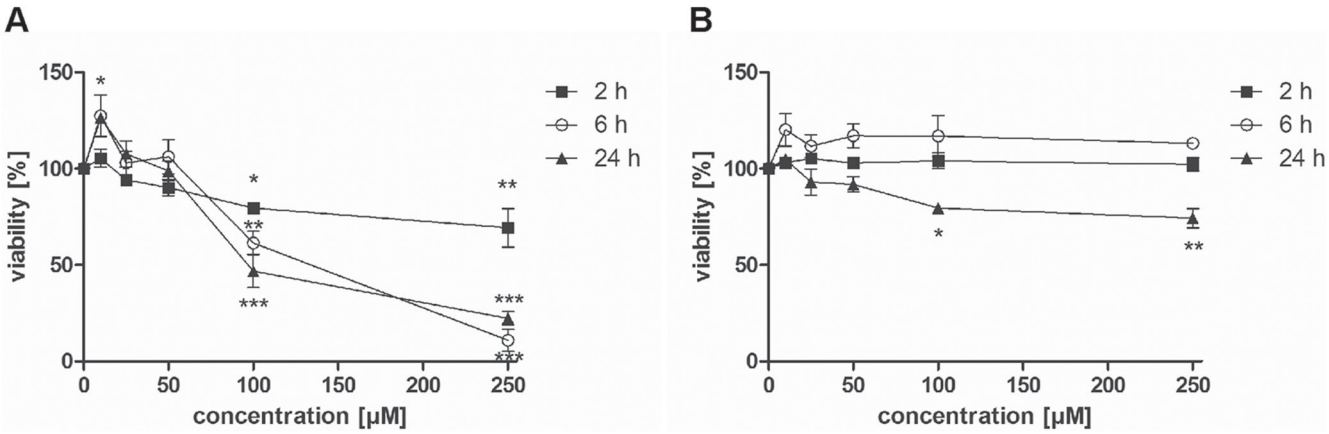

Fig. 3. CORM-401, but not iCORM-401 lowers cell viability of HepG2 cells in a dose- and time-dependent manner. Cellular viability was determined at different concentrations and time points with the MTT assay. Results of CORM-401 (A) and iCORM-401 (B) treatment are shown. Control was set to 100% cell viability (control absorbance values ranged from 0.5 to 0.65); positive control (2 mM H_2O_2) was used for background subtraction (positive control absorbance values ranged from 0.14 to 0.16). Results represent means of three independent experiments ± SEM. ANOVA analysis with Dunnett's post-hoc test was performed for determination of statistical significances. * $p \leq .05$; ** $p \leq .01$; *** $p \leq .001$.

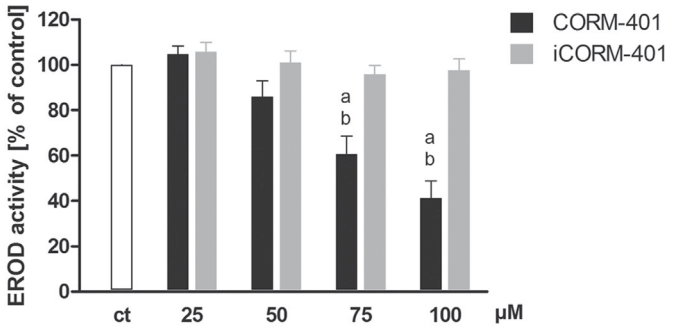

Fig. 4. Inhibition of EROD activity in HepG2 cells by CORM-401. Cells were pre-treated with 1 µM 3-MC for 24 h and then incubated for 2 h with different concentrations (25 µM–100 µM) of CORM-401, iCORM-401 or medium only (ct). Next, assay medium was added (2.5 µM ethoxyresorufin, 10 µM dicoumarol) and EROD activity was measured fluorometrically. Fluorescence (λ_{ex}: 535 nm/λ_{em}: 590 nm) of the newly formed resorufin was recorded over 30 min. Activity was calculated as increase in relative fluorescence units per min. Control was set to 100%. Values are means ± SEM of three independent experiments. ANOVA analysis with Bonferroni's post-hoc test was performed for determination of statistical significances. (a) treatment vs. ct with $p \leq .05$; (b) CORM-401 vs. respective iCORM-401 with $p \leq .05$. ct = control, 3-MC = 3-methylcholanthrene.

CYP1A2 as target enzyme. Representative chromatograms of the reaction mixture under control conditions (0 and 1 h) and after 1 h incubation with 100 µM CORM-401 or 100 µM iCORM-401 are shown in Fig. 5A-D. A quantitative evaluation of nortriptyline formation is given in Fig. 5E. The signals at retention times of 8.8 and 9.6 min were assigned to nortriptyline and amitriptyline, respectively. No nortriptyline was found at 0 h (blank value; Fig. 5B). After 1 h of incubation (control without CORM-401/iCORM-401) about 800 pmol of nortriptyline were formed (Fig. 5A). When CORM-401 was present in the reaction mixture, a concentration dependent inhibition of nortriptyline formation was observed. Nortriptyline formation was decreased statistically significant to about 400 pmol with 10 µM CORM-401 and to about 300 pmol when using 100 µM CORM-401 (Fig. 5C + E). In the presence of iCORM-401 (10–100 µM), about 750 pmol nortriptyline were formed after 1 h of incubation, due to a minor inhibitory effect. Nortriptyline formation was significantly lower for CORM-401 compared to iCORM-401 at all concentrations applied. We conclude that CYP1A2-dependent *N*-demetylation is efficiently inhibited by CORM-401-mediated CO release.

4. Discussion

CO is known to bind to heme-containing proteins, such as hemoglobin, modulating their biological function. Via this mechanism CO also inhibits the activity of CYP enzymes when present at the target site (Leemann et al., 1994). Inhibition has been demonstrated e.g. in liver microsomal fractions purged with CO gas. Such a treatment completely inactivates CYP enzymes and was used as a control in studies on xenobiotic metabolism (Parise et al., 2015) or for the determination of CYP content of biological samples using difference spectroscopy (Dong et al., 2018).

In recent years it has been suggested, that CO is a signalling molecule and CO-releasing molecules (CORMs) delivering CO at low concentrations attracted attention in basic research as well as drug development (Hopper et al., 2018; Motterlini and Foresti, 2017). In the present study we addressed the question, whether CO delivered by CORMs inhibits the activity of CYP enzymes and thus may modulate phase I metabolism of xenobiotics.

Here we used CORM-401 as a model substance for CO delivering compounds. CORM-401 and the corresponding inactive CORM-401 (iCORM-401) were tested for CO release in the Mb assay. In accordance with literature (Fayad-Kobeissi et al., 2016), CO release was detected with CORM-401, but not with iCORM-401 (Fig. 1). Consequently, upon incubation of recombinant CYP1A1 with CORM-401, but not with iCORM-401, EROD activity was decreased in a concentration dependent manner (Fig. 2). This demonstrates for the first time an inhibitory effect of CORM-derived CO on CYP activity in-vitro. Additionally, effects of CORM-401 on EROD activity in living HepG2 cells were studied and comparable results to the cell-free EROD assay were obtained. CORM-401, but not iCORM-401 decreased EROD activity in HepG2 cells in a concentration dependent manner (Fig. 4). At the concentrations of CORM-401 and iCORM-401 applied in the assay no effect on cellular viability was found (Fig. 3). Since release of CO by CORM-401 requires the close presence of suitable CO acceptors such as heme proteins (Crook et al., 2011) we conclude, that CO is released intracellularly with CYP enzymes as acceptors. This links the signalling molecule CO specifically to a physiological relevant target aside from heme proteins of the respiratory chain. It further shows that intracellular CO release can in principle be monitored in living cells by measuring inhibition of CYP activity.

We further demonstrated, that CORM-401 derived CO modifies the CYP-dependent metabolism of the antidepressant drug, amitriptyline. A major pathway of its metabolism is the *N*-demethylation to nortriptyline by CYP enzymes such as CYP1A2 and other members of the CYP

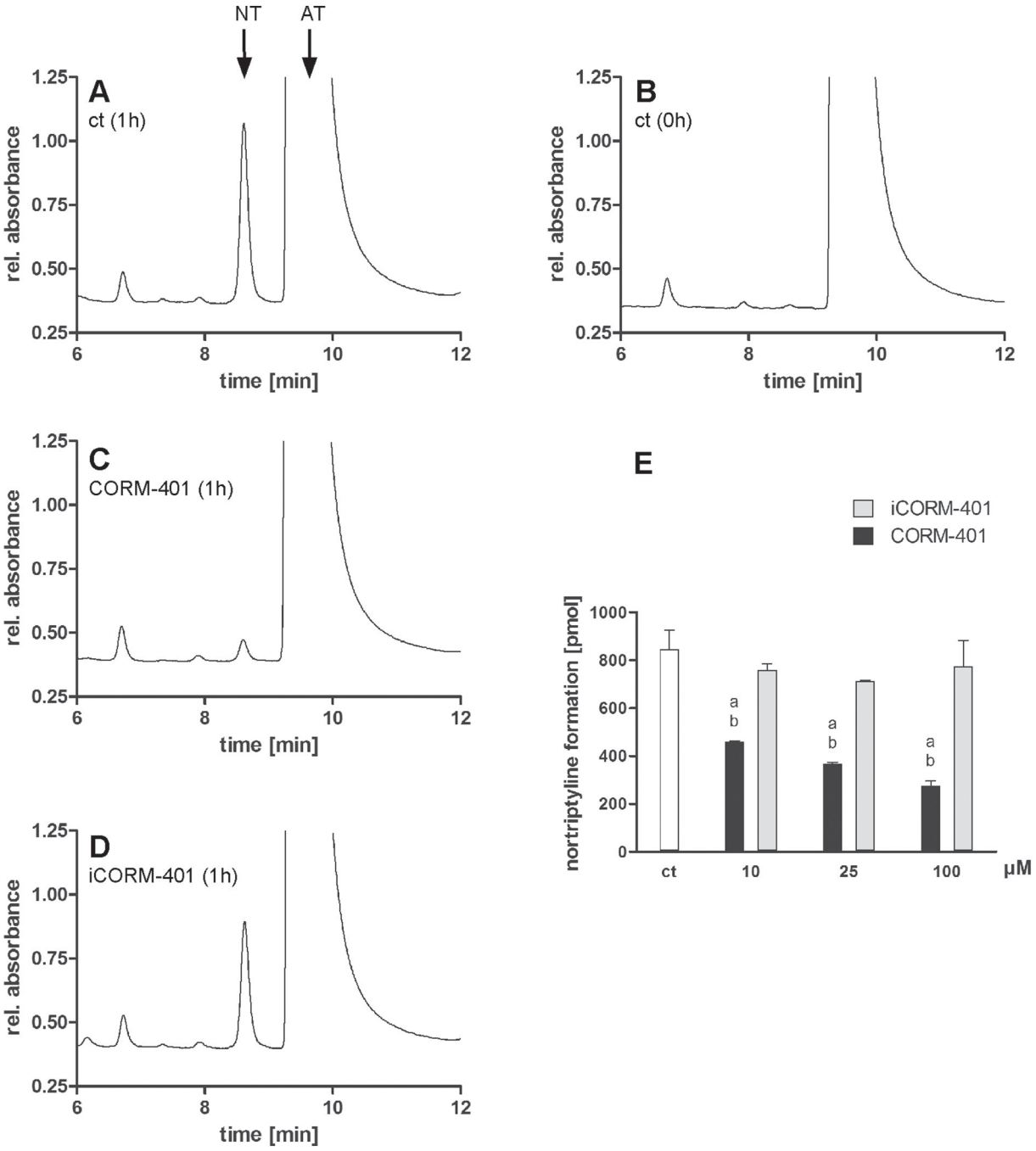

Fig. 5. CYP mediated metabolism of amitriptyline is inhibited by CORM-401. Assay mixture consisted of 100 µM amitriptyline, 5 pmol CYP1A2 enzyme, 200 µM NADPH and CORM-401, iCORM-401 or PBS (solvent control, ct), respectively in a 0.1 M potassium phosphate buffer (pH 7.2). After 1 h of incubation, the reaction was stopped with TCA. The mixture was centrifuged for 5 min at 10,000*g* and the supernatant was analyzed by HPLC. Representative chromatograms of control, 1 h incubation (A), control, 0 h incubation (B), 100 µM CORM-401 (C) and 100 µM iCORM-401 (D) are shown. Quantification of nortriptyline formation is given in E. Values are means ± SEM of three independent experiments. ANOVA analysis with Bonferroni's post-hoc test was performed for determination of statistical significances. (a) treatment vs. ct with $p \leq .05$; (b) CORM-401 vs. respective iCORM-401 with $p \leq .05$. AT = amitriptyline, ct = control, NT = nortriptyline, TCA = trichloroacetic acid.

family (Venkatakrishnan et al., 1998). Formation of nortriptyline was inhibited by CORM-401 exposure, while iCORM-401 had only minor effects (Fig. 5). This observation is of interest because several CORMs are currently under drug development for treatment of distinct diseases such as sickle cell anemia (Misra et al., 2017; Keipert, 2016) or delayed cerebral ischemia after subarachnoid haemorrhage (Dhar et al., 2017) (for review see: Hopper et al., 2018). Since the proposed mechanism of CORM-mediated CYP inhibition (binding of CO to prosthetic heme group) is of general nature, other CYPs may be implicated and inhibited as well. Based on the present data a potential interference of CORMs with the CYP-mediated xenobiotic metabolism of other drugs (drug-drug interaction) should be taken into account (Reinen et al., 2018). However, it should be noted here, that it was not the goal of this study to discuss CORM-401 itself as a possible drug, but merely use it as a representative for a compound class.

The findings may also be of interest considering CORMs to be used for the prevention of biological activation of xenobiotics by CYP enzymes. In a recent study it was shown, that CORM-A1 abolished

acetaminophen mediated hepatotoxicity in mice (Upadhyay et al., 2018). In addition to antioxidative activities mediated by CO, which were suggested to be the underlying mechanism, we propose that also inhibition of CYP enzymes contributes to the reported beneficial effect of CORM-A1. The inhibition of the enzyme might prevent formation of the reactive metabolite NAPQI and thus interfere with hepatotoxicity (Dahlin et al., 1984). In another study CORM-2 was used to modulate the pulmonary vascular tone of isolated perfused mouse lungs. No spectral alterations correlating with CO-CYP binding were found by tissue spectrophotometry during the study. The authors concluded from these findings, that no CO-dependent CYP inhibition occurred, but did not measure actual CYP enzyme activity. Furthermore, it should be mentioned, that CORM-2 was applied with an erythrocytes containing perfusate solution in which the erythrocytes possibly acted as a CO sink (Pak et al., 2016). However, future studies are required to decipher the set of molecular targets of CORMs.

Acknowledgments

This work was funded by the Deutsche Forschungsgemeinschaft (DFG, German Research Foundation) – Projektnummer 190586431 – SFB 974 – Project B09 (ASR) and Projektnummer STA699/3-1 (WS).

References

Babu, D., Leclercq, G., Motterlini, R., Lefebvre, R.A., 2017. Differential effects of CORM-2 and CORM-401 in murine intestinal epithelial MODE-K cells under oxidative stress. Front. Pharmacol. 8, 31.

Braud, L., Pini, M., Muchova, L., Manin, S., Kitagishi, H., Sawaki, D., Czibik, G., Ternacle, J., Derumeaux, G., Foresti, R., Motterlini, R., 2018. Carbon monoxide-induced metabolic switch in adipocytes improves insulin resistance in obese mice. JCI Insight 3.

Burke, M.D., Mayer, R.T., 1974. Ethoxyresorufin: direct fluorimetric assay of a microsomal O-dealkylation which is preferentially inducible by 3-methylcholanthrene. Drug Metab. Dispos. 2, 583–588.

Crook, S.H., Mann, B.E., Meijer, A.J., Adams, H., Sawle, P., Scapens, D., Motterlini, R., 2011. [$Mn(CO)_4\{S_2CNMe(CH_2CO_2H)\}$], a new water-soluble CO-releasing molecule. Dalton Trans. 40, 4230–4235.

Dahlin, D.C., Miwa, G.T., Lu, A.Y., Nelson, S.D., 1984. N-acetyl-p-benzoquinone imine: a cytochrome P-450-mediated oxidation product of acetaminophen. Proc. Natl. Acad. Sci. U. S. A. 81, 1327–1331.

Dhar, R., Misra, H., Diringer, M.N., 2017. SANGUINATE (PEGylated carboxyhemoglobin bovine) improves cerebral blood flow to vulnerable brain regions at risk of delayed cerebral ischemia after subarachnoid hemorrhage. Neurocrit. Care. 27, 341–349.

Dong, A.N., Pan, Y., Palanisamy, U.D., Yiap, B.C., Ahemad, N., Ong, C.E., 2018. Site-directed mutagenesis of cytochrome P450 2D6 and 2C19 enzymes: expression and spectral characterization of naturally occurring allelic variants. Appl. Biochem. Biotechnol. 186, 132–144.

Fayad-Kobeissi, S., Ratovonantenaina, J., Dabire, H., Wilson, J.L., Rodriguez, A.M., Berdeaux, A., Dubois-rande, J.L., Mann, B.E., Motterlini, R., Foresti, R., 2016. Vascular and angiogenic activities of CORM-401, an oxidant-sensitive CO-releasing molecule. Biochem. Pharmacol. 102, 64–77.

Garcia-Gallego, S., Bernardes, G.J., 2014. Carbon-monoxide-releasing molecules for the delivery of therapeutic CO in vivo. Angew. Chem. Int. Ed. Eng. 53, 9712–9721.

Hopper, C.P., Meinel, L., Steiger, C., Otterbein, L.E., 2018. Where is the clinical breakthrough of heme oxygenase-1/carbon monoxide therapeutics? Curr. Pharm. Des. 24 (20), 2264–2282.

Kaczara, P., Proniewski, B., Lovejoy, C., Kus, K., Motterlini, R., Abramov, A.Y., Chlopicki, S., 2018. CORM-401 induces calcium signalling, NO increase and activation of pentose phosphate pathway in endothelial cells. FEBS J. 285, 1346–1358.

Keipert, P.E., 2016. Clinical evaluation of MP4CO: a phase 1b escalating-dose, safety and tolerability study in stable adult patients with sickle cell disease. Adv. Exp. Med. Biol. 923, 23–29.

Leemann, T., Bonnabry, P., Dayer, P., 1994. Selective inhibition of major drug metabolizing cytochrome P450 isozymes in human liver microsomes by carbon monoxide. Life Sci. 54, 951–956.

Ling, K., Men, F., Wang, W.C., Zhou, Y.Q., Zhang, H.W., Ye, D.W., 2018. Carbon monoxide and its controlled release: therapeutic application, detection, and development of carbon monoxide releasing molecules (CORMs). J. Med. Chem. 61 (7), 2611–2635.

Lubet, R.A., Nims, R.W., Mayer, R.T., Cameron, J.W., Schechtman, L.M., 1985. Measurement of cytochrome P-450 dependent dealkylation of alkoxyphenoxazones in hepatic S9s and hepatocyte homogenates: effects of dicumarol. Mutat. Res. 142, 127–131.

Misra, H., Bainbridge, J., Berryman, J., Abuchowski, A., Galvez, K.M., Uribe, L.F., Hernandez, A.L., Sosa, N.R., 2017. A phase Ib open label, randomized, safety study of SANGUINATE in patients with sickle cell anemia. Rev. Bras. Hematol. Hemoter. 39, 20–27.

Motterlini, R., Foresti, R., 2017. Biological signaling by carbon monoxide and carbon monoxide-releasing molecules. Am. J. Phys. Cell Physiol. 312, C302–C313.

Motterlini, R., Clark, J.E., Foresti, R., Sarathchandra, P., Mann, B.E., Green, C.J., 2002. Carbon monoxide-releasing molecules: characterization of biochemical and vascular activities. Circ. Res. 90, E17–E24.

Musameh, M.D., Green, C.J., Mann, B.E., Motterlini, R., Fuller, B.J., 2010. CO liberated from a carbon monoxide-releasing molecule exerts a positive inotropic effect in doxorubicin-induced cardiomyopathy. J. Cardiovasc. Pharmacol. 55, 168–175.

Pak, O., Bakr, A.G., Gierhardt, M., Albus, J., Strielkov, I., Kroschel, F., Hoeres, T., Hecker, M., Ghofrani, H.A., Seeger, W., Weissmann, N., Sommer, N., 2016. Effects of carbon monoxide-releasing molecules on pulmonary vasoreactivity in isolated perfused lungs. J. Appl. Physiol. 120, 271–281.

Parise, R.A., Eiseman, J.L., Clausen, D.M., Kicielinski, K.P., Hershberger, P.A., Egorin, M.J., Beumer, J.H., 2015. Characterization of the metabolism of benzaldehyde dimethane sulfonate (NSC 281612, DMS612). Cancer Chemother. Pharmacol. 76, 537–546.

Reinen, J., Smit, M., Wenker, M., 2018. Evaluation of strategies for the assessment of drug-drug interactions involving cytochrome P450 enzymes. Eur. J. Drug Metab. Pharmacokinet. 43, 737–750.

Upadhyay, K.K., Jadeja, R.N., Thadani, J.M., Joshi, A., Vohra, A., Mevada, V., Patel, R., Khurana, S., Devkar, R.V., 2018. Carbon monoxide releasing molecule A-1 attenuates acetaminophen-mediated hepatotoxicity and improves survival of mice by induction of Nrf2 and related genes. Toxicol. Appl. Pharmacol. 360, 99–108.

Venkatakrishnan, K., Greenblatt, D.J., Von Moltke, L.L., Schmider, J., Harmatz, J.S., Shader, R.I., 1998. Five distinct human cytochromes mediate amitriptyline N-demethylation in vitro: dominance of CYP 2C19 and 3A4. J. Clin. Pharmacol. 38, 112–121.

3 DISCUSSION

3.1 General discussion

All organisms are exposed to potentially hazardous, exogenous stressors. These stressors include all sorts of chemical and physical noxae such as xenobiotics, natural compounds, toxins, drugs, heavy metals or radiation, challenging the organism on the cellular level (Fig 1). For cytoprotection, different cellular stress response pathways have evolved to counteract the various stressors and enable survival of the organism. Among the different stress response pathways, the Nrf2/Keap1 system orchestrates cellular defense against electrophilic stressors, including prooxidative and alkylating agents (Baird and Yamamoto, 2020). Keap1 is the cytosolic anchor protein of Nrf2, which is at resting state marked with ubiquitin for degradation. Upon reaction of an oxidative/electrophilic compound with Cys residues of Keap1, the interaction with Nrf2 is abrogated. Nrf2 is then released from Keap1 and translocates into the nucleus to form a heterodimer with sMaf proteins. This dimer is a functional transcription factor, and triggers gene expression of ARE-containing defense enzymes (Otsuki and Yamamoto, 2020) including those for antioxidant defense (e.g. SOD, GPx) against oxidative stressors or phase II xenobiotic metabolism (e.g. GST, UGT) for elimination of electrophilic alkylating agents (Sies et al., 2017, Galal et al., 2015). HO-1 is also typically highly upregulated upon Nrf2/Keap1 activation (Medina et al., 2020). HO-1 catalyzes the degradation of heme to biliverdin, iron and CO and is therefore thought to be responsible for the major part of stress-induced CO signaling (Motterlini and Foresti, 2017). Fig 7 shows a proposed model for the implication of CO signaling in cellular stress response including findings from this thesis as well as from literature.

To study effects of stress-induced CO signaling, suitable tools for CO detection and application in model systems needed to be established (*Manuscript 2*). For biochemical detection of CO, three assays based on heme-protein activity were applied: the Mb binding assay, a CYP activity assay (EROD) and oxygen consumption measurements for respiratory chain activity and thus indirectly the binding of CO to cytochrome *c* oxidase. The frequently applied and commercially available CORM-2, CORM-3 and CORM-401 have then been tested in the aforementioned assays for their suitability as CO delivery systems. CORM-2 and CORM-3 showed a quick CO release in the Mb assay (5 min), residual CO activity of respective iCORMs and a lack of storage stability at room temperature and -20 °C (Fig 1 of *Manuscript 2*). Additionally, putative non-CO related activities of CORM-2 hampered its use in CYP activity experiments (Fig 2 of *Manuscript 2*). Non-CO related side effects of CORM-2 and CORM-3 (modulation of ion

channel activity or antimicrobial effects) have also been described in literature and were related to the activity of reactive ruthenium species (Gessner et al., 2017, Southam et al., 2018). In contrast, CORM-401 transferred CO to Mb continuously over a period of 50 min and maintained CO releasing capacity upon storage for seven days at room temperature and -20 °C. Furthermore, iCORM-401 did not release any CO or interfered with enzyme activity assays (Fig 1+2 of *Manuscript 2*). The suitability of CORM-2 and CORM-3 was also limited in oxygen consumption measurements due to oxygen consuming activities of the compounds already observed in cell-free control experiments and CO release in the extracellular space due to thermally controlled ligand exchange (Fig 3+5 of *Manuscript 2*). CORM-401, however, did not interfere with high resolution respirometry nor XF technology and the expected inhibition of cellular respiration upon exposure of MEFs to CORM-401 was found in both set ups (Fig 3-5 of *Manuscript 2*). The CO release from CORM-401 depends on the close presence of CO acceptor molecules (heme proteins) and is therefore considered to take place mainly intracellular. However, a controversial discussion, whether the location of release is of importance for a small molecule such as CO that can easily pass membranes, is still going on (Soboleva et al., 2019, Soboleva et al., 2018). As a conclusion of *Manuscript 2*, CORM-401 was selected as a suitable CO delivery tool for further experiments, while CORM-2 and CORM-3 were considered unsuitable for the study of CO signaling due to undesired side effects of the compounds. For the investigation of CO effects on the mitochondrial respiratory chain, advantages of XF technology (low cell numbers and amounts of consumables per assay, semi-automation and higher number of treatment groups per assay) outweigh those of high resolution respirometry (direct oxygen measurement via electrode and short measurement intervals of seconds). To study the modulation of intracellular heme proteins and CO targets not related to mitochondrial function, the EROD assay is usable for the determination of CYP enzyme activity.

Since most of the further experiments were also performed in MEFs treated with CORM-401, the SRB assay was applied next for cytotoxicity testing and dose finding purposes. In the investigated time frame (0 – 240 min), only the highest CORM-401 concentration tested (100 µM) led to a significant decrease of cell viability (Fig 3A), while iCORM-401 showed no effect (Fig 3B). Hence, 50 µM CORM-401 was selected as a non-cytotoxic concentration usable for further experiments with MEFs.

The regulatory effects of CO on mitochondrial function and subsequent signal transduction were analyzed in more detail in *Manuscript 3*. Using XF technology, a CO-specific effect pattern was found after acute CORM-401 application in the mito stress test. This effect pattern

comprises a decreased maximal respiration and ATP production and an increased proton leakage (Fig 2 of *Manuscript 3*), which is in accordance with findings from other groups (Kaczara et al., 2015, Braud et al., 2018). The decrease of maximal respiration and ATP production is most likely ascribable to the well-known inhibition of cytochrome *c* oxidase (complex IV) by CO (Petersen, 1977, Pankow and Ponsold, 1984). The increase of proton leakage, however, has been discussed to be the result of CO modulating the activity of different channels such as P_iC, ANT or BK_{Ca} (Lo Iacono et al., 2011, Long et al., 2014, Kaczara et al., 2015). Importantly, very similar effects were found when different cell types (NHDFs, HepG2 and MCF-7 cells) were tested under the same conditions (Fig S2 of *Manuscript 3*), demonstrating the general validity of this approach. When analyzing the effect of endogenously produced CO on mitochondrial function the same effect pattern (decreased maximal respiration and ATP production, increased proton leakage) was observed. Under the conditions tested here, the enzyme substrate (heme) seems to be the limiting factor for CO production, rather than HO-1 protein levels, suggesting for the first time, that endogenous CO signaling might in part be substrate regulated. Although this is supported by the observation, that *Hmox1* overexpressing cells showed no further modulation of CO-related effects, the results found under *Hmox1* knock down conditions can not completely be assigned. Here, the observed CO-specific effect could also be mediated by residual HO-1 or HO-2 enzyme activity.

It is well-known that upon inhibition of the respiratory chain by CO an unintended electron transfer to oxygen can occur, generating ROS (Bilban et al., 2006, Zuckerbraun et al., 2007). However, it is also described, that CO signaling exerts protective effects against prooxidative agents (Babu et al., 2017). In *Manuscript 3* slightly elevated ROS levels were found after CORM-401 exposure. However, at the same time CO also modulated intracellular glucose utilization and metabolism was quickly directed from glycolysis towards PPP and via glyceraldehyde-3-phosphate channeled back into glycolysis. This prominent burst through the oxidative part of PPP suggests NADPH regeneration as a major goal for this CO-mediated metabolic rewiring. This is in line with increased NADPH levels found in endothelial EA.hy926 cells following CORM-401 treatment (Kaczara et al., 2018). It should be noted, that ROS are prominent inducers of PPP and NADPH is needed for antioxidant defense in general (Kuehne et al., 2015). Thus, a signal transduction pathway starting with inhibition of the respiratory chain by CO, thereby producing a mild oxidative stress that causes a prominent and quick metabolic rewiring towards PPP and NADPH production is a likely scenario to take place (Fig 7). This might also explain the contradictory reports about pro- and antioxidative effects of CO signaling (Lin et al., 2019, Kaczara et al., 2016, Babu et al., 2017).

An inhibition of the respiratory chain is typically associated with a lowered ATP production, which was also found for CORM-401 with the mito stress test (Fig 2 of *Manuscript 3*). In the ATP rate assay this observation was confirmed (Fig 4) and additionally it was found that the impact of CO on mitochondrial ATP production is much greater than on the glycolytic ATP production, which was also slightly decreased, probably due to the shift of glucose metabolism towards PPP. The decreased mitochondrial ATP production was accompanied by significantly increased levels of ADP and AMP, while ATP concentrations were only moderately affected (Fig 5). This could be caused by adenylate kinase, an enzyme catalyzing the transfer of a phosphate group from one ADP to another, thereby generating ATP and AMP (Klepinin et al., 2020). Due to the unique characteristics of the enzymatic reaction (reaction takes place near to the enzymatic equilibrium) and the relative abundances of ATP, ADP and AMP being 100, 10 and 1, respectively (Beis and Newsholme, 1975), relatively small changes of ATP concentrations lead to large increases in AMP levels (Dzeja and Terzic, 2009). Upon inhibition of mitochondrial ATP production, first the ADP concentration is expected to increase. ADP would then be used by adenylate kinase to generate ATP and AMP. Via this mechanism the cell maintains ATP levels and additionally promotes AMP-mediated signaling. After exposure of cells to CORM-401 an activation of the key AMP-sensing enzyme AMPK was determined via analysis of the phosphorylation site Thr172 of AMPKα. The signal was then further transduced and activation of ULK1, an AMPK target, was determined via analysis of the phosphorylation status at Ser555 (Fig 6). Phosphorylation of $ULK1^{Ser555}$ is a marker for mitophagy induction under different stress conditions (Egan et al., 2011, Laker et al., 2017). Upon activation, ULK1 can translocate to the outer mitochondrial membrane and phosphorylate the mitophagy receptor FUNDC1 (Tian et al., 2015, Wu et al., 2014). Active FUNDC1 is recognized by LC3, which is processed and ultimately leads to the engulfment of the mitochondrion by the autophagosome and finally degradation of the organelle (Park and Koh, 2020). Thus, it is likely, that CO signaling is transduced via the AMP-AMPK-ULK1 pathway, and leads to the induction of mitophagy (Fig 7). Another possibility of CO-mediated mitophagy induction is described in *Manuscript 1* and comprises the activation of different channels (P_iC, ANT or BK_{Ca}) leading to a leakage of protons from the mitochondrial intermembrane space into the matrix (Lo Iacono et al., 2011, Long et al., 2014, Kaczara et al., 2015). As a result of proton leakage, the mitochondrial membrane potential ($\Delta\Psi_m$) is decreased, which was also observed after CORM treatment (Kaczara et al., 2016). Loss of $\Delta\Psi_m$ is in general used by the cell as a control measure for mitochondrial quality. Upon loss of $\Delta\Psi_m$ usually the Pink1/Parkin-mediated mitophagy pathway is induced for the degradation of mitochondria with low $\Delta\Psi_m$

values (Fig 7) (Zimmermann and Reichert, 2017). However, while the CO-mediated mitophagy induction via Pink1/Parkin has been shown to be protective under different stress conditions such as inflammation, doxorubicin-mediated cardiotoxicity or hyperoxia (Kim et al., 2018, Chen et al., 2019, Suliman et al., 2017, Hull et al., 2016), a study proofing this signal transduction pathway is still missing. Nevertheless, evidence for the stimulation of two different mitophagy inducing pathways (AMP-AMPK-ULK1 and $\Delta\Psi_m$-Pink1/Parkin) by CO highlights the importance of this event. It can be speculated, that both pathways may compensate for each other in case of a malfunction of one, in order to ensure the ultimate goal of this signaling pathways: the degradation of defective mitochondria.

The removal of defective mitochondria via mitophagy is only one aspect of mitochondrial quality control mechanisms. Mitophagy and its control via CO signaling ensures, that defective mitochondria do not mediate damage to other cellular components by e.g. extensive ROS production. Nevertheless, mitochondria must be resynthesized via mitochondrial biogenesis in order to balance energy metabolism on the long-term. A CO-mediated induction of mitochondrial biogenesis, leading to increased levels of mitochondrial mass and ATP is well described in the literature and summarized in *Manuscript 1*. Interestingly, a key regulator of mitochondrial biogenesis, PGC-1α, is a substrate of AMPK. AMPK can regulate mitochondrial biogenesis either by directly phosphorylating PGC-1α or via inducing its gene expression. An AMPK-mediated induction of mitochondrial biogenesis via activation of PGC-1α was shown for astrocytes treated with CORM-2 (Choi et al., 2017). It was furthermore shown, that AMPK activity offers protection against various injuries such as diabetes, inflammation, ischemia reperfusion or obesity (Wu and Zou, 2020). It can thus be speculated, that CO might act protective under at least some of these conditions through the activation of AMPK signaling (Braud et al., 2018, Kim et al., 2018). With respect to mitochondrial homeostasis the data of this thesis and reports from literature suggest a dual regulatory role of CO signaling on mitochondrial quality control mechanisms (mitophagy/mitochondrial biogenesis) leading to a preservation of mitochondrial functionality as a response to cellular stress (Fig 7).

CYPs are a group of heme proteins involved in the phase I of xenobiotic metabolism, and contribute to cellular stress response via detoxification of foreign compounds. However, CYPs can also form electrophilic metabolites from their substrates, leading to a bioactivation of the parent compound (Schmidt et al., 2013). It is also well-known, that CO is a potent CYP inhibitor via binding to the prosthetic heme group and CO gas was often used as a control application for the determination of microsomal CYP activity (Parise et al., 2015, Dong et al., 2018). However, in *Manuscript 4* it was demonstrated for the first time, that CYP activity can also be

modulated by low amounts of CO *in vitro*. CORM-401 was used for intracellular CO delivery to living HepG2 cells. Via this imitation of endogenous CO production, a decrease of EROD activity was observed at non-cytotoxic CORM-401 concentrations (Fig 3+4 of *Manuscript 4*). The connection of CO signaling to CYP enzyme activity represents a putative feedback inhibition in the electrophile stress response pathway (Fig 7). If a xenobiotic is bioactivated to an electrophile by CYPs, this metabolite would activate the Nrf2/Keap1 pathway and thereby induce gene expression of phase II xenobiotic metabolism enzymes (GST, UGT) for its own detoxification. At the same time HO-1 would be induced for CO signaling and subsequent CYP inhibition for prevention of more electrophile formation.

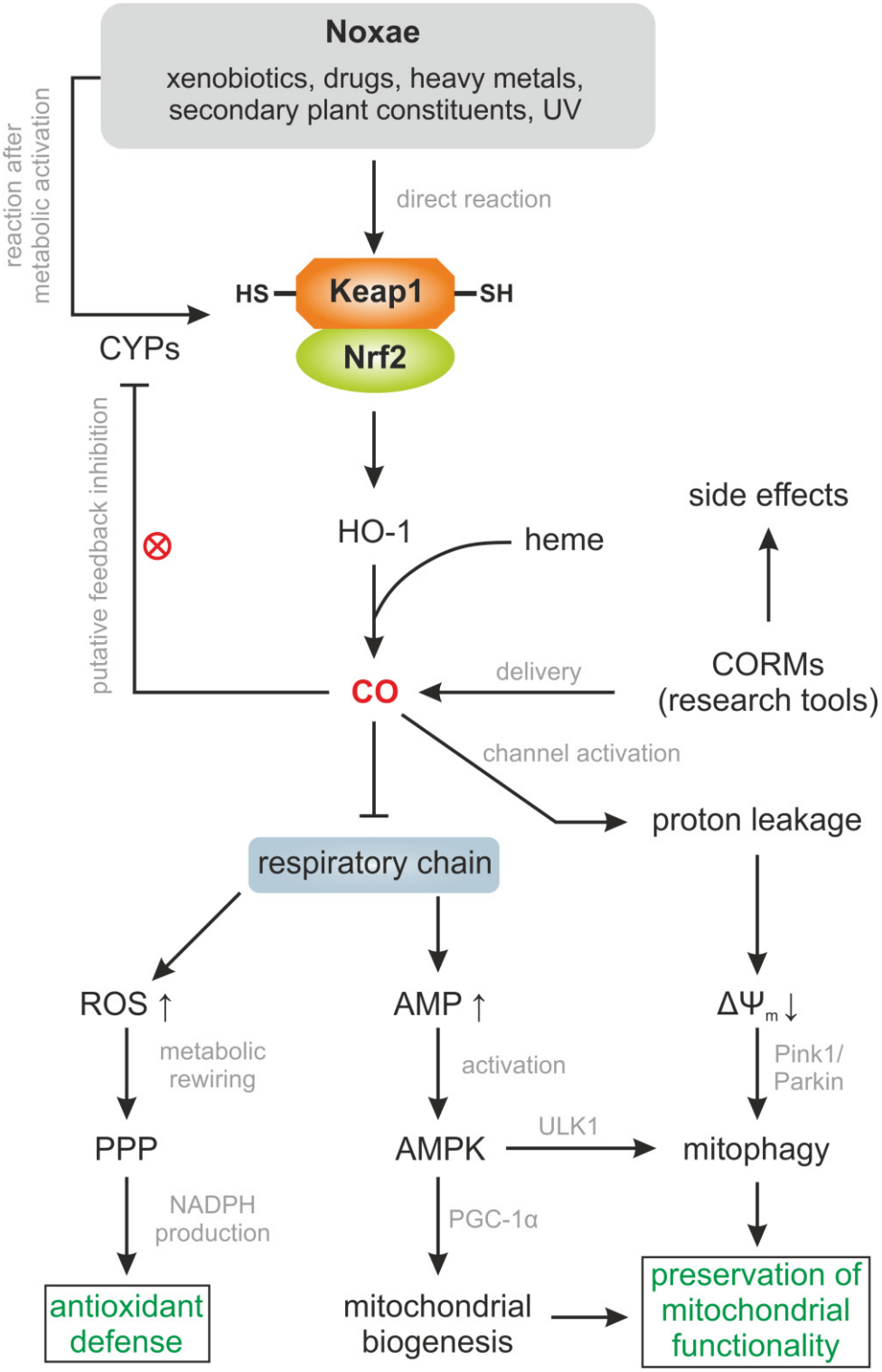

Figure 7: Proposed model for the implication of CO signaling in cellular stress response.

3.2 Concluding remarks

During the last two decades CO produced by heme oxygenases is increasingly considered to be a gaseous signaling molecule with cytoprotective properties. This thesis aimed to elucidate the role of CO signaling as an integral part of cellular stress response. For this purpose, biochemical

tools for CO detection (Mb assay, EROD assay, oxygen consumption measurements) and delivery (CORMs) were established and tested for their suitability to study CO signaling in model systems. These tools were then used to study direct effects of CO signaling on mitochondrial function and the transduction of the signal to secondary events. It was found, that CO exposure inhibited mitochondrial respiration, and that this primary event is transduced in two different signaling pathways: (i) a mild ROS production followed by a metabolic rewiring towards PPP and NADPH production and (ii) an increase of AMP levels followed by an activation of the AMP-sensing protein AMPK and subsequent activation of ULK1, an mitophagy inducing kinase. Via these two pathways CO signaling is considered to be implicated in the cellular stress response for antioxidant defense and preservation of mitochondrial functionality. Although these events were studied using CORM-401 as research tool, the most prominent findings on metabolic changes were also observed upon endogenous CO production via heme oxygenases. Furthermore, it was demonstrated, that CO signaling modulates enzyme activity of CYPs in living cells. CYPs were used as a non-mitochondria related target heme protein and its modulation by CO signaling represents a putative interconnection with other stress response pathways. It is therefore concluded, that CO signaling is an integral part of cellular stress response and as such involved in the regulation of antioxidant defense, mitochondrial homeostasis and possibly xenobiotic metabolism via an indirect mechanism.

3.3 Future perspectives

As a part of this thesis, CO signaling was not only studied using CORMs as research tools, but also endogenous CO production by heme oxygenases was investigated. In this context the question was raised, whether CO signaling might at least in part be substrate regulated. Obviously, the complete answer to this question was beyond the scope of this work and needs further investigations in future studies. Until now, little is known about the response of heme biosynthesis, and thus substrate provision for heme oxygenases, upon exogenous stressors that induce HO-1 expression. Does an upregulation of HO-1 protein levels imply and induction of heme biosynthesis via positive feedback regulation of heme concentrations? Does an increased heme biosynthesis lead to modulations of the TCA cycle which provides succinyl-CoA for the generation of δ-aminolevulinic acid, the first step of heme biosynthesis? It should also be noted, that the final steps of heme biosynthesis take place in the mitochondrial matrix, while heme oxygenases are C-terminally anchored in the ER, facing the cytosol. This leads to the question,

how enzyme and substrate meet for CO signaling. Translocation of HO-1 from ER towards mitochondria has already been shown and might be a starting point for future experiments.

Another perspective for future work on CO signaling relates to the further integration and interconnection of CO signaling with other pathways of cellular stress response. The modulation of CYP enzyme activity by CO could be investigated not only in terms of xenobiotic metabolism, but also with regard to lipid signaling. CYPs catalyze oxidations of endogenous substrates and are thereby involved in the regulation of various lipophilic signaling compounds including eicosanoids, retinoic acid, cholecalciferol, or steroid hormones. Via modulation of CYP activity, CO signaling could be connected to processes such as inflammation, growth and development, or calcium homeostasis.

List of publications

Publications

Walter, M., Stahl, W., Brenneisen, P., Reichert, A.S., **Stucki, D.**, 2019. Carbon monoxide releasing molecules 401 (CORM-401) modulates phase I metabolism of xenobiotics. *Toxicol In Vitro* 59, 215-220.

Stucki, D., Krahl, H., Walter, M., Steinhausen, J., Hommel, K., Brenneisen, P., Stahl, W., 2020. Effects of frequently applied carbon monoxide releasing molecules (CORMs) in typical CO-sensitive model systems – A comparative *in vitro* study. *Arch Biochem Biophys* 687, 108383.

Stucki, D., Steinhausen, J., Westhoff, P., Krahl, H., Brilhaus, D., Massenberg, A., Weber, A.P.M., Reichert, A.S., Brenneisen, P., Stahl, W., 2020. Endogenous carbon monoxide signaling modulates mitochondrial function and intracellular glucose utilization: impact of the heme oxygenase substrate hemin. *Antioxidants (Basel)* 9.

Stucki, D., Stahl, W., 2020. Carbon monoxide – beyond toxicity? *Toxicol Lett* 333, 251-260.

Talks

Walter, M., Brenneisen, P., Stahl, W., **Stucki, D.** Carbon monoxide releasing molecule 401 (CORM-401) modulates phase I metabolism of the tricyclic antidepressant amitriptyline. 4th German Pharm Tox Summit, Stuttgart, February 2019.

Stucki, D., Steinhausen, J., Brilhaus, D., Westhoff, P., Weber, A.P.M., Stahl, W. Carbon monoxide – a novel stress response mediator? 5th German Pharm Tox Summit, Leipzig, March 2020.

Poster

Stucki, D., Brenneisen, P., Reichert, A.S., Stahl, W. Carbon monoxide releasing molecule 401 (CORM-401) modulates mitochondrial energetics of murine embryonic fibroblasts (MEFs). MITOchats, Cologne, July 2019.

References

BABU, D., LECLERCQ, G., MOTTERLINI, R. & LEFEBVRE, R. A. 2017. Differential Effects of CORM-2 and CORM-401 in Murine Intestinal Epithelial MODE-K Cells under Oxidative Stress. *Front Pharmacol,* 8**,** 31.

BAIRD, L. & YAMAMOTO, M. 2020. The Molecular Mechanisms Regulating the KEAP1-NRF2 Pathway. *Mol Cell Biol,* 40.

BEACH, T. E., PRAG, H. A., PALA, L., LOGAN, A., HUANG, M. M., GRUSZCZYK, A. V., MARTIN, J. L., MAHBUBANI, K., HAMED, M. O., HOSGOOD, S. A., NICHOLSON, M. L., JAMES, A. M., HARTLEY, R. C., MURPHY, M. P. & SAEB-PARSY, K. 2020. Targeting succinate dehydrogenase with malonate ester prodrugs decreases renal ischemia reperfusion injury. *Redox Biol,* 36**,** 101640.

BEIS, I. & NEWSHOLME, E. A. 1975. The contents of adenine nucleotides, phosphagens and some glycolytic intermediates in resting muscles from vertebrates and invertebrates. *Biochem J,* 152**,** 23-32.

BILBAN, M., BACH, F. H., OTTERBEIN, S. L., IFEDIGBO, E., D'AVILA, J. C., ESTERBAUER, H., CHIN, B. Y., USHEVA, A., ROBSON, S. C., WAGNER, O. & OTTERBEIN, L. E. 2006. Carbon monoxide orchestrates a protective response through PPARgamma. *Immunity,* 24**,** 601-10.

BRAUD, L., PINI, M., MUCHOVA, L., MANIN, S., KITAGISHI, H., SAWAKI, D., CZIBIK, G., TERNACLE, J., DERUMEAUX, G., FORESTI, R. & MOTTERLINI, R. 2018. Carbon monoxide-induced metabolic switch in adipocytes improves insulin resistance in obese mice. *JCI Insight,* 3.

CARLING, D., ZAMMIT, V. A. & HARDIE, D. G. 1987. A common bicyclic protein kinase cascade inactivates the regulatory enzymes of fatty acid and cholesterol biosynthesis. *FEBS Lett,* 223**,** 217-22.

CHEN, Y., JOE, Y., PARK, J., SONG, H. C., KIM, U. H. & CHUNG, H. T. 2019. Carbon monoxide induces the assembly of stress granule through the integrated stress response. *Biochem Biophys Res Commun,* 512**,** 289-294.

CHOI, Y. K., KIM, J. H., LEE, D. K., LEE, K. S., WON, M. H., JEOUNG, D., LEE, H., HA, K. S., KWON, Y. G. & KIM, Y. M. 2017. Carbon Monoxide Potentiation of L-Type Ca(2+) Channel Activity Increases HIF-1alpha-Independent VEGF Expression via an AMPKalpha/SIRT1-Mediated PGC-1alpha/ERRalpha Axis. *Antioxid Redox Signal,* 27**,** 21-36.

CHOI, Y. K., PARK, J. H., BAEK, Y. Y., WON, M. H., JEOUNG, D., LEE, H., HA, K. S., KWON, Y. G. & KIM, Y. M. 2016. Carbon monoxide stimulates astrocytic mitochondrial biogenesis via L-type Ca(2+) channel-mediated PGC-1alpha/ERRalpha activation. *Biochem Biophys Res Commun,* 479**,** 297-304.

COBURN, R. F., BLAKEMORE, W. S. & FORSTER, R. E. 1963. Endogenous carbon monoxide production in man. *J Clin Invest,* 42**,** 1172-8.

DAVIES, S. P., HELPS, N. R., COHEN, P. T. & HARDIE, D. G. 1995. 5'-AMP inhibits dephosphorylation, as well as promoting phosphorylation, of the AMP-activated protein kinase. Studies using bacterially expressed human protein phosphatase-2C alpha and native bovine protein phosphatase-2AC. *FEBS Lett,* 377**,** 421-5.

DE LA FUENTE, I. M., CORTÉS, J. M., VALERO, E., DESROCHES, M., RODRIGUES, S., MALAINA, I. & MARTÍNEZ, L. 2014. On the dynamics of the adenylate energy system: homeorhesis vs homeostasis. *PLoS One,* 9**,** e108676.

DONG, A. N., PAN, Y., PALANISAMY, U. D., YIAP, B. C., AHEMAD, N. & ONG, C. E. 2018. Site-Directed Mutagenesis of Cytochrome P450 2D6 and 2C19 Enzymes:

Expression and Spectral Characterization of Naturally Occurring Allelic Variants. *Appl Biochem Biotechnol,* 186**,** 132-144.

DZEJA, P. & TERZIC, A. 2009. Adenylate kinase and AMP signaling networks: metabolic monitoring, signal communication and body energy sensing. *Int J Mol Sci,* 10**,** 1729-72.

EGAN, D. F., SHACKELFORD, D. B., MIHAYLOVA, M. M., GELINO, S., KOHNZ, R. A., MAIR, W., VASQUEZ, D. S., JOSHI, A., GWINN, D. M., TAYLOR, R., ASARA, J. M., FITZPATRICK, J., DILLIN, A., VIOLLET, B., KUNDU, M., HANSEN, M. & SHAW, R. J. 2011. Phosphorylation of ULK1 (hATG1) by AMP-activated protein kinase connects energy sensing to mitophagy. *Science,* 331**,** 456-61.

GALAL, A. M., WALKER, L. A. & KHAN, I. A. 2015. Induction of GST and related events by dietary phytochemicals: sources, chemistry, and possible contribution to chemoprevention. *Curr Top Med Chem,* 14**,** 2802-21.

GESSNER, G., SAHOO, N., SWAIN, S. M., HIRTH, G., SCHONHERR, R., MEDE, R., WESTERHAUSEN, M., BREWITZ, H. H., HEIMER, P., IMHOF, D., HOSHI, T. & HEINEMANN, S. H. 2017. CO-independent modification of K(+) channels by tricarbonyldichlororuthenium(II) dimer (CORM-2). *Eur J Pharmacol,* 815**,** 33-41.

HARDIE, D. G. 2004. The AMP-activated protein kinase pathway--new players upstream and downstream. *J Cell Sci,* 117**,** 5479-87.

HAWLEY, S. A., BOUDEAU, J., REID, J. L., MUSTARD, K. J., UDD, L., MÄKELÄ, T. P., ALESSI, D. R. & HARDIE, D. G. 2003. Complexes between the LKB1 tumor suppressor, STRAD alpha/beta and MO25 alpha/beta are upstream kinases in the AMP-activated protein kinase cascade. *J Biol,* 2**,** 28.

HERZIG, S. & SHAW, R. J. 2018. AMPK: guardian of metabolism and mitochondrial homeostasis. *Nat Rev Mol Cell Biol,* 19**,** 121-135.

HULL, T. D., BODDU, R., GUO, L., TISHER, C. C., TRAYLOR, A. M., PATEL, B., JOSEPH, R., PRABHU, S. D., SULIMAN, H. B., PIANTADOSI, C. A., AGARWAL, A. & GEORGE, J. F. 2016. Heme oxygenase-1 regulates mitochondrial quality control in the heart. *JCI Insight,* 1**,** e85817.

ISHIGAMI, I., ZATSEPIN, N. A., HIKITA, M., CONRAD, C. E., NELSON, G., COE, J. D., BASU, S., GRANT, T. D., SEABERG, M. H., SIERRA, R. G., HUNTER, M. S., FROMME, P., FROMME, R., YEH, S. R. & ROUSSEAU, D. L. 2017. Crystal structure of CO-bound cytochrome c oxidase determined by serial femtosecond X-ray crystallography at room temperature. *Proc Natl Acad Sci U S A,* 114**,** 8011-8016.

KACZARA, P., MOTTERLINI, R., KUS, K., ZAKRZEWSKA, A., ABRAMOV, A. Y. & CHLOPICKI, S. 2016. Carbon monoxide shifts energetic metabolism from glycolysis to oxidative phosphorylation in endothelial cells. *FEBS Lett,* 590**,** 3469-3480.

KACZARA, P., MOTTERLINI, R., ROSEN, G. M., AUGUSTYNEK, B., BEDNARCZYK, P., SZEWCZYK, A., FORESTI, R. & CHLOPICKI, S. 2015. Carbon monoxide released by CORM-401 uncouples mitochondrial respiration and inhibits glycolysis in endothelial cells: A role for mitoBKCa channels. *Biochim Biophys Acta,* 1847**,** 1297-309.

KACZARA, P., PRONIEWSKI, B., LOVEJOY, C., KUS, K., MOTTERLINI, R., ABRAMOV, A. Y. & CHLOPICKI, S. 2018. CORM-401 induces calcium signalling, NO increase and activation of pentose phosphate pathway in endothelial cells. *FEBS J,* 285**,** 1346-1358.

KIM, H. J., JOE, Y., RAH, S. Y., KIM, S. K., PARK, S. U., PARK, J., KIM, J., RYU, J., CHO, G. J., SURH, Y. J., RYTER, S. W., KIM, U. H. & CHUNG, H. T. 2018. Carbon monoxide-induced TFEB nuclear translocation enhances mitophagy/mitochondrial biogenesis in hepatocytes and ameliorates inflammatory liver injury. *Cell Death Dis,* 9**,** 1060.

KIM, J., KUNDU, M., VIOLLET, B. & GUAN, K. L. 2011. AMPK and mTOR regulate autophagy through direct phosphorylation of Ulk1. *Nat Cell Biol,* 13**,** 132-41.

KLEPININ, A., ZHANG, S., KLEPININA, L., REBANE-KLEMM, E., TERZIC, A., KAAMBRE, T. & DZEJA, P. 2020. Adenylate Kinase and Metabolic Signaling in Cancer Cells. *Front Oncol,* 10**,** 660.

KUEHNE, A., EMMERT, H., SOEHLE, J., WINNEFELD, M., FISCHER, F., WENCK, H., GALLINAT, S., TERSTEGEN, L., LUCIUS, R., HILDEBRAND, J. & ZAMBONI, N. 2015. Acute Activation of Oxidative Pentose Phosphate Pathway as First-Line Response to Oxidative Stress in Human Skin Cells. *Mol Cell,* 59**,** 359-71.

LAKER, R. C., DRAKE, J. C., WILSON, R. J., LIRA, V. A., LEWELLEN, B. M., RYALL, K. A., FISHER, C. C., ZHANG, M., SAUCERMAN, J. J., GOODYEAR, L. J., KUNDU, M. & YAN, Z. 2017. Ampk phosphorylation of Ulk1 is required for targeting of mitochondria to lysosomes in exercise-induced mitophagy. *Nat Commun,* 8**,** 548.

LEEMANN, T., BONNABRY, P. & DAYER, P. 1994. Selective inhibition of major drug metabolizing cytochrome P450 isozymes in human liver microsomes by carbon monoxide. *Life Sci,* 54**,** 951-6.

LIN, C. C., HSIAO, L. D., CHO, R. L. & YANG, C. M. 2019. Carbon Monoxide Releasing Molecule-2-Upregulated ROS-Dependent Heme Oxygenase-1 Axis Suppresses Lipopolysaccharide-Induced Airway Inflammation. *Int J Mol Sci,* 20.

LO IACONO, L., BOCZKOWSKI, J., ZINI, R., SALOUAGE, I., BERDEAUX, A., MOTTERLINI, R. & MORIN, D. 2011. A carbon monoxide-releasing molecule (CORM-3) uncouples mitochondrial respiration and modulates the production of reactive oxygen species. *Free Radic Biol Med,* 50**,** 1556-64.

LONG, R., SALOUAGE, I., BERDEAUX, A., MOTTERLINI, R. & MORIN, D. 2014. CORM-3, a water soluble CO-releasing molecule, uncouples mitochondrial respiration via interaction with the phosphate carrier. *Biochim Biophys Acta,* 1837**,** 201-9.

MARSIN, A. S., BERTRAND, L., RIDER, M. H., DEPREZ, J., BEAULOYE, C., VINCENT, M. F., VAN DEN BERGHE, G., CARLING, D. & HUE, L. 2000. Phosphorylation and activation of heart PFK-2 by AMPK has a role in the stimulation of glycolysis during ischaemia. *Curr Biol,* 10**,** 1247-55.

MEDINA, M. V., SAPOCHNIK, D., GARCIA SOLÁ, M. & COSO, O. 2020. Regulation of the Expression of Heme Oxygenase-1: Signal Transduction, Gene Promoter Activation, and Beyond. *Antioxid Redox Signal,* 32**,** 1033-1044.

MOTTERLINI, R., CLARK, J. E., FORESTI, R., SARATHCHANDRA, P., MANN, B. E. & GREEN, C. J. 2002. Carbon monoxide-releasing molecules: characterization of biochemical and vascular activities. *Circ Res,* 90**,** E17-24.

MOTTERLINI, R. & FORESTI, R. 2017. Biological signaling by carbon monoxide and carbon monoxide-releasing molecules. *Am J Physiol Cell Physiol,* 312**,** C302-c313.

MUNDAY, M. R., CAMPBELL, D. G., CARLING, D. & HARDIE, D. G. 1988. Identification by amino acid sequencing of three major regulatory phosphorylation sites on rat acetyl-CoA carboxylase. *Eur J Biochem,* 175**,** 331-8.

NANDI, A., YAN, L. J., JANA, C. K. & DAS, N. 2019. Role of Catalase in Oxidative Stress- and Age-Associated Degenerative Diseases. *Oxid Med Cell Longev,* 2019**,** 9613090.

NEBERT, D. W., WIKVALL, K. & MILLER, W. L. 2013. Human cytochromes P450 in health and disease. *Philos Trans R Soc Lond B Biol Sci,* 368**,** 20120431.

OTSUKI, A. & YAMAMOTO, M. 2020. Cis-element architecture of Nrf2-sMaf heterodimer binding sites and its relation to diseases. *Arch Pharm Res,* 43**,** 275-285.

PANKOW, D. & PONSOLD, W. 1984. Effect of carbon monoxide exposure on heart cytochrome c oxidase activity of rats. *Biomed Biochim Acta,* 43**,** 1185-9.

PARISE, R. A., EISEMAN, J. L., CLAUSEN, D. M., KICIELINSKI, K. P., HERSHBERGER, P. A., EGORIN, M. J. & BEUMER, J. H. 2015. Characterization of the metabolism of benzaldehyde dimethane sulfonate (NSC 281612, DMS612). *Cancer Chemother Pharmacol,* 76**,** 537-46.

PARK, S. Y. & KOH, H. C. 2020. FUNDC1 regulates receptor-mediated mitophagy independently of the PINK1/Parkin-dependent pathway in rotenone-treated SH-SY5Y cells. *Food Chem Toxicol,* 137**,** 111163.

PECORELLA, S. R., POTTER, J. V., CHERRY, A. D., PEACHER, D. F., WELTY-WOLF, K. E., MOON, R. E., PIANTADOSI, C. A. & SULIMAN, H. B. 2015. The HO-1/CO system regulates mitochondrial-capillary density relationships in human skeletal muscle. *Am J Physiol Lung Cell Mol Physiol,* 309**,** L857-71.

PETERSEN, L. C. 1977. The effect of inhibitors on the oxygen kinetics of cytochrome c oxidase. *Biochim Biophys Acta,* 460**,** 299-307.

ROSS, F. A., JENSEN, T. E. & HARDIE, D. G. 2016. Differential regulation by AMP and ADP of AMPK complexes containing different γ subunit isoforms. *Biochem J,* 473**,** 189-99.

SCHATZSCHNEIDER, U. 2015. Novel lead structures and activation mechanisms for CO-releasing molecules (CORMs). *Br J Pharmacol,* 172**,** 1638-50.

SCHMIDT, J., KOTNIK, P., TRONTELJ, J., KNEZ, Ž. & MAŠIČ, L. P. 2013. Bioactivation of bisphenol A and its analogs (BPF, BPAF, BPZ and DMBPA) in human liver microsomes. *Toxicol In Vitro,* 27**,** 1267-76.

SIES, H., BERNDT, C. & JONES, D. P. 2017. Oxidative Stress. *Annu Rev Biochem,* 86**,** 715-748.

SOBOLEVA, T., ESQUER, H. J., ANDERSON, S. N., BERREAU, L. M. & BENNINGHOFF, A. D. 2018. Mitochondrial-Localized Versus Cytosolic Intracellular CO-Releasing Organic PhotoCORMs: Evaluation of CO Effects Using Bioenergetics. *ACS Chem Biol*.

SOBOLEVA, T., SIMONS, C. R., ARCIDIACONO, A., BENNINGHOFF, A. D. & BERREAU, L. M. 2019. Extracellular vs Intracellular Delivery of CO: Does It Matter for a Stable, Diffusible Gasotransmitter? *J Med Chem,* 62**,** 9990-9995.

SOUTHAM, H. M., SMITH, T. W., LYON, R. L., LIAO, C., TREVITT, C. R., MIDDLEMISS, L. A., COX, F. L., CHAPMAN, J. A., EL-KHAMISY, S. F., HIPPLER, M., WILLIAMSON, M. P., HENDERSON, P. J. F. & POOLE, R. K. 2018. A thiol-reactive Ru(II) ion, not CO release, underlies the potent antimicrobial and cytotoxic properties of CO-releasing molecule-3. *Redox Biol,* 18**,** 114-123.

STUCKI, D., BRENNEISEN, P., REICHERT, A. S. & STAHL, W. 2018. The BH3 mimetic compound BH3I-1 impairs mitochondrial dynamics and promotes stress response in addition to its pro-apoptotic key function. *Toxicol Lett,* 295**,** 369-378.

STUCKI, D. & STAHL, W. 2020. Carbon monoxide - beyond toxicity? *Toxicol Lett,* 333**,** 251-260.

SULIMAN, H. B., KEENAN, J. E. & PIANTADOSI, C. A. 2017. Mitochondrial quality-control dysregulation in conditional HO-1-/- mice. *JCI Insight,* 2**,** e89676.

TAILLÉ, C., EL-BENNA, J., LANONE, S., BOCZKOWSKI, J. & MOTTERLINI, R. 2005. Mitochondrial respiratory chain and NAD(P)H oxidase are targets for the antiproliferative effect of carbon monoxide in human airway smooth muscle. *J Biol Chem,* 280**,** 25350-60.

TIAN, W., LI, W., CHEN, Y., YAN, Z., HUANG, X., ZHUANG, H., ZHONG, W., CHEN, Y., WU, W., LIN, C., CHEN, H., HOU, X., ZHANG, L., SUI, S., ZHAO, B., HU, Z., LI, L. & FENG, D. 2015. Phosphorylation of ULK1 by AMPK regulates translocation of ULK1 to mitochondria and mitophagy. *FEBS Lett,* 589**,** 1847-54.

TOYAMA, E. Q., HERZIG, S., COURCHET, J., LEWIS, T. L., JR., LOSÓN, O. C., HELLBERG, K., YOUNG, N. P., CHEN, H., POLLEUX, F., CHAN, D. C. & SHAW, R. J. 2016. Metabolism. AMP-activated protein kinase mediates mitochondrial fission in response to energy stress. *Science,* 351**,** 275-281.

VOGEL, C. F. A., VAN WINKLE, L. S., ESSER, C. & HAARMANN-STEMMANN, T. 2020. The aryl hydrocarbon receptor as a target of environmental stressors - Implications for pollution mediated stress and inflammatory responses. *Redox Biol,* 34**,** 101530.

WHITLOCK, J. P., JR. 1999. Induction of cytochrome P4501A1. *Annu Rev Pharmacol Toxicol,* 39**,** 103-25.

WU, S. & ZOU, M. H. 2020. AMPK, Mitochondrial Function, and Cardiovascular Disease. *Int J Mol Sci,* 21.

WU, W., TIAN, W., HU, Z., CHEN, G., HUANG, L., LI, W., ZHANG, X., XUE, P., ZHOU, C., LIU, L., ZHU, Y., ZHANG, X., LI, L., ZHANG, L., SUI, S., ZHAO, B. & FENG, D. 2014. ULK1 translocates to mitochondria and phosphorylates FUNDC1 to regulate mitophagy. *EMBO Rep,* 15**,** 566-75.

XU, C., LI, C. Y. & KONG, A. N. 2005. Induction of phase I, II and III drug metabolism/transport by xenobiotics. *Arch Pharm Res,* 28**,** 249-68.

ZIMMERMANN, M. & REICHERT, A. S. 2017. How to get rid of mitochondria: crosstalk and regulation of multiple mitophagy pathways. *Biol Chem,* 399**,** 29-45.

ZUCKERBRAUN, B. S., CHIN, B. Y., BILBAN, M., D'AVILA, J. C., RAO, J., BILLIAR, T. R. & OTTERBEIN, L. E. 2007. Carbon monoxide signals via inhibition of cytochrome c oxidase and generation of mitochondrial reactive oxygen species. *Faseb J,* 21**,** 1099-106.

Eidesstattliche Erklärung

Ich versichere an Eides statt, dass die vorliegende Dissertation „Implication of carbon monoxide signaling in cellular stress response“ von mir selbstständig und ohne unzulässige fremde Hilfe unter Beachtung der „Grundsätze zur Sicherung guter wissenschaftlicher Praxis an der Heinrich-Heine-Universität Düsseldorf“ erstellt worden ist. Diese Arbeit wurde weder in gleicher noch in abgewandelter Form bei einer anderen Institution zur Prüfung vorgelegt. Vorherige, erfolgreiche oder erfolglose Promotionsversuche habe ich nicht unternommen.

Düsseldorf, den 8. September 2020

_____

David Stucki

Danksagung

Ich möchte mich bei einigen Leuten bedanken die mir während dieser Arbeit mit Rat und Tat zur Seite gestanden haben.

Zunächst gilt mein Dank meinem erstklassigen Doktorvater Prof Wilhelm Stahl für die Stellung des interessanten Themas und die tolle Betreuung meiner Arbeit. Willi, ich möchte dir insbesondere dafür danken, dass ich viele eigene Ideen in dieses Projekt einbringen und untersuchen konnte. Auch danke ich dir dafür, dass du mir während der experimentell schwierigen ersten Phase meiner Arbeit immer wieder Mut gemacht und Zuversicht verbreitet hast – offensichtlich hattest du recht, irgendwann macht es *klick*. Danke auch, dass ich die Verantwortung übernehmen durfte Studenten zu betreuen sowie Freiheiten zur Teilnahme an Kongressen und zur toxikologischen Weiterbildung von dir bekommen habe.

Ich möchte mich ebenfalls bei Prof Vlada Urlacher für die Übernahme des Zweitreferats und den anregenden Diskussionen während der Betreuungsgespräche, sowie bei Prof Gerhard Fritz für die Betreuung und Hinweise zu meiner Arbeit und den Vorträgen aus toxikologischer Sichtweise und bei Prof Peter Brenneisen für die anregenden Diskussionen in den Gruppen-Seminaren bedanken.

Natürlich möchte ich mich auch bei der gesamten Arbeitsgruppe Stahl für die tolle Zeit und Arbeitsatmosphäre in den letzten Jahren bedanken…

Bei Peter Graf für die vielen lustigen und ernsthaften Gespräche über verschiedenste Themen von Politik, Witzen oder den aktuellen Corona-Zahlen, aber auch für zahlreiche nützliche Tipps und Tricks zur technischen Machbarkeit von eigentlich allem Möglichen im Labor. Lieber Peter, vielen Dank für die tolle Zeit mit dir zusammen im Büro, ich werde sie sehr vermissen.

Bei Heide Krahl für die technische Unterstützung im Labor von Zellen splitten bis Seahorse Experimenten. Auch wenn wir mittlerweile nicht mehr in einem Büro sitzen, so war es doch eine einprägsame Zeit – ich sag nur: ich guck‘ dann mal.

Bei Sarah Zerres für ihre Geduld und Verständnis bei der ein oder anderen ausufernden Diskussion von Peter und mir, für die Begrünung des Büros und Erläuterungen zu den verschiedensten Ninja-Prüfungen.

Natürlich möchte ich mich auch bei meinen ehemaligen Studis Katrin Hommel, Moritz Walter, Julia Steinhausen und Annika Massenberg bedanken. Es war eine sehr schöne Erfahrung eure Arbeiten betreuen zu können und ich glaube ich habe dabei mindestens genauso

viel gelernt wie ihr (hoffentlich) auch. Ich habe mich über die Zusammenarbeit mit jedem einzelnen von euch wirklich sehr gefreut und möchte mich für das Vertrauen bedanken das ich von euch erhalten habe.

Ein großer Dank geht auch an alle Mitglieder der Arbeitsgruppe Brenneisen, die *Brennis*. Vielen Dank für die schöne Zeit im Labor und natürlich in der Mensa, für die vielen Hilfestellungen, anregenden Diskussionen und im allgemeinen wunderbare Arbeitsatmosphäre, an Claudia Wyrich, Dr Claudia von Montfort, Lisa Haasler, Lara Ebbert, Niklas Klahm und alle anderen die in den letzten Jahren Teil des Teams waren.

Auch bei Prof Andreas Reichert und seiner Arbeitsgruppe möchte ich mich für die gute Zusammenarbeit und gemeinsamen Diskussionen in den zahlreichen Seminaren und Workshops bedanken. Danke auch an Drs Arun Kondadi und Marcel Zimmermann für die zahlreichen Tipps und Hilfestellungen beim Klonieren und der Fluoreszenzmikroskopie, auch wenn es leider keine Imaging Daten in die Arbeit geschafft haben. Thanks guys. Danke auch an Andrea Borchardt für die netten Pausen vor der Türe. Es war immer unterhaltsam und entspannend.

Ein weiterer Dank geht auch an Prof Andreas Weber für die Kooperation bei der Metabolomanalyse und an Drs Philipp Westhoff und Dominik Brilhaus für die Hilfe und Beratung bei der Planung der entsprechenden Experimente und natürlich auch für die Durchführung und Auswertung der Analysen selber.

Ich möchte mich ebenfalls bei meinen Eltern bedanken die mich mit einem gewissen Drang Dinge zu verstehen und zu diskutieren ausgestattet haben und ohne deren Unterstützung während meines gesamten Studiums ich erst gar nicht in die Lage gekommen wäre an einer Doktorarbeit zu werkeln. Vielen Dank dafür, ich habe euch beide sehr lieb.

Zu guter Letzt gilt mein Dank natürlich auch meiner Freundin Sarah die mich all die Jahre sehr unterstützt, motiviert und besonders in der schwierigen Anfangszeit der Arbeit aufgebaut hat. Es war doch teilweise eine sehr fordernde Zeit und ich bin dir dankbar, dass du mich durch ebendiese begleitet hast – das hat sie viel angenehmer und schöner werden lassen. Danke, dass du immer für mich da warst mein Schatz, ich liebe dich sehr!